The role of auxin response in patterning the thallus of the liverwort *Marchantia polymorpha*

Thesis submitted for the degree of Doctor of Philosophy

By

Eduardo Flores-Sandoval
B.Sc.

March, 2013

School of Biological Sciences

Monash University
Victoria 3800
Australia

A mi familia y amigos

Declaration

This thesis contains no material that has been accepted for the award of any other degree or diploma in any university or institution. This thesis contains no material previously published or written by another person except where due reference is made in the text.

Eduardo Flores-Sandoval

ACKNOWLEDGEMENTS

This work would not have been possible without the help and guidance of John Bowman. John has given me the necessary tools and freedom to conduct independent research, all in a relaxed and friendly environment. John has gift to make science exciting and interesting, this was most useful when the project reached difficult stages of failed experiments and little understanding. John's support was constant (maybe except when he was writing his book -just joking John) and his expertise has helped me put this thesis in a wider historical context. I especially thank him for his friendship, generosity and countless stories, BBQs, beers in St. Kilda, and runs and hikes in the beautiful australian bush.

I thank Sandra Floyd for her help in the initial phases of this project, setting up experimental work in *Marchantia* as well as her constructive criticism to establish an initial testable hypothesis. I thank her for organizing lab logistics for so many years.

Magnus Eklund has significantly helped me in the last part of this project with experimental work, many skills in the lab and stimulating discussions. His enthusiasm and easiness to collaborate make me think that the work with *Marchantia* could be of interest to a wider scientific community. His specific contributions are noted in the last chapter of the thesis.

Professor Takayuki Kochi and Dr. Kmizune Ishizaki from Kyoto University have provided valuable information as well as valuable plasmids for the establishment of *Marchantia* as an experimental system in the lab.

John Alvarez has also kindly helped me develop some basic skills and knowledge in molecular and developmental biology, as well as great techniques to throw ice in sneaky ways to lab members, and the introduction to cat-video culture.

Scanning Electron Microscopy was learnt with the friendly assistance of Joan Clark from Monash Micro Imaging.

Many of my previous and current lab mates have kept an enjoyable and sweet atmosphere in the lab, especially with their "delightful" taste in music. Their quiet office work was mostly appreciated when I was desperately trying to finish this thesis. I thank their everyday scientific collaboration and help in troubleshooting, the lunch moments in the system's garderns, the usual breaks to complain about life, the clayton road Indonesian food times, and their alcohol excesses out there in the real world. Most of us, just a bunch of young guys from far away lands trying to survive the phD/science life. In chronological order, as far as I remember: The moss master Keiko Sakakibara, Dyani Lewis, Pia Sappl, Chris Zalewski, Karen Yip, Lukas Brand, Yuval Eshed (all these guys are ancestral branches of the Bowman lab), Tom Dierschke, Chihiro Furumizu, Yuki Hirakawa, Joseph Ryan, Tezz Quon and Moritz Rövekamp.

David Smyth and the Smyth lab have provided useful plasmids such as 3XVENUSN7, as well as helpful discussions, research advice and the opportunity to get involved in a teaching experience of plant development in the School of Biological Sciences.

I thank the people at the School of Biology and from Melbs whom I have shared true friendship, it would be unfair to try to list them all.
Alex Rijavec and all my housemates and close friends living in Melbourne kept me grounded in a the real world, and became something very close to a family.
Loud Music sessions and Running were particularly useful to write this thesis. This document was written in a combination of places: 442 Abbotsford Street North Melbourne, 30 Greeves Street St Kilda, State Library of Victoria, University of Melbourne Library, Hargrave-Andrew Library at Monash University, and room 247 phD student office of the Bowman Lab.

This phD program was funded by the National Science Council of Mexico (Consejo Nacional de Ciencia y Tecnología), John Bowman, and in the last stages by the School of Biological Sciences of Monash University, I thank them all for that. Fionna Hibbert helped organizing a big file of paperwork for many Monash related issues.

Last but not least, a mi familia, Samuel, Silvia, Ruben y Pichin, que siempre me dieron su apoyo para estudiar ciencia y su cariño incondicional. Han sido largos años lejos de ustedes pero los tengo siempre mi corazón. Gracias por visitarme y pasearse conmigo por aqui!

Any limitations on the quality of this work are my sole responsibility.

Eduardo Flores Sandoval

ABSTRACT

In the liverwort *Marchantia polymorpha,* the phytohormone auxin controls the development of specific organs in different developmental stages. Pharmacological experiments show that in the haploid generation young gemmalings develop rhizoids in response to auxin, while in a mature thallus, auxin promotes the growth of gemmae cup rims, controls the spacing of gemmae cups and affects the formation of air chambers. A phylogenetic evaluation of genes involved in auxin biology across land plants indicates that most major families involved in auxin synthesis, transport, conjugation and response exist in *Marchantia* as single representatives, possibly resembling the genome of the common ancestor of all land plants. Auxin insensitive plants were created by overexpression of a chimeric protein consisting of the endogenous *TOPLESS* (*MpTPL*) co-repressor fused to protein-protein interaction domains 3 and 4 (D34) encoded by AUX/IAA or ARF genes of 6 *Marchantia* loci. Overexpression of these fusion proteins creates extremely small plants that lack a clear establishment of dorsi-ventral polarity and exhibit an overall disorganized patterning. Only the D34 of *MpARF3* did not produce aberrant patterning phenotypes, suggesting that the MpARF3 protein has low interaction affinities with MpARF1, MpARF2 and MpAUX/IAA. In *Marchantia*, TPL likely acts as a co-repressor in the auxin signaling pathway, as ectopic expression of *TOPLESS* inhibits the formation of gemma cups, while a dominant negative version of *TPL* (TPL^{N176H}) promotes meristem production (bifurcation), as well as abnormal gemmae cups in the thallus. To begin the dissection of specific roles of ARFs, we focus on *MpARF3*, a transcription factor orthologous to class C *ARFs* (*ARF10/16/17*) of *Arabidopsis* and which is regulated by *microRNA160*. Overexpression of the endogenous *MpmiR160* greatly inhibits meristem bifurcation and produces gemmae-less plants. Conversely, expression of miR-resistant *MpARF3* transforms the thallus into juvenile undifferentiated tissue, and when expressed at only low doses increases bifurcation rates of the thallus. Thus, *miR160*-regulation of class C *ARFs* existed in the common ancestor of all land plants and it is plausible that the ancestral role of class C ARFs was the promotion undifferentiated developmental stages, as this is a shared character with *Arabidopsis*.

Taken together, my experiments demonstrate a crucial role of auxin as a morphogenetic trigger across all land plants. In addition, I assign specific roles for auxin in nearly all life stages and tissues of the gametophyte of *Marchantia*, a member of the basal most lineage of land plants.

TABLE OF CONTENTS

GENERAL INTRODUCTION

Land plants have complex life cycles with an alternation of generations, in which both the haploid and diploid generations are multicellular. The haploid generation, or gametophyte, produces haploid gametes that fuse and produce a diploid generation. The diploid generation, or sporophyte, produces haploid spores via meiosis. Compared to charophycean (freshwater) algal relatives, key innovations of land plants involve mitotic divisions that produce a multicellular sporophyte before undergoing meiosis, meristematic tissue in a diploid generation and the capacity to pattern three-dimensional structures from meristems in both the diploid and haploid generations (Bowman et al., 2007). While land plants form a monophyletic clade, the early diverging lineages within land plants reside in a paraphyletic grade in which Liverworts are sister to all land plants, followed by Mosses and Hornworts. These three lineages have a haploid dominant life cycle where the gametophyte is free living and compose the paraphyletic group called the Bryophytes. In comparison, the Tracheophytes, or plants with vascular tissue, have a diploid dominant life cycle and are comprised of the Lycophytes, Ferns, and Seed Plants (Gymnosperms and Angiosperms). A comparative approach using the newly available genomes of species of almost each lineage of land plants, combined with the tools of developmental genetics and molecular biology may help show how the diversity of land plants evolved by co-opting pre-existing developmental pathways to pattern new morphologies (Bowman et al., 2007).

Genetic and physiological studies have revealed that in angiosperms, the phytohormone auxin or indole-3-acetic acid (IAA), controls central aspects of plant development in both haplod and diploid generations (Walker and Estelle, 1998; Woodward and Bartel, 2005; Guilfoyle and Hagen, 2007; Vanneste and Friml, 2009; Finet and Jaillais, 2012). Auxin was first discovered in the 1930s and named after the greek term *auxein*, which means “to grow or to increase”. Auxin triggers growth and tissue differentiation in places where it accumulates, perhaps acting as a morphogenetic trigger (Benkova et al., 2009). In the model flowering plant species *Arabidopsis thaliana,* a balance between auxin biosynthesis, transport and conjugation regulate the spatial distribution of auxin, leading to activation of

transcriptional responses that control a variety of morphological and physiological processes. In the sporophytic generation of *Arabidopsis thaliana*, an auxin maximum provides a cue for the establishment of the apical-basal axes of the young embryo and the establishment of the root meristem (Hardtke and Berleth, 1998; Hamann et al., 1999; Friml et al., 2003). In mature sporophytes, auxin maxima provide positional cues for the emergence of new organs such as leaves, floral organs, and the establishment of vascular tissue, lateral roots and root hairs (Reinhardt et al., 2000; Mattsson et al., 2003). Auxin also regulates graviotropic and phototropic responses and the dormancy of lateral buds (Hobbie and Estelle, 1994; Liscum and Briggs, 1996; Chen et al., 1998; Muller et al., 1998; Esmon et al., 2006). The phenotypes of loss-of-function alleles in genes encoding auxin perception, biosynthesis, transport and response machinery converge into a meristem-less embryo that fails to establish the basic apical-basal polarity and patterning (Hardtke et al., 2004; Dharmasiri et al., 2005b; Cheng et al., 2007; Petrasek and Friml, 2009). In the gametophytic generation, auxin controls the identity and disposition of cells composing the small female gametophyte, although in this case only auxin biosynthesis may create differential distribution of the hormone, or alternatively auxin is transported into the gametophyte from the sporophyte (Pagnussat et al., 2009).

It has been speculated that an increase in complexity of the auxin genetic toolkit (metabolism, synthesis, transport and signaling genes) is correlated with an increased complexity in land plant architecture, from bryophytes to flowering plants (Cooke et al., 2002) .

The present thesis uses the liverwort *Marchantia polymorpha* to understand the developmental role of auxin in a member of the basal most lineage of land plants. *Marchantia* is emerging as a new model system for plant genetics, possibly bearing the most simplified auxin genetic toolkit known for embryophytes. I use a pharmacological and genetic approach to study the morphogenetic effects of auxin transcriptional responses, specifically in the haploid generation of *Marchantia* and discuss my results in the context of evolutionary biology.

The first chapter of this thesis is a literature review explaining the discovery of the auxin signaling pathway in flowering plants, focusing on the role of *Auxin Response Factors* (*ARFs*) in controlling the transcriptional output of auxin perception. It also briefly explores genetic mechanisms of auxin synthesis, transport and conjugation.

Chapter two is a revision on forward and reverse genetics that allowed to understand the importance of *ARFs* in patterning *Arabidopsis* development, and how these discoveries converged with their cloning through biochemical methods (seen in chapter 1).

Chapter three deals with a phylogenetic classification of *ARFs* and several other members of the auxin genetic toolkit of embryophytes. It presents evolutionary scenarios to understand what was the ancestral auxin genetic toolkit of land plants as well as evolutionary scenarios for the origin of *ARFs*.

Chapter four is a morphological description of the model system of this thesis, *Marchantia polymorpha*, and provides a literature review on developmental studies explaining transitions from a spore into a mature thallus, focusing in the haploid generation.

Chapter five deals with the developmental effects of exogenous auxin and auxin inhibitors in the haploid generation of development, and mixes observations made in this work with previous reports in the literature.

Chapter six deals with the use of the endogenous *TOPLESS* corepressor of *Marchantia* to disrupt overall auxin response and the developmental effects associated with disruption of multiple sets of *ARFs*.

Chapter seven reports on the role of *MpARF3* in patterning development of *Marchantia* and its putative role as promoter of undifferentiated cells states and how its activity may be independent of the auxin signaling pathway.

CHAPTER 1

Functional description of auxin signaling in angiosperm model organisms

Because the main experimental work of this thesis focuses on auxin transcriptional responses, I'll explain the current state of knowledge of the molecular mechanisms of auxin signaling and how they were discovered in *Arabidopsis thaliana*. It is necessary, however, to start with a brief introduction of how plants control auxin distribution throughout development before explaining the auxin signaling pathway.

General mechanisms of auxin distribution.

*Auxin biosynthesis***.** There are two main pathways of auxin biosynthesis described for angiosperms, the tryptophan (Trp) dependent and the tryptophan independent pathways (Mashiguchi et al., 2011; Finet and Jaillais, 2012). The genetic basis for the tryptophan independent pathway has not been clearly elucidated, although mutations in tryptophan biosynthesis enzymes *trp2-1* and *trp3-1* still posses free IAA compared to the wild type, suggesting that plants create auxin in a tryptophan independent fashion (Ouyang et al., 2000; Finet and Jaillais, 2012).

While several pathways to convert Trp to auxin may exist, there are only two clearly described so far in detail and they are named after the intermediaries between Trp and IAA. First, the indole-3-acetaldoxime (IAOx) pathway, which is Brassicales specific, is carried out by *CYP79B2* and *CYP79B3*, encoding cytochrome P450 monooxygenases (Zhao et al., 2002). The second is the indole-3-pyruvate (IPA) pathway, whose machinery seems to be conserved in all land plants. A recent study has placed two types of enzymes, one encoded by *TRYPTOPHAN AMINOTRANSFERASE OF ARABIDOPSIS* (*TAA*) genes and the second encoded by *YUCCA* (*YUC*) genes as members of a single pathway (Mashiguchi et al., 2011). Enzymes encoded by *TAA* and its paralogues catalyze the transition from Trp to IPA and enzymes encoded by the *YUCCA* paralogues catalyze the rate-limiting step of IPA conversion into IAA (Mashiguchi et al., 2011). In *Arabidopsis* there are 3 TAA paralogues (*TAA1, TAR1* and *TAR2*) and 11 YUC paralogues (*YUC1-11*). Multiple mutants of the *TAA* paralogues, such as the *wei8 tar2* double mutant, are severely

impaired in embryonic and postembryonic development (Stepanova et al., 2008). *YUC1* overexpression under control of the 'constitutive' cauliflower mosaic virus 35S promoter (*pCaMV35S*) exhibit increased levels of free IAA as well as phenotypes characteristic of those observed when plants are grown in the presence of high levels of exogenous auxin, such as elongated hypocotyls, epinastic leaves, and enhanced apical dominance, and these phenotypes depend on *TAA1* activity (Zhao et al., 2001; Stepanova et al., 2011). Conversely, *yuc1 yuc4 yuc10 yuc11* quadruple mutants lack a hypocotyl, a root meristem, floral organs and resemble auxin transport, response and perception mutants described in the following sections (Cheng et al., 2007). *YUC1* expression, as characterized by *in situ* hybridization, is in the apical region of the globular stage embryo and is later restricted to the apical meristem and cotyledons in the heart stage, and subsequently exclusively in the apical meristem in mature embryos. *YUC4* exhibits a similar expression pattern, except that it is also expressed in the apical regions of cotyledons in the mature embryo (Cheng et al., 2007). Simultaneous expression of *TAA1* and *YUC1* by pCaMV35S increased formation of root hairs, adventitious and lateral roots compared to single *YUC1* overexpression (Mashiguchi et al., 2011).

Polar auxin transport. Three main protein families control auxin transport: AUX/LAX influx carriers, PIN efflux carriers and ABCB efflux carriers (Petrasek and Friml, 2009). The importance of auxin transport for *Arabidopsis* development was identified using forward genetic screens.

Influx carriers were initially discovered by characterizing an agravitropic *auxin resistant 1* mutant (*aux1*), which was resistant to exogenous application of a synthetic auxin 2,4-D (dichlorophenoxyactetic acid). *aux1* was the founding member of a family of 4 *Arabidopsis* genes (*AUX1*, *LAX1*, *LAX2* and *LAX3*) encoding transmembrane proteins similar to aminoacid permeases, and are involved in root graviotropism, lateral root formation, hypocotyl phototropism, root hair development (*AUX1*) and phyllotaxis (*AUX1* and *LAX1-3*) (Bennett et al., 1996; Petrasek and Friml, 2009).

Efflux carriers were also identified from the study of several *Arabidopsis* mutants: *pin1* is a mutant with defects in organ initiation (a pin-like organ is formed instead of a flower) and phyllotaxy (Okada et al., 1991), defects that can be phenocopied by pharmacological inhibition of auxin efflux using NPA (1-

naphthylphthalamic acid) (Okada et al., 1991). Defects of *pin1* mutants can be rescued by microapplication of endogenous auxin (IAA) to pin-formed apices of *pin1* plants (Reinhardt et al., 2000). The *PIN1* gene encodes a protein with transmembrane regions separated by a hydrophilic loop (Galweiler et al., 1998). Several independently identified mutants, *agraviotropic 1* (*agr1*), *wavy roots 6* (*wav6*) and *ethylene insensitive root 1* (*eir1*), are mutant alleles of another *PIN* family member, *PIN2*, in *Arabidopsis* (Chen et al., 1998; Luschnig et al., 1998; Muller et al., 1998; Utsuno et al., 1998). The *PIN* gene family in *Arabidopsis* consists of 8 genes (Vieten et al., 2007), classified in two functional subgroups. A first subgroup is composed of *PIN1*, *PIN2*, *PIN3*, *PIN4* and *PIN7*, which encode proteins that are localized in the plasma membrane and act as efflux carriers between cells. They are involved in a variety of developmental processes including embryogenesis, lateral organ formation, vascular development, phylotaxis, vein formation, shoot and root graviotropism and phototropism.

Single *pin* mutants can complete embryogenesis, but *pin1 pin3 pin4 pin7* quadruple mutants are defective in the establishment of apical-basal polarity, resembling quadruple *yuc1 yuc4 yuc10 yuc11* mutants (Benkova et al., 2003; Friml et al., 2003). However, neither *aux1/lax* nor *abcb* multiple mutants display such strong embryonic phenotypes suggesting a major role for PINs in patterning the embryo As reviewed in Petrasek and Friml, 2009: In the 1 cell embryo, PIN7 pumps auxin out of the upper side of suspensor cells, resulting in auxin accumulation in the apical cell. PIN1 is inferred to distribute auxin evenly throughout the apical embryonic region through the octant stage. Embryonic apical basal polarity is established in the early globular stages, when coordinated PIN1 and PIN7 polarity rearrangements create a downwards flow of auxin that results in auxin accumulation in the hypophysis, the uppermost cell of the suspensor and precursor of the root meristem. In the heart stage embryo, additional auxin maxima are inferred to be formed at the positions of the initiating cotyledons mainly by the action of PIN1 and ABCB19: *pin1 abcb1* and *pin1 abcb1 abcb19* mutants show fused cotyledons compared to single *pin1* and *abcb1 abcb19* double mutants (Friml et al., 2003; Dhonukshe et al., 2007; Petrasek and Friml, 2009) (Mravec et al., 2008).

A second functional group of PIN proteins, comprised of PIN5, PIN6 and PIN8, has a reduced middle hydrophilic loop and potentially regulates auxin exchange

between the endoplasmic reticulum (ER) and the cytosol, thus regulating intracellular auxin homeostasis (Mravec et al., 2009; Ding et al., 2012).

ABCB proteins are orthologues of the mammalian ATP-binding cassette subfamily B-type transporters similar to the multidrug resistance/phosphoglycoprotein family. They have been studied less thoroughly than PIN proteins, but some reported roles include embryogenesis, lateral root formation, root hair development root, hypocotyl graviotropism, hypocotyl phototropism and leaf shape (Noh et al., 2001). Some ABCB proteins in plants have binding affinity to NPA (Murphy et al., 2002).

A recently described protein family of *PIN-LIKE* proteins (*PILS*) also regulates intracellular auxin accumulation at the ER, such family resembles PIN5 like proteins in having a single central hydrophilic loop flanked by 5 transmembrane domains on each side but only show 10-18% amino acid similarity with PIN proteins. PILS are conserved throughout land plants and are even found in unicellular algae *Chlamydomonas reinhardtii* and *Ostreococcus tauri*, taxa that lack PIN proteins, suggesting that *PIN* genes may have evolved from *PILS*-like ancestors (Barbez et al., 2012).

Auxin conjugation. Maintenance of homeostatic levels of intracellular auxin in angiosperms also depends on enzymatic reactions that store auxin as inactive conjugates, in which IAA is linked to amino acids, sugars or peptides (Woodward and Bartel, 2005; Finet and Jaillais, 2012). GH3 family proteins are amido synthetases that are classified in two functional types: Group I is involved in jasmonic acid conjugation and group II is involved in auxin conjugation by linking IAA to sugars, or amino acids (Sztein et al., 2000; Staswick et al., 2005; Terol et al., 2006). Group II GH3s have been identified as early auxin response genes and rapidly regulate the effects of exogenous auxin in a negative feedback loop (Hagen and Guilfoyle, 1985). In *Arabidopsis* members include *GH3.2* (*YDK*), *GH3.5*, *GH3.6* (*DFL1*) and *GH3.17*, all able to catalyze IAA conjugation to amino acids (Staswick et al., 2005). Overexpression of *GH3.2* (*ydk1-D allele)* and *GH3.6 (dfl1-D allele)* results in plants with reduced lateral roots and short hypocotyls and dwarf phenotypes in adult plants, phenotypes observed in plants with deficient auxin levels (Nakazawa et al., 2001; Takase et al., 2003; Takase et al., 2004). Additional components of the conjugation machinery include *IRL1/ILL* amidohydrolases, which release free IAA from conjugates (Woodward and Bartel, 2005). Compared to seed plants, where up to 90%

of total IAA is stored as conjugates, liverworts have up to 30% of the total IAA levels as free IAA, suggesting a less elaborate way of conjugating auxin (Sztein et al., 2000). Liverworts have slower rates of IAA conjugation and it's been proposed that conjugates in liverworts cannot be reversed back to free IAA (Sztein et al., 1999). Mosses have a more sophisticated machinery to conjugate and hydrolyze conjugates back to free IAA levels. In the moss *P. patens*, double knockouts of *PpGH3*-1 and *PpGH3*-2 result in growth inhibition (excessive levels of free IAA are inhibitory), high levels of free IAA and almost no IAA-amide conjugates (Ludwig-Muller et al., 2009b). Interestingly, the two PpGH3 proteins can form amino acid conjugates with both auxin and jasmonic acid, although *PpGH3*-2 has more affinity with auxin than *PpGH3*-1 (Ludwig-Muller et al., 2009b).

To summarize, the levels of free auxin in a cell depend upon the rate of biosynthesis, polar transport, inactivation via conjugation to amino acids or sugars, and finally on hydrolysis of inactive conjugates to revert them to free IAA. Specific gene families with multiple paralogues control all of these processes in angiosperms. Free IAA levels then determine the transcriptional response described in the next section.

The Auxin signaling pathway.

Discovery of Auxin induced genes.

The first attempts to unravel auxin signaling, from perception to an eventual genetic response used two main strategies (Liu et al., 1994; Abel and Theologis, 1996). First, forward genetic screens were used to identify auxin resistant and auxin transport inhibitor resistant mutants with defects in auxin physiology. From these screens it was possible to positionally clone genes such as *TIR1 (auxin transport inhibitor response 1)*, which encodes and F-box protein that is the main auxin receptor in *Arabidopsis* (Ruegger et al., 1998) and AXR1 which is a ubiquitin-activating enzyme (E1), the first enzyme in the ubiquitin conjugation pathway (Leyser et al., 1993). A second strategy involved the cloning of genes rapidly induced by auxin, that is, genes transcribed before the phenotypic effects of auxin application are observed. Such screens led to the identification of the *cis*-regulatory elements

conferring auxin inducibility, and eventually the cloning of the response factors binding to such *cis*-elements and elucidation of the signaling pathway *in reverse*.

The first auxin-induced genes to be cloned and sequenced were named *AUX22* and *AUX28,* identified from cDNA libraries from auxin treated soybean hypocotyls (Ainley et al., 1988). In parallel, screens in pea hypocotyls identified additional auxin induced genes, named *Ps-IAA4/5* and *Ps-IAA6* (Theologis et al., 1985). Because both *AUX* and *PS-IAA* genes had homology with each other, they were the founders of a large gene family now known as the *AUX/IAAs*. *AUX/IAAs* are rapidly transcribed 5 to 60 minutes after auxin application and posses four conserved domains (I to IV) shared among most members of the family. *AUX/IAAs* were later cloned in *Arabidopsis*, which has 29 paralogues (Abel et al., 1995).

Other screens of early auxin-inducible genes, identified not only members of the *AUX/IAA* superfamily but also several unrelated classes of genes: *GH2/4* (Hagen et al., 1988), *GH3* (Hagen et al., 1991) and *SMALL AUXIN UP RNA* (*SAUR*) genes (McClure et al., 1989). The functions of proteins encoded by the *GH3* genes was described in the previous section, but the functions of the *SAUR* and *GH2/4* genes remain largely unknown. The sequences of these transcripts showed that *AUX/IAAs*, *SAURs* and *GH3s* did not have a DNA binding domain and, thus, the transcription factors responsible for creating a proper auxin signaling output were yet to be found. Furthermore, it was not known whether *AUX/IAAs* acted to promote or repress the auxin signaling pathway.

Discovery of Auxin Response Elements (AuxRE)

The identification of *cis*-regulatory regions associated with auxin-inducible genes was found by promoter deletion analysis of *PS-IAA4/5.* A relatively short promoter fragment was able to induce reporter gene transcription in response to auxin in pea and tobacco cells. This fragment was named an Auxin Response Element (AuxRE) and was divided into 2 functional domains A and B (Ballas et al., 1993). Domain A is qualitative auxin responsive element whereas domain B acts as a quantitative enhancer. Domain A has the tandem sequence 5'-**TGTCCC**(N_6)**TGTCAC**(N_9)**GAGACA**-3'. Domain B had the core sequence 5'-CACATGCTCATGTTTC-3' (Oeller et al., 1993; Ballas et al., 1995). A similar study dissecting a soybean SAUR promoter showed that a minimal 30bp region (NDE) 5'-**TGTCTC**NNNNNNGGTCCAT-3'was sufficient to confer auxin inducibility (Li et

al., 1994). Additional promoter analysis of the soybean GH3 gene found 2 domains of 11 bp (D1) 5'-CCTCG**TGTCTC**-3' and 32 bp (D4) that are auxin inducible and share similar sequences (Liu et al., 1994). Thus, a consensus AuxRE has the sequence 5'-**TGTCTC**-3', although nucleotide 5 of the consensus sequence is variable in the *PS-IAA4/5* AuxRE. The consensus sequence is shared amongst unrelated auxin inducible genes and is often found in some sort of repeat. In the soybean GH3 promoter, it was shown that domains D1 and D4 are composite AuxREs as they have an adjacent or overlapping upstream constitutive element that drives constitutive expression on its own if fused to a minimal promoter, but in AuxREs they enhance expression only in the presence of auxin. The first artificial auxin inducible promoters were designed by fusing an heterologous GAL4 minimal element to the conserved AuxRE core sequence (Ulmasov et al., 1995).

Discovery of Auxin Response Factors (ARFs)

AuxREs share some similarity with glucocorticoid response elements (GREs) in animal cells. GREs also have adjacent overlapping DNA binding sites (constitutive elements) and the preferred binding site for the glucocorticoid receptor is a palindrome (Ulmasov et al., 1997a). Following this idea, Ulmasov *et al* (1997a) created another artificial auxin responsive promoter P3(4x) consisting of 4 palindromic tandem copies of inverted repeats of the core 5'-**TGTCTC**-3' element (**GAGACA**N_3**TGTCTC**ccaaagg)x4 that activates GUS in response to auxin in transfected carrot protoplasts. This construct was used as bait for a yeast-one hybrid experiment screening for *Arabidopsis thaliana* cDNAs encoding proteins that could bind the P3(4x) sequence. Four members of a new family of transcription factors, named Auxin Response Factors (ARFs), were identified in that initial study (ARF1, ARF3, IAA24/ARF5 and ARF2/ARF1-BP) and a total of 23 ARFs are now known to exist in *Arabidopsis* (Guilfoyle and Hagen, 2007).

Protein sequences of ARFs have 2 domains homologous to independent protein families. The NH_2-terminal end of ARF proteins encodes a B3 DNA binding domain, similar to other transcription factors such as VIP1/ABI3 that are not involved in auxin signaling and rather specifically bind to *cis*-elements in ABA (Abscisic acid) responsive promoters (McCarty et al., 1991). The COOH- terminal end of ARF proteins are homologous to domains III and IV of AUX/IAAs, with the exception of ARF3, 13 and 17 that lack both domains (Guilfoyle and Hagen, 2007). Yeast two-

hybrid experiments were used to show that domains III and IV allow protein-protein interaction and the formation of ARF-ARF homodimers, ARF-ARF heterodimers, ARF-AUX/IAA heterodimers and AUX/IAA homodimers (Kim et al., 1997; Ulmasov et al., 1997a; Ulmasov et al., 1997b). The middle region of ARF proteins, carboxyl to the B3 domain, contains putative activator or repressor domains (ADs or RDs, respectively) depending on amino acid compositions of specific ARF proteins, although both are rich in serine (S).

Co-transfection experiments in carrot protoplast measuring the capacity of plasmids encoding ARF effectors to activate GUS reporter driven by GH3 promoter or the P3(4X) promoter showed that ARF ADs are rich in glutamine (Q) residues (for example ARF6) while ARF RDs are enriched in proline (P) residues (for example ARF1) (Ulmasov et al., 1999b). Fusions of several ARF putative ADs or RDs with yeast GAL4 DNA binding domain were used test their capacity to activate a GUS reporter driven by GAL4 DNA binding sites in carrot protoplasts confirming this result (Tiwari et al., 2003). Out of the 23 *Arabidopsis* ARFs only ARF5, 6, 7, 8 and 19 were found to be activators while the remainder act as repressors (Ulmasov et al., 1999b; Guilfoyle and Hagen, 2001, 2007). The ARF B3 domain functions independently of other domains, as it does not play a role in activation, repression or dimerization (Ulmasov et al., 1999b). Although Domains III and IV provide auxin responsiveness to reporter assays (Guilfoyle and Hagen, 2001) they can also influence DNA binding efficiency because ARF binding to AuxREs is stabilized when ARFs dimerize with each other *in vitro* (Ulmasov et al., 1999a).

ARF proteins can bind to inverted (5'-**GAGACA**N**TGTCTC**-3') or everted repeats (5'-**TGTCTC**N**GAGACA**-3') of AuxREs with the optimal spacing between repeats for ARF1 binding being 7 to 8 nucleotides (Ulmasov et al., 1997a). A single P3 promoter palindrome is insufficient for ARF1 binding, while 2 and 4 repeats create one and two ARF1 complexes respectively. A single everted repeat of the natural *PS-IAA4/5* promoter created a single ARF1 complex. Gel-shift assays showed that only mutations in the first 4 nucleotides of the AuxRE compromise ARF binding and auxin responsiveness in ARF1, ARF2, ARF4, ARF5, ARF6 and ARF8 (Ulmasov et al., 1997a, 1999a). Therefore sequences such as 5'-**TGTCCC**-3' and 5'-**TGTCAC**-3' such as those found in the promoter of *Ps-IAA4/5* also act as putative AuxREs (Ulmasov et al., 1997a). Divergent spatio-temporal patterns of gene expression might avoid competition of ARF proteins for similar AuxREs, or if ARFs form a complex

with other transcription factors, such additional partners could also provide binding specificity to promoters of target genes (Ulmasov et al., 1999a).

Development of DR5 auxin response reporter.

Random mutagenesis of AuxREs were used to find artificial auxin inducible promoters that could be used to indicate *ARF* activity maxima. The minimal 11bp GH3 AuxRE element (D1) was used to find that substitutions outside the core 5'-**TGTCTC**-3' element could either increase (DR5) or decrease (D1-6) auxin responsiveness in transient assays in carrot protoplasts and transgenic *Arabidopsis* seedlings (Table 1) (Ulmasov et al., 1997b).

Element	Sequence	Relative GUS activity
D1(8x)	5′-CCTCG**TGTCTC**-3′	1250
D1-5(8x)	5′-CCTCG**TGgaTC**-3′	500
D1-6(8x)	5′-aaaaa**TGTCTC**-3′	0
DR5 (8x)	5′-CCTtt**TGTCTC**-3′	2500
DR5m3(8x)	5′-CCTtt**TGgCTC**-3′	0
DR5m5(8x)	5′-CCTtt**TGTCcC**-3′	2000

Table 1. Internal mutations in the 5'-**TGTCTC**-3' change the auxin responsiveness of AuxREs. Some external mutations (D1-6) decrease auxin responsiveness but others (DR5) increase two-fold auxin responsiveness compared to the WT D1 element of the GH3 promoter. GUS activity is shown as approximate values in response to auxin (Ulmasov et al., 1997b).

DR5 is composed of 8 simple tandem repeats (no inverted or everted repeats) and has less basal activity than 8 tandem repeats of the natural GH3 D1 element, as well as greater auxin inducibility than either the D1(8x) or P3(4x) palindromic artificial promoters. It was found that six copies of DR5 has almost an equal inducibility as DR5(8x) in carrot protoplast transient assays. Consistent with previous results only mutations in the 5th nucleotide of the core 5'-**TGTCTC**-3' element did not affect auxin inducibility. Gel shift assays showed that ARF1 bound in vitro to DR5(8X), although with less efficiency compared to the binding of ARF1 to the P3(4x) artificial promoter, suggesting that ARFs prefer everted repeats as binding sites (Ulmasov et al., 1997b).

DR5 has been used as a reporter for auxin response, however, it should be kept in mind that it only measures the relative output of auxin signaling through ARFs present in a cell or tissue, which may be a combination of both positive and

negatively acting ARFs. DR5 has been used in several developmental studies in angiosperms trying to tie the role of developmental modifications with auxin signaling (Sabatini et al., 1999). In the moss *Physcomitrella patens* DR5:GUS shows limited staining unless exogenous auxin is applied. Furthermore, GUS expression is detectable only after 3 days of auxin application when driven by the DR5 promoter (Bierfreund et al., 2003). In the liverwort *Marchantia polymorpha* DR5 failed to drive GUS reporter expression after exogenous auxin application (Ishizaki et al., 2012).

AUX/IAAs act as short-lived auxin signalling repressors.

A common property of inducible systems is that activation of transcriptional responses is accompanied by the production of a repressor that eventually deactivates and resets the hormonal response (Abel and Theologis, 1996). Although *AUX/IAAs* do not bind to AuxREs *in vitro*, overexpression of several AUX/IAAs in carrot cells (*Aux22, Ps-IAA4/5 and Ps-IAA6*) disrupts auxin inducibility of DR5, P3(4x) and D1 artificial promoters driving reporter genes, suggesting they are the early induced repressors that reset the auxin signaling pathway. Because yeast two hybrid experiments showed that AUX/IAAs and ARFs form heterodimers via interactions with domains III and IV, it was suggested that AUX/IAAs form repressor complexes when attached to ARFs that inhibit their own production in a negative feedback loop (Ulmasov et al., 1997b). This opened the question of how preexisting AUX/IAAs proteins detach from ARFs to allow ARF transcriptional activity in response to auxin.

Screens for *Arabidopsis* mutants that failed to respond exogenous auxin identified dominant and semi-dominant mutations in nine AUX/IAA genes: *IAA3/shy2-2, IAA6/shy1-1, IAA7/axr2-1, IAA12/Bdl, IAA14/slr1-1, IAA17/axe3-1, IAA18/iaa18-1, IAA19/msg2, IAA28/iaa28-1* (Liscum and Reed, 2002). All of these mutants were shown to have a single amino acid substitution in domain II in the conserved motif GWPPV (Leyser et al., 1996; Rouse et al., 1998). The use of second site mutagenesis screens, found a series of revertants that restore mutants to a wild-type phenotype, and involve a disruption of conserved domains III and IV, which compromise the dimerization capacity of AUX/IAAs with ARFs or result in premature stop codons, suggesting that the original dominant alleles are gain-of-function mutations (Rouse et al., 1998; Tian and Reed, 1999; Nagpal et al., 2000; Ouellet et al., 2001; Tiwari et al., 2001). Using fusions of domain II of AUX/IAAs with luciferase demonstrated that domain II acts as an auxin-responsive degradation

signal, and using versions of domain II that mimic dominant mutations eliminated auxin responsiveness (Worley et al., 2000). Further biochemical analyses showed that dominant mutant alleles of AXR3-1/IAA17, AXR2-1/IAA7 and SHY2-2/IAA3 proteins have an increased stability and steady-state levels (Ouellet et al., 2001). This suggested that AUX/IAAs detach from ARFs via protein degradation.

As described previously, the role of AUX/IAA proteins as repressors of auxin signaling is supported by the fact that at least sixteen AUX/IAA proteins decrease the transcription of reporter lines driven by AuxREs such as P3(4x):GUS in carrot protoplast assays (Tiwari et al., 2001). However, there are exceptions. For example, an auxin responsive construct SAUR pro:GUS exhibited an increased expression pattern in recessive *axr3/iaa17-1* background, suggesting that this particular type of AUX/IAA does not act as a repressor of the auxin signaling pathway (Leyser et al., 1996). It is not known whether this achieved by AXR3/IAA17 sequestering other AUX/IAAs, or by interacting with repressor ARF proteins, allowing activator ARF proteins to transcribe genes without competition.

AUX/IAAs are degraded by auxin receptor TIR1 in the presence of auxin.

Mutant alleles of *TRANSPORT INHIBITOR RESISTANT1* (*TIR1*) were initially isolated by screening for mutations conferring resistance to the growth-inhibiting properties of auxin transport inhibitors naphthylphathalamic acid (NPA) and 2-carboxyphenyl-3-phenylpropane-1,2-dione (CPD) (Ruegger et al., 1997). *TIR1* encodes an F-box protein with leucine rich repeats (Ruegger et al., 1998). TIR1 interacts with the cullin AtCUL1 and SKP-1 like proteins (ASK1 and ASK2) to form the SCF^{TIR1} (Skip/Cullin/F-box) E3 ubiquitin ligase complex that confers substrate specificity to the ubiquitin pathway (Gray et al., 1999). TIR1 belongs to a family of 6 closely related F-box proteins named AFBs (Auxin signaling F-box) (Dharmasiri et al., 2005b). In *tir1 afb2 afb3* triple mutants the expression of DR5:GFP is severely curtailed with or without auxin induction and a delayed the degradation of AXR/IAA17 is observed (Dharmasiri et al., 2005b). A *tir1-1 afb1-1 afb2-1 afb3-1* quadruple mutant shows a range of phenotypes with the most severe lacking a root and hypocotyl and having a single cotyledon, with no elongation in response to light (Dharmasiri et al., 2005b). Proteasome inhibitors, as well as *tir-1* mutants, were shown to increase the stability of reporter constructs overexpressing *AXR2/IAA7* and *AXR3/IAA17* fused to GUS (pCaMV35S:AXR2/3:GUS), while the application of

auxin reduced the levels of these translational fusions *(Gray et al., 2001)*. This suggested that the targets of the SCF^{TIR1} E3 ubiquitin ligase are AUX/IAAs. Protein immunoprecipitation was used to show that AXR2/IAA7 and AXR3/IAA17 interact with the SCF^{TIR1} complex while single amino acid substitutions in proteins encoded by *axr2-1* and *axr3-1* disrupted the interaction with SCF^{TIR1}. A small peptide consisting only of Domain II of AXR2 was sufficient to form a complex with SCF^{TIR1} and applied auxin enhanced the interaction between AUX/IAAs and SCF^{TIR1} (Gray et al., 2001). It was later shown that auxin acts as a molecular glue that enhances the interaction between TIR1 and AUX/IAAs and does not induce conformational changes in the SCF complex (Tan et al., 2007).

At the protein level, F-box proteins confer target specificity to the SCF complex, the amino-terminus of TIR1 mediates interaction with SKP1 and the carboxyl-terminal end mediates protein-protein interaction to select the targets. The Cullin and RBX1 protein catalyzes the transfer of activated ubiquitin to the target protein (Moon et al., 2004). Thus, TIR1 and its closely related paralogues act as auxin receptors in *Arabidopsis*, with the ligand auxin promoting the interaction between $SCF^{TIR1}$and AUX/IAAs. Expression of TIR1 in a heterologous system –using *Xenopus laevis* embryos- was sufficient to detect auxin-mediated interaction between TIR1 and AUX/IAA proteins (Dharmasiri et al., 2005a; Kepinski and Leyser, 2005).

A recent study shows that efficient auxin binding requires the assembly of a co-receptor complex composed of an AUX/IAA protein bound to TIR1. Because there are 29 AUX/IAAs and 6 TIR/AFBs, different co-receptor complexes combinations show different auxin binding affinities (Villalobos et al., 2012).

Other proteins that bind to auxin have been identified, but do not appear to act as receptors. For example, ABP1 (AUXIN BINDING PROTEIN 1) binds to auxin in the endoplasmic reticulum, but there is no link between ABP and auxin regulated gene expression (Napier et al., 2002).

AUX/IAA domain I interacts with TPL corepressor to inactivate ARFs

Suppressive intragenic mutations that inactivate proteolysis resistant AUX/IAAs were also found in domain I of AUX/IAAs, although their significance was not clear as domain I is not involved in dimerization with ARFs or AUX/IAAs (Rouse et al., 1998; Tiwari et al., 2001). Domain I is composed of a core sequence of LxLxL and is known as an ethylene-responsive element binding factor-associated

amphiphilic repression motif (EAR). EAR motifs were initially identified in both AUX/IAAs and ethylene responsive element binding factors (ERFs) (Kagale et al., 2010). A particular type of ERF (known as class II ERFs) were identified as active repressors of transcription because they are capable of interacting with components of the basal transcription machinery or with histone deacetlyases (HDACs), which modify chromatin structure and prevent other transcriptional activators from binding target cis-elements (Kagale et al., 2010). In *Arabidopsis*, a total of 219 proteins of 21 different transcription factor families, regulating developmental, hormonal and stress pathways, possess an EAR motif (Kagale et al., 2010).

Yeast two hybrid assays showed that domain I of AUX/IAAs interacted with the CTLH domain (C-terminal to LisH) of TOPLESS, a member of the GROUCHO/TUP1/LEUNIG family of corepressors with a total of 5 paralogues (*TPL* plus *TOPLESS-RELATED* (*TPR*)) in *Arabidopsis* (Szemenyei et al., 2008).

TOPLESS was initially identified in forward genetic screens of embryo polarity, with the dominant negative allele *tpl-1* causing transformation of the shoot pole into a root pole at 29°C, creating a double root seedling (Long et al., 2002). At lower temperatures, *tpl-1* embryos fail to form a shoot apical meristem and have fused cotyledons (Long et al., 2002). *TOPLESS* was identified by positional cloning and an asparagine (N) to histidine (H) in amino acid 176 (N176H) was determined to be responsible for the *tpl-1* phenotype. Suppressor screens identified intragenic mutations that reduced or abolished gene function (as in the case of dominant AUX/IAA mutants), suggesting that *tpl-1* is a gain-of-function allele. However, a pentuple loss-of-function mutant combination of all the TOPLESS related genes had a phenotype similar to that of *tpl-1*, indicating that the *tpl-1* allele is a dominant negative allele and the *tpl-1* phenotype is similar to losing all TPL and TPRs activities (Long et al., 2006).

TOPLESS is expressed throughout the *Arabidopsis* embryo but at especially high levels in the embryo proper during early embryogenesis and in developing vasculature in later stages of development (Long et al., 2006). Homozygous translational fusions of wild-type TPL protein fused to GFP were able to rescue the *tpl-1* phenotype, while translational fusions of the dominant negative TPL^{N176H} protein fused to GFP conferred the *tpl-1* mutant phenotype. These results suggest a dosage effect can enhance or suppress the phenotypic effects of the *tpl-1* protein.

An extragenic suppressor screen identified loss-of-function mutations in histone acetyl transferase GCN5 (*HAG1*) suppressed the *tpl-1* phenotype. HAG1 is recruited to promoters by transcription factors and acetylates the N-terminal tail of histone H3, facilitating active gene expression (Kuo et al., 1996). If TPL is involved in repression, the *tpl-1* allele would allow uncontrolled expression of its targets. This idea is supported by the fact that loss-of-function *hag* mutants suppress the phenotypic effects of *tpl-1* mutants, as uncontrolled expression of TPL targets would be diminished by lack of HAG-mediated coactivation. Conversely, mutations in *HISTONE DEACETYLASE 19* (*HDA19*), involved in repressive gene regulation, exhibit similar phenotypes as *tpl-1* mutants. Furthermore, *hda19 tpl-1* double mutants exhibit an enhanced *tpl-1* phenotype at lower temperatures. These observations are consistent with TPL being a corepressor and that a complex formed between TPL/TPR proteins and histone deacetlyases, such as HDA19, is necessary to repress root-promoting genes in the shoot apex during early embryogenesis (Long et al., 2006).

Given that TPL lacks any known DNA binding domains, other proteins must provide specificity between the repressor complex formed by TPL/HDA and its targets. As previously mentioned, a yeast two hybrid screen was used to discover that multiple AUX/IAAs including IAA12/BDL bind to TPL (Szemenyei et al., 2008). Genetic analyses were performed to elucidate the significance of this interaction: *bdl-1* mutants are gain-of-function proteolysis resistant alleles of a P74S mutation in the degron domain II that confers protein stability and repression of auxin responsive genes even in the presence of auxin. *bdl-1* mutants resemble loss-of-function *ARF5/MP* mutants, in which seedlings lack the hypocotyl and roots as well as having decreased vasculature (Berleth and Jurgens, 1993; Hardtke and Berleth, 1998; Hamann et al., 1999). *tpl-1* suppressed the *bdl-1* phenotype with *tpl-1 bdl-1* seedlings able to form roots, hypocotyls, cotyledon vasculature and restored auxin responsive DR5:GFP expression. Therefore, the effects of the proteolysis resistant *bdl-1* protein are mitigated if the *TPL* corepressor is non-functional, allowing *ARF5/MP* activity. Consistent with this, *IAA12*/*BDL* loss-of-function mutations enhanced the *tpl-1* phenotype at 21°C (Szemenyei et al., 2008).

Biomolecular Fluorescence Complementation (BiFC) experiments in tobacco demonstrated that an interaction between TPL and ARF5/MP only occurred in the presence of stabilized IAA12/BDL. This suggested that IAA12/BDL acts as a bridge

allowing indirect interaction between ARF5/MP and TPL in the absence of auxin, and that ARFs provide DNA binding specificity to the complex by binding to AuxREs. In the presence of auxin, IAA12/BDL is degraded releasing ARF5/MP from the repressor complex and allowing it to activate transcription of its targets. This scenario was confirmed by expressing a chimeric TPL protein fused to domains III and IV of BDL/IAA12 (TPL-BDL). This chimeric protein should be able to interact with ARF5/MP in an auxin insensitive fashion due to absence of degron domain II of AUX/IAAs. TPL-BDL driven by IAA12/BDL promoter exhibited a similar phenotype as *arf5/mp* and *bdl-1* mutants, presumably by permanently high jacking *ARF5/MP* to the repressor complex (Szemenyei et al., 2008).

Summary of the auxin signaling pathway in Arabidopsis.

Limiting the scenario to activating ARFs such as MONOPTEROS: in the absence of auxin, the 5 activating ARFs are kept in repressor complexes by interacting with AUX/IAAs (29 in *Arabidopsis*) via homologous protein-protein interaction domains III/IV. AUX/IAAs in turn interact via an EAR domain I (LXLXL) with the co-repressor TPL that recruits histone deacetylases to the complex and maintains the DNA to which ARFs are bound in an inactive chromatin state (Long et al., 2006; Szemenyei et al., 2008). In the presence of auxin, the auxin receptor TIR1/AFB F-box tags AUX/IAAs for degradation in the proteosome via interaction with degron domain II of AUX/IAA proteins, releasing ARF proteins from the repressive complex (Gray et al., 2001; Dharmasiri et al., 2005a; Kepinski and Leyser, 2005). ARF proteins are allowed to associate with histone acetylases and activate downstream targets. Target genes include *SAUR* (encoding proteins of mostly unknown function), *GH3* (encoding conjugators of free auxin) and *AUX/IAA* (encoding repressors of ARF proteins) genes, which are rapidly transcribed in response to auxin to reset the inducible system and repress ARF activity, creating a negative feedback loop. ARF proteins also target genes responsible for determining a variety of morphogenetic pathways such as those directing the development of roots, hypocotyls, and vascular tissue (in the case of *ARF5/MP*) (Berleth and Jurgens, 1993; Hardtke and Berleth, 1998; Hamann et al., 1999).

A novel degradation based auxin sensor in Arabidopsis

Because potentially every class of ARF could recognize and bind the DR5 synthetic promoter, it is now considered that DR5 shows the final output activity of combinations of activating and repressing ARF proteins rather than the actual level of auxin in the cell. A recent study introduced a new auxin sensor: a fusion of the degron domain II of IAA28 (the most stable DII) with a fluorescent reporter expressed under control of a constitutive promoter (*pCaMV35S*:*DII-VENUS*, *DII-VENUS* for short); *VENUS* is degraded in the presence of auxin due to interactions with the SCF^{TIR} complex (Brunoud et al., 2012). Comparisons of *DR5:VENUS* with *DII-VENUS* show divergent expression patterns, and in particular *DII-VENUS* is degraded in places where DR5 is not expressed. Application of exogenous auxin degrades the signal of *DII-VENUS* after 30 min. In a *tir1 afb1 afb2 afb3* quadruple mutant a ubiquitous distribution of *DII-VENUS* was observed and mutations in DII mimicking dominant proteolysis resistant alleles of AUX/IAA proteins showed no degradation in response to auxin. *DII-VENUS* did not appear to interfere with endogenous auxin signaling in the plant. As a test of physiological processes monitored by this auxin sensor, it was demonstrated that *DII-VENUS* was degraded in the lower side of roots after 30 min of a 90° gravity treatment, corroborating that roots bend in response to gravity by accumulating auxin in specific parts of the plant. In the shoot apical meristem (SAM) *DII-VENUS* was progressively degraded in organ primordia, showing also redistribution of auxin throughout the SAM in different time points (Brunoud et al., 2012). In particular, *DII-VENUS* was degraded in the central regions of both vegetative and inflorescence meristems, indicating the presence of predicted auxin maxima that is not seen with DR5 reporters (Vernoux et al., 2011).

Different types of ARFs in Arabidopsis

Previous phylogenetic analyses classified *Arabidopsis* ARF genes into four distinct subfamilies (Liscum and Reed, 2002; Remington et al., 2004). One lineage is composed of 5 activators (*ARF5/MP, 6, 7, 8 and 19*), with a Q-rich content in their middle regions. In *Arabidopsis*, two members of this family (*ARF6* and *ARF8)* are regulated by *microRNA167* (*miR167*) (Wu et al., 2006). A second lineage sister to the activators, based on previously published phylogenies, is composed of *ARF3/ETTIN* and *ARF4*. This lineage is composed of repressors of transcription with SL/G and SLP-rich repressor domains. Both *ETTIN* and *ARF4* are post-transcriptionally

targeted by *TASiRNA3 (Trans-Activating Short interfering RNA)*, which is produced after cleavage of the *TAS3* transcript by *microRNA390* (*miR390*) (Williams et al., 2005; Fahlgren et al., 2006; Garcia et al., 2006). Sister to *ETTIN* and *ARF4* is a third lineage composed of very closely related *ARF* repressors (*ARF* 1, 2, 9, 11, 18 and 12-15, 20-23) seven of which are found clustered close the centromere of chromosome 1 of *Arabidopsis* (*ARF* 12, 13, 14, 15, 20, 21, 22 and 23) and may have originated recently from a series of tandem duplications within the flowering plant linage leading to *Arabidopsis*. This type of tandem ARF is not present in rice and therefore are not conserved throughout land plants (Guilfoyle and Hagen, 2007). Genes of both the *ARF5/MP* and *ARF3/ETTIN* lineages possess conserved domains 3 and 4, although some genes, such as *ETTIN* in *Arabidopsis*, have lost this domain. Finally, a fourth lineage of ARF genes is composed of *ARF10*, *ARF16*, and *ARF17*. They are thought to act mainly as repressors and possess SPL-rich and S-rich middle regions. In *Arabidopsis*, all members of this lineage are post-transcriptionally regulated by *microRNA160* (*miR160*) (Mallory et al., 2005) and have more divergent domains 3 and 4, as compared with other lineages of ARF genes (Remington et al., 2004).

Different ARF lineages interact distinctively with AUX/IAAs proteins.

Recent analyses of protein-protein interactions of all *Arabidopsis* ARF and AUX/IAA proteins assessed by yeast two hybrid screens, suggest that the topology of the network has three principal features: 1. AUX/IAA proteins interact with themselves, 2. AUX/IAA proteins interact with ARF activators (ARF5-8, 19) and 3. ARF repressors have almost no interactions with other proteins in the network (Vernoux et al., 2011). These results imply that many ARF repressors regulate gene expression independently of auxin maxima, as degradation of AUX/IAA proteins by TIR1 would not affect their activity. However, all ARF proteins potentially compete for the same targets as they both recognize similar Auxin Response Elements. These results have led to the view that in the absence of auxin, the activator ARF proteins are kept in check by AUX/IAA proteins, whereas the repressor ARF proteins can repress genes containing an ARE. In the presence of auxin, the activator ARF proteins are released from repression via degradation of the AUX/IAA proteins and can compete for AREs. In this scenario, it is the balance between the levels of activator and repressor ARFs and their relative affinities for AREs that would dictate whether

genes are activated and to what level in response to auxin. However, this scenario does bring up the question as to why two types of repressor *ARFs* are necessary.

After reviewing the main components of the auxin signaling pathway as well as the proposed mechanisms of action, the following chapter will focus on understanding the developmental roles of *ARFs* in angiosperm embryogenesis, as a background for our own developmental studies.

CHAPTER 2

Developmental description of auxin signaling in angiosperm model organisms

INTRODUCTION

In this second chapter I describe the developmental effects of Auxin Response in the model species, *Arabidopsis thaliana*, focusing on selected examples of the three main families of *ARFs* classified in the previous chapter: class A (*ARF5/MP* and *ARF7/NPH4*), class B (*ARF3*/*ETTIN* and *ARF4*) and class C (*ARF10, ARF16* and *ARF17*). Because our experimental work with *Marchantia* focuses on the role of class C orthologues, these genes will be discussed more thoroughly.

Of the 23 *Arabidopsis ARFs* only a fraction has been studied because many single mutants as well as single over expressing lines are indistinguishable from the wild type. *Marchantia polymorpha* only has 3 *ARFs* and therefore it is an attractive system to understand the basic and perhaps ancestral functions of all classes of *ARFs*.

Embryo development in Arabidopsis.

Embryo development in *Arabidopsis* will be discussed briefly as many ARFs have roles in patterning the earliest developmental stages of the sporophyte. Embryo development starts with an asymmetric cell division of the zygote: the smaller apical daughter cell creates the octant proembryo that consists of two tiers of four cells (embryo proper). The upper tier develops into the shoot meristem and cotyledons, while the lower tier (central region) generates the hypocotyl, embryonic root and upper tier of root meristem. The basal daughter cell of the zygote creates a single file of 7-9 extraembryonic cells called the suspensor, and only the uppermost cell adjacent to the proembryo adopts an embryonic fate. This uppermost cell gives rise to the hypophysis, which generates the quiescent center and the lower tier of the root meristem. Thus the root meristem is of mixed clonal origin (Jurgens, 2001). A subsequent round of divisions in the embryo creates the dermatogen (16 cells), followed by globular, triangular (or transition), heart, torpedo and bent cotyledon stages (Laux et al., 1994). An *Arabidopsis* embryo has both apical-basal and radial polarity. The basic elements of the apical-basal pattern include the shoot meristem,

cotyledons, hypocotyl, root and the root meristem. Radial patterning (not discussed further in this work) includes concentrically arranged tissues of epidermis, ground tissue and vascular tissue.

Roles of Class A ARFs: ARF5/MP* and *ARF7/NPH4

The first systematic search for mutations affecting spatial patterning of plant embryogenesis using forward genetics identified nine loci affecting apical-basal and radial patterning of the *Arabidopsis* embryo (Mayer et al., 1991).

The *monopteros* (*mp*) mutation was initially isolated due to its clear disruption of the apical-basal patterning of the embryo: *mp* seedlings lack a hypocotyl and root. Thus, *mp* plants have only a shoot meristem and cotyledons that ends basally in a conical structure, called the 'basal peg', that does not have any root features or internal organization. In the earliest stages of development, *mp* mutants have an altered orientation of the first division plane of the apical daughter of the zygote, resulting in double-octant proembryos (Berleth and Jurgens, 1993; Hamann et al., 1999). The hypophysis fails to undergo the cell divisions that would form the quiescent center and the lower stem cells of the root meristem. Cotyledons vary from two to one with intermediate forms showing fusion, and a fraction of *mp* mutants lack a shoot apical meristem. *mp* cotyledons have vascular strands that are not reticulated: The vascular strands in *wt* cotyledons are interconnected with two half-circles extending inside the blade whereas *mp* cotyledons have a single reduced central strand of vascular tissue (Mayer et al., 1991; Berleth and Jurgens, 1993). All vascular strands in the organs of *mp* mutants are incompletely differentiated and insufficiently connected (Przemeck et al., 1996). When grown on auxin media, wounded *mp* seedlings are able to form roots from the wounded site, suggesting that the *MONOPTEROS* gene in not necessary for the formation of roots, and this has allowed study of mutant traits in post embryonic stages (Berleth and Jurgens, 1993). In mature stages, *mp* mutants have pin-like organ primordia that fail to differentiate into inflorescences, such as those phenotypes observed in *pin1* mutants and NPA treated plants (Przemeck et al., 1996).

The *MONOPTEROS* gene was cloned by positional cloning and it encodes a 902 amino acid protein with high similarity to Auxin Response Factors, in particular with cDNA clone of *IAA24* found in the initial study describing ARFs (Ulmasov et al., 1997a). Since then, *MP* has been classified as *ARF5*, and it was shown to be an

activator of transcription in carrot protoplast assays, eliciting a "positive" transcriptional output of the auxin signaling pathway (Hardtke and Berleth, 1998; Tiwari et al., 2003). *In situ* hybridization shows broad expression of the *MP* transcript in early globular embryos across all sub-edpidermal cells, and in the heart-stage embryos expression is confined to central domains and the midlines of the cotyledons and the embryo axis. In torpedo-stage embryos expression is further restricted to the center of embryonic organs, and ultimately restricted to provasculature and differentiating vascular strands in mature embryos (Hardtke and Berleth, 1998). In leaf primordia, expression is ubiquitous and later restricted to vascular tissues in mature leaves. Flower organs have confined *MP* expression in vascular tissues, being more pronounced in the gynoecium, particularly in developing ovules. In mature roots, *MP* was expressed in the central cylinder (Hardtke and Berleth, 1998).

Auxin-insensitive *bodenlos (bdl)* mutants are identical to *mp* mutants in that they fail to initiate an embryonic root meristem. *BODENLOS* mutants were isolated due to their insensitivity to auxin analogue 2,4-D. The *bdl mp* double mutants exhibit a phenotype similar to single mutants suggesting a shared role in a single developmental pathway (Hamann et al., 1999). It was later shown that the *bdl* phenotype was a result of a single amino acid substitution in conserved proteolysis domain II (QVVGWPP) of *AUX/IAA12*. The *bdl* mutation creates a proteolysis resistant AUX/IAA that constitutively maintains ARF5 in a repressive complex even in the presence of auxin. This provided one of the initial links to connect short-lived inhibitory and auxin induced AUX/IAA proteins and ARF transcription factors (see chapter one for description of the signaling pathway) (Hamann et al., 1999).

Further analyses on the synergistic role of activating *ARFs* in embryo development was shown by multiple loss-of-function analysis, combining mutations in *MP* with those in a closely related paralogue, *ARF7*/*NPH4*. NPH4 mediates auxin-dependent cell expansion in mature hypocotyl and *nph4* mutations were isolated in screens identifying non-phototrophic mutants that fail to grow towards blue light in dark conditions (Stowe-Evans et al., 1998; Harper et al., 2000). ARF5/MP and ARF7/NPH4 interact readily in yeast two hybrid assays and share similar expression patterns. *In situ* hybridization shows that *NPH4* transcripts are present at the heart stage embryo particularly in cotyledons and basal part of the embryo, and throughout the embryo in mature stages. In mature plants *NPH4* is expressed ubiquitously but at higher levels in young organs (Hardtke et al., 2004). Weak mp^{G92} alleles with lesions

close to the C-terminal regions still have two cotyledons with ramified vascular strands. However, *mp*^{G92} *nph4-1* double mutants have single cotyledons in greater proportions than *mp*^{G92} single mutants and a 60% of double mutants do not form cotyledons at all, resulting in club shaped seedlings. Double mutants with the strong *mp*^{G12} alleles (with lesions in the N-terminal region, i.e. *nph4-1 mp*^{G12}), fail to initiate cotyledons and vascular cell differentiation creating a homogenous club shaped embryo without organs (Hardtke et al., 2004).

Gain-of-function alleles of *NPH4* (*CaMV35S:NPH4)* lines were undistinguishable from wild type, however*, CaMV35S:MP* lines show distorted flowers that sometimes terminate in pin-shaped inflorescences, suggesting possible co-suppression of the transgene. Transcriptionally, however, *CaMV35S:MP* and *mp* lines show converse expression patterns, as the former enhances auxin response and the later diminishes auxin responses. It has therefore been postulated that pin-shape inflorescences can be created by either saturating or depleting primordia with auxin responses, although this is still controversial (Mattsson et al., 2003). *CaMV35S:NPH4 CaMV35S:MP* lines result in plants with delayed rosette leave formation, rosette leaves have hyponastic leaf blades and short petioles. Leaf blades and petioles are twisted and small irregular leaves are formed in older rosettes. Inflorescence meristems never produce flower primordia, terminating exclusively in pin-shaped inflorescences (Hardtke et al., 2004).

A more recent study creating truncated versions of *MP* (*MPΔ*) that lack domains 3 and 4, and thus maintain the protein free from interacting with AUX/IAA repressors, have different effect as compared to *CaMV35S:MP* lines including: increased expression levels of auxin inducible genes and *DR5*:*GFP*, vascular tissue abundance, narrow and pointy lateral organs filled with parallel vasculature, and increased rooting (Krogan et al., 2012). The effects of this type of construct suggest constitutive action and should be tested, in combination with NPH4*Δ* for more accurate gain-of-function effects of ARF activators in *Arabidopsis*.

Roles of Class B ARFs: ETTIN/ARF3 and ARF4

ETTIN (*ETT*) encodes a clade B repressing ARF that lacks domains III and IV of protein-protein interaction and allows interaction with ARFs and AUX/IAAs (Kim et al., 1997; Ulmasov et al., 1997a; Tiwari et al., 2003). Because of this deletion, it has been postulated that *ETTIN*/*ARF3* regulates gene expression independently of the

presence of auxin in the cell, although it might compete with other ARFs for the same targets.

The original *ett-1* phenotype is pleiotropic although restricted to the flower with the following modifications: sepal and petal number are increased, stamen number and anther formation are decreased and the gynoecium morphology is severely affected. The wild type apical-basal disposition of carpel structures consists of stigma, style, ovary and internodes. The stigma and style sit on top of a bilocular ovary and in turn the ovary sits on top of a short internode. The ovary is composed of two lateral valves and two medial furrows (Sessions et al., 1997). The weak *ett-2* allele has a slight reduction in valve formation and pronounced outgrowth of the medial ovary. Intermediate *ett-3* alleles have a more severe valve reduction and more proliferation of adaxial style tissue apically and basally; the internodes are big and composed of abaxial style tissue. The strong *ett-1* allele has no valves and long covered apically by style tissue and basally by internode tissue (Sessions et al., 1997). Therefore, in *ett* mutants there is a destabilized establishment of the regional boundaries of the apical and basal limits of the carpel valves (Sessions et al., 1997). In the wild type, abaxial epidermal cells of petals are composed of cubic cells while adaxial ones are conical. In *ett-1* and *ett-11* lines, petals show conical cells in both abaxial and adaxial sides of the epidermis, suggesting a partial loss of abaxial identity in *ett* mutants (Pekker et al., 2005).

In situ hybridization shows that in early stages of flower development, *ETT* transcripts are detected throughout the inflorescence meristem and in sites of provascular differentiation. *ETT* RNA is particularly concentrated in new floral meristems. In later stages, *ETT* is expressed in petal, stamen and carpel primordia, particularly in abaxial domains of stamens and gynoecium. In mature flowers *ETT* expression is restricted to the procambial strand in stamens and carpels (Sessions et al., 1997). *ETT* is detected throughout the shoot apical meristem (SAM), but it is expressed at high levels in young leaf primordia and in older primordia it is restricted to lateral leaf margins, vascular bundles and stipules. In early organs, *ETT* is expressed in provascular tissues and later confined to the procambium (Pekker et al., 2005).

Second site suppressor screens identified loss-of-function mutations in *ETT* as suppressors of mis-expression of the GARP-type transcriptional repressor *KANADI*, a factor involved in establishing abaxial organ polarity (Pekker et al., 2005). Ectopic

expression of *KANADI1* (*KAN1*) or *KAN2* results in abaxialization of leaves and abolishment of lateral leaf expansion (Eshed et al., 2001). The petal and stamen specific *APETALA3* promoter was used to mis-express *KAN1*, resulting in flowers with either radialized stamens and no petals or radialized petals and fertile stamens (Pekker et al., 2005). Mutagenized seeds of fertile *AP3:KAN1* plants were screened in the M2 generation for suppressors of the radialized petal phenotype. One of the suppressors had normal petals but a malformed gynoecium with reduced valves and basally expanded style tissue. Allelism tests confirmed the suppressor as a new allele of *ETT (ett-11)*, thus confirming the role of *ETTIN* in abaxial-adaxial patterning in flower development (Pekker et al., 2005). *ett-1* plants are also able to suppress ectopic *KAN* driven by leaf specific *ANT* promoter, suggesting that *ETT* is an integral component of the abaxial KAN activity in leaves as well.

The most closely related paralogue of *ETT*, *ARF4* shows no aberrant phenotype in *arf4-1* and *arf4-2* single mutants. However, *ett-1 arf4-1* double mutants resemble *kan1-2 kan2-1* double mutants, with narrow, dark-green leaves that develop ectopic blade outgrowths on their abaxial sides, although such outgrowths occur later in plant development compared to *kan1-2 kan2-1* mutants (Pekker et al., 2005). Flowers of *ett-1 arf4-1* had altered phyllotaxis, short sepals with abaxial protrusions, narrow petals and sterile and malformed stamens. There were extra petals and sepals and reduced number of stamens. The gynoecium of *ett-1 arf4-1* was devoid of ovary? tissue, placenta was shifted upwards and ovules could be found in the distal end in both adaxial and abaxial sides. *ARF4* expression is not detected in the SAM as *ETT* but it is restricted to abaxial domains of young leaf primordia. As leaves expand, *ARF* expression is restricted to the phloem. *ARF4* is also detected in low levels throughout inflorescence and flower meristems and later in development resolves? in all initiating floral organ primordia and bracts. In late stages, expression is restricted to the phloem (Pekker et al., 2005).

CaMV35S:ETT resemble the wild type although with leaves that slightly curl downward and flower organs that bend outwards at maturity, and the transgene was able to almost rescue double *ett-1 arf4-1* plants. *CaMV35S:ARF4* plants are indistinguishable from the wild type but the transgene is able to partially rescue *ett-1* mutants and completely rescue *arf4-1* mutants (Pekker et al., 2005). No double *CaMV35S:ETT CaMV35S:ARF4* have been reported in the literature.

Post-transcriptional regulation of class B ARF genes also exists in *Arabidopsis*. In *Arabidopsis*, *ta-siRNAs* derived from a *TAS3* RNA precursor negatively regulates *ARF3* and *ARF4* mRNA in an *ARGONAUTE7 (AGO7)*-dependent manner. *ta-siRNA3* biogenesis depends on cleavage of primary *TAS3* transcripts by *miR390* that recognizes two *miR390* binding sties in the *TAS3* transcript. Cleavage is followed by production of double stranded RNA (dsRNA) by RNA-DEPENDENT RNA POLYMERASE6 (RDR6) using the cleaved product as a template. DICER-LIKE4 (DCL4) processes the resulting dsRNA into phased 21-nucleotide *ta-siRNAs,* some of which are complementary to *ARF3* and *ARF4*, allowing recognition and cleavage by *AGO7* (Allen et al., 2005). Therefore, mutations in the *ta-siRNA* biogenesis pathway such as *ago7* or *rdr6* increase expression levels of *ETT* and *ARF4*. Furthermore, *TAS3* is expressed in adaxial sides of early leaf primordia (complementary to *ETT* and *ARF4*), thus down-regulating *ETT* and *ARF4* in the adaxial leaf domain (Garcia et al., 2006).

In *Arabidopsis ARF3*/*ETT* has two ta-siRNA recognition sites called A and B. Silent mutations were introduced in the coding sequence of *ETT*/*ARF3* that create a *tasiRNA*-insensitive mutant and the transcript was driven by its own promoter (*pARF3*:*ARF3mut*). This experiment increased transcriptional levels of *ARF3* compared to *pARF3:ARF3* controls and the wild type. Phenotypically, *pARF3*:*ARF3mut* plants created dominant accelerated phase-change phenotypes when combined with *rdr6-15* mutations, producing abaxial trichomes two leaf positions ahead of the wild type. These plants also had severe leaf curling, lobed leaves (serrated leaves) with ectopic radial leaf primordia that emerged from the margin of the petiole near the base of the leaf or from the tips of veins, near the sinuses of the lobes on the abaxial surface. This leaf serration is reminiscent of *KNOX* gene overexpression and of other double mutants such as *rdr6 asymetric leaves 2* (*as2*) (Li et al., 2005). Flowers of *pARF3:ARF3 rdr6* and *pARF3:ARF3m6 rdr6* plants had narrow, twisted and downwardly curled sepals and petals, short stamens without pollen, and the gynoecium was irregular in shape and split open at the apical end. Gynoecia expanded in wide siliques with unfertilized ovules. Valve tissue was folded on itself on apical ends and there was almost no style or stigmatic tissue. Ectopic organs resembling gynoecia formed from the placenta and filled the apices of the gynoecia, these organs were associated with expression of the *ARF3* transgenes (Fahlgren et al., 2006). Affected carpels of *pARF3:ARF3m6 rdr6* also had split septa

resembling *SPATULA* mutants, a gene with putative AuxREs in its promoter and negatively regulated by *ETT* as reported by genetic analysis (Heisler et al., 2001).

Endogenous *miR390* as well as four copies of *TAS3*-like transcripts with the two canonical *miR390* binding sites have been found in the moss *Physcomitrella patens* (Axtell et al., 2006; Axtell et al., 2007). Moss *ta-siRNAs* derived from the *TAS3*-like moss loci and also regulates orthologues of *Arabidopsis ARF3* and *ARF4* in moss. Moss *rdr6* mutants show accelerated transition of leafy gametophores from protonemata (Talmor-Neiman et al., 2006). The same study could not find any evidence of *mir390* expression in *Selaginella moellendorffi.* Target predictions using the block 1(+) *ta-siRNAs* recovered three putative targets of *PpTAS3a-d*: Phypa1_1129196, an AP2 domain gene that has been demonstrated to be a target of block 1(+) using RLM-RACE. Two additional AP2 domain genes are putative targets. Block 2(-) *ta-siRNAs* were predicted to target four transcripts, two of which encoded orthologues to *ETT* and *ARF4*. Cleavage products were detected for both *ARF* mRNAs, demonstrating *TAS3*-derived *ta-siRNA* regulation was conserved in the common ancestor of mosses and angiosperms. Additionally a moss specific miR1219 also targets endogenous *ARF* RNAs which are putative ARF3/4 orthologues (Axtell et al., 2007).

Role of Class C ARFs: ARF10 ARF16 and ARF17.

In *Arabidopsis* mutations of clade C *ARF* paralogues (*AtARF10*, *AtARF16*, *AtARF17*) have not been detected through forward genetic screens and have been studied using reverse genetics. All paralogues are negatively regulated by *miR160* (Mallory et al., 2005; Wang et al., 2005; Liu et al., 2007). In plants, miRNA *(miR)* genes are transcribed into primary miRNAs (*pri-miRNAs*), *pri-miRs* form a stem loop as a result of non exact base complementarity between miR and miR* sequences (Meyers et al., 2008). Stem loops are recognized by DICER (RNase III-type endonuclease) that produces 21 nucleotide *miRNA* duplexes that have two-nucleotide 3' overhangs. miRNAs duplexes are loaded into a RNA-induced silencing complex (RISC) where they provide specificity by complementary base pairing to allow *ARGONAUTE* (*AGO*)-catalyzed cleavage of target mRNAs as well as translational repression (Hammond, 2005).

Class C ARFs are considered repressors of transcription (Ulmasov et al., 1999b; Tiwari et al., 2003; Okushima et al., 2005), and their interaction with

AUX/IAAs is limited (Vernoux et al., 2011). They form an independent phylogenetic lineage that possibly predates the origin of land plants (De Smet et al., 2011; Finet et al., 2012).

Loss-of-function phenotypes.

Single *arf10* or *arf16* loss-of-function mutants do not display obvious developmental abnormalities (Mallory et al., 2005; Okushima et al., 2005). Overexpression of any one of the three endogenous *Arabidopsis miR160* precursors using the CaMV35S promoter (*pCaMV35S:MIR160a, b and c*) displayed reduced root length and an increase in lateral root number (Wang et al., 2005). *pCaMV35S:MIR160c* plants also exhibit a lack of root bending in response to gravity, and the root tip shows frequent changes of direction after 4-d-old vertically grown seedlings are rotated 90° clockwise. In *Arabidopsis*, gravity is thought to be sensed by root cap columella cells which contain starch granules called amyloplasts. *pCaMV35S:MIR160c* plants had swollen root caps with extra cells and no amyloplasts, perhaps explaining the absence of graviotropic responses (Wang et al., 2005). The *arf10-2 arf16-2* double mutant displayed a similar phenotype to *pCaMV35S:MIR160c* plants (loss of collumela cells), although lateral root production was not affected. When analyzed at the transcriptional level, it was noted that *arf10-3 arf16-3* lines have increased expression of activator *ARF6* but down-regulation of the activator *ARF8*. This crosstalk between ARF genes maintains a balance between ARF repressors and activators and could explain the lack of change in lateral root production, and suggests regulatory feedbacks between activating and repressing ARFs in *Arabidopsis* (Gutierrez et al., 2009). Analysis of the mitotic marker line *pCYC1At:CDB-GUS*, which is expressed in cells actively dividing, shows that *pCaMV35S:MIR160c* plants have expanded domains of active cell division in both the collumela root cap region and the quiescent center (QC), whereas wild-type plants only have active cell division above the QC. Both QC (QC25) and columella initial (J2341) markers were expanded in *pCaMV35S:MIR160c* plants, suggesting that *ARF16* is a negative regulator of stem cell identity or activity (Wang et al., 2005).

Controversy on role of class C ARFs as negative regulators of stem cell identity comes from studies dealing with totipotent and non-totipotent *Arabidopsis* calli (Qiao et al., 2012). A comparative transcriptomics approach was used to detect *microRNAs* differentially expressed in the two types of calli. It was found that

totipotent calli had low transcriptional levels of *miR160* compared to non-totipotent calli when grown on shoot inducing media. In contrast, overexpression of *miR160* (*pCaMV35S:MIR160)* in cultured *Arabidopsis* cells *in vitro* compromised shoot regeneration. This suggests that at least in cultured cells, loss of class C ARF activity results in a loss of cell totipotency, challenging the results obtained for root phenotypes (Qiao et al., 2012).

Although not published, *pCaMV35S:MIR160* lines also produce phenotypic effects in the shoot as the stipules are transformed into leaves and flowers have a degree of male sterility (John Alvarez, personal communication), suggesting that the role of these genes goes beyond determining root cap formation and repressing lateral root formation.

Gain-of-function phenotypes.

Embryonic effects of gain-of-function of a class C *ARF* were observed via a *Ds* transposon insertion 1635 bp downstream of the *MIR160a* gene, which produces a partial loss-of-function allele that inhibits *MIR160a* expression in aerial organs but not in roots. This mutant was named *floral organs on carpels* (*foc*), for flowers of this mutant produce inflorescences from siliques (Liu et al., 2010). Compared to wild-type embryos, the suspensor cells of *foc* mutants, divide in both transversal and longitudinal planes, creating a double-filed suspensor that eventually produces abnormal hypophyses. The embryo proper (derived from the apical cell of the zygote) also fails to differentiate normally, creating a non-spherical and asymmetric embryo at the octant stage and dermatogen stages. At the heart stage cotyledons are asymmetric. Furthermore, embryo development of *foc* plants is severely retarded, as 2 days after pollination, 93% wild type embryos (N=150) reach the dermatogen stage, while 51% of *foc* embryos were at quadrant or octant stages (Liu et al., 2010).

Pleiotropic effects in several developmental processes occur when class C ARF genes are mis-regulated. Silent mutations that affect the *miR160*-binding site of *ARF17* were used to create a miRNA resistant version of *ARF17* (*mARF17*), which was expressed under its own promoter (*pARF17:mARF17)* and developmental effects were compared plants expressing the wild-type control (*pARF17:ARF17*) (Mallory et al., 2005). *pARF17:mARF17* plants had leaf margin serration, reduced plant size, short roots and hypocotyls, decreased root branching, accelerated flowering time, altered phyllotaxy, reduced petal size, abnormal stamens, reduced fertility and a few

plants died before the transition to flowering (Mallory et al., 2005). Progeny of hemizygous *pARF17:mARF17* plants segregated embryos with three (10-14%) or four cotyledons (3-4%), and cotyledons were lobed and curled downwards. Overexpressing *mARF17* using the 35S promoter showed similar phenotypes although the severity of leaf curling, floral organ defects and premature death were greater (Mallory et al., 2005).

Developmental effects of expression of *mARF16* by its own promoter (*pARF16:mARF16*) include diminished lateral roots than wild-type (opposite to *pCaMV35S:miR160*) but no evident changes in root cap formation or columella formation. Wang et al (2005) report that *mARF16* plants have a consumed basal portion of the root meristem. *pCaMV35S:mARF16* plants often die, but survivors had miniaturized organs (reduced cell number and size), serrated and upcurled leaves and aberrant flowers with reduced fertility (Wang et al., 2005).

Wild-type and miR resistant versions of *ARF10* expressed under their own promoter and fused to GFP (*pARF10:ARF10-GFP* vs. *pARF10:mARF10-GFP*) have also been studied. *mARF10* plants show small (weak lines) to extremely small (strong lines) rosette leaves with serrations. Seedlings with the narrowest leaves died before reaching a juvenile stage. Flowers of weak lines had contorted and elongated petals and produced twisted siliques (Liu et al., 2007). 4/100 *pARF10:mARF10-GFP* seedlings had three cotyledons and three true leaves emerging at one time, and 70% of the seedlings showed bent cotyledons.

In *Arabidopsis* calli, expression of miR resistant *ARF10* produced high levels of shoot regeneration, as well as elevated expression of *CLAVATA3*, *CUP-SHAPED COTYLEDON1* and *-2*, and *WUSCHEL* transcription factors, genes involved in the maintenance of totipotency of the shoot apical meristem (Qiao et al., 2012). These effects in addition to serration in leaves (a phenotype reminiscent of loss of determinacy, which can be achieved reactivating meristem identity genes in leaf margins), and the production of inflorescences from siliques (which might be caused by reactivation of inflorescence meristem programs within carpels) (Liu et al., 2010), suggests that class C ARFs might be involved in the induction or maintenance of totipotent cell states.

Expression patterns.

Northern blots were initially used to discover that *ARF10*, *ARF16*, *ARF17* and the *miR160* transcript are widely expressed in roots, rossette leaves, stems, cauline leaves, buds, flowers, siliques and seedlings (Mallory et al., 2005). In the embryo, *in situ* hybridization shows that *ARF16* is expressed in the vascular primordium at the heart stage, and in cotyledons and procambium in the late heart stage (Liu et al., 2010). *pARF16:GFP-ARF16* showed expression in hypophyseal cells in the heart-stage and remained in the basal region of the embryo. In the mature root, translational fusions of *ARF16* (*pARF16:GFP-ARF16*) showed expression in collumela, emerging lateral root cap cells and progenitor stem cells (apical root region). Conversely, the promoter of *miR160c* (*pMIR160C:GUS*) showed expression in the vascular bundles of primary and lateral roots and was not found in the apical root region. A translational fusion using a *miR* resistant version of *ARF16* (*pARF16:GFP-mARF16*) has expanded expression of GFP in the vascular bundles, suggesting that the *ARF16* promoter drives expression in this region but ARF16 mRNA is restricted by the action of *miR160* (Wang et al., 2005). The *MONOPTEROS* mutant mp^{U55} lacks any *ARF16* expression in the root, using the *pARF16:GFP-ARF16* reporter, suggesting a role of *ARF16* in patterning the root (Wang et al., 2005). In the shoot, *ARF16* showed high expression in juvenile leaves and diminished in older leaves, whereas *pMIR160C:GUS* was undetectable in juvenile leaves and was only present in older leaves (Wang et al., 2005).

ARF17 expression using *in situ* hybridization shows expression in cotyledons and the central embryo domain at the heart stage (Liu et al., 2010).

The *ARF10* promoter fused to *GUS* showed expression in the radicle tip of germinating seeds before the rupture of the testa and endosperm. It also showed expression in the root in post-germinative stages. In later stages of development, *pARF10*:*GUS* is also detected in vascular tissues of leaves and roots (Liu et al., 2007). *In situ* hybridizations show that *ARF10* expression is activated in root explants grown in shoot inducing media after a period of growth in callus inducing media, furthermore *ARF10* expression is accumulated in initiation sites of new leaves and shoots. Conversely, *MIR160a* expression is accumulated in root explants grown in callus inducing media but is lost after transfer to shoot inducing media (Qiao et al., 2012).

Detailed expression patterns of the *MIR160a* promoter fused to GUS and including the 3'region that confers expression in aerial organs, show a broad expression pattern. In the embryo it is expressed in middle regions of cotyledons and hypocotils. In younger seedlings expression is strong in vascular tissue of cotyledons and young leaves, shoot and root tips, lateral roots, vascular tissue of mature leaves and young flower buds. In the flower it is strongly expressed in anthers, carpel internodes and developing embryos (Liu et al., 2010). *In situ* hybridization was used to show that *miR160* is expressed mostly in the embryo proper at octant and dermatogen stages, and throughout the embryo in globular and triangular stages. At the heart stage it is expressed in cotyledon primordia and in vascular primordia. At the torpedo stage, *miR160* is expressed only in cotyledon and hypocotyl epidermal cells (Liu et al., 2010).

The 3'region of the *MIR160a* UTR has three putative AuxREs and transcriptional fusions of the endogenous *MIR160a* promoter -including its 3'UTR- with GUS, show that treatment with exogenous auxin increases the expression patterns of *MIR160a* in a qualitative way, also quantitative RT-PCR shows expression of MIR160a in seedlings is upregulated by auxin. This suggests a regulatory feedback loop between ARFs and *MIR160a* (Liu et al., 2010).

In situ hybridization of *ARF10*, *ARF16* and *ARF17* in the *foc* background shows an increase of expression levels and sometimes expansion of domains (in the case of *ARF17*) in embryo development. Because these genes are already expressed throughout the embryo, it can be proposed that the phenotypes seen in *foc* mutants are caused by a quantitative gradual increase of class C *ARF* transcripts rather than a discreet activation of these genes.

Summarizing, *MIR160* precursors and class C *ARFs* have antagonistic expression patterns in mature organs, suggesting qualitative regulation. In the root, class C expression is limited to meristematic tissue and when *miR160* regulation is abolished, class C ARFs expand to vascular bundles. In aerial parts, class C *ARFs* are expressed in young leaves and shoots and *MIR160* precursors have increased expression in older leaves. Interestingly, all class C *ARFs* and the *MIR160a* precursor are expressed throughout the embryo, suggesting a quantitative rather than qualitative regulation of class C *ARFs* in the earliest stages of development, i.e. class C *ARFs* work in a dose dependent fashion.

Downstream effects in AuxREs of class C ARF mis-expression.

Although considered a repressor, rosette leaf tissue of 30-d-old *pARF17:mARF17* plants showed increased activity of *GH3.3* and *GH3.2/YDK1* but down-regulation of *GH3.5* and *DFL1/GH3.6* (Mallory et al., 2005). The *GH3* up-regulated genes are group II *GH3*-like proteins that conjugate IAA to amino acids *in vitro* and are rapidly transcribed in response to exogenous auxin. They are predicted to decrease active IAA levels in the cell (Staswick et al., 2005). Dominant *ydk1-D* alleles that overexpress *YDK1/GH3.2* phenocopy *pARF17:mARF17* plants, showing reduced primary root length, reduced lateral root number, reduced hypocotyl length as well as reduced apical dominance.

Two AUX/IAA genes (*IAA1* and *IAA5*) and three SAUR genes (*SAUR-AC1*, *SAUR28* and *SAUR63*) were upregulated in the *pARF16:mARF16* background compared to wild type (Wang et al., 2005). *ARF16* expression is upregulated in a late fashion in response to exogenous auxin (5 hours after treatment) and translational fusions are induced 12 hrs after treatment.

When co-expressing either *pARF17:mARF17* (Mallory et al., 2005) or *pARF16:mARF16* (Wang et al., 2005) with the auxin response reporter *pDR5:GUS*, *GUS* activity increases in cotyledons, leaf margins and cotyledons compared to the wild type controls but no drastic change of *DR5:GUS* is observed in the root. These experiments are significant given that both *ARF16* and *ARF17* would directly bind to the AuxREs in the DR5 promoter. They are considered to be repressors but they increase the activity of *pDR5:GUS* in rosette leaves in *Arabidopsis*, suggesting they could act as activators or cause activation of *pDR5:GUS* via secondary effects (Mallory et al., 2005; Wang et al., 2005). Converse experiments show contradictory data and agree with the proposition that class C *ARFs* are repressors: in *pDR5:GUS foc* lines (where *MIR160a* is compromised in aerial tissue), *pDR5*:*GUS* expression is decreased in anthers and carpels of pollinated flowers, i.e. class C *ARFs* are repressing the DR5 promoter (Liu et al., 2010). Embryonic *pDR5*:*GUS* expression is also reported to be diminished in a *foc* background but there is no detailed spatial expression information in embryos (Liu et al., 2010). 50 μM NAA induction of *pDR5:GUS foc* reports no increase of expression in inflorescences compared to the wild type, suggesting a degree of auxin insensitivity in a gain-of-function *ARF10*, *ARF16* and *ARF17* background. This is significant as auxin would release class A activator ARFs from repressive complex, but the ectopic expression of class C ARF

repressors in a *foc* background could inhibit the capacity of class A ARFs to activate AuxREs in the DR5 promoter (Liu et al., 2010).

When root *pDR5:GUS* expression is analyzed in *p35S:MIR160c* background there is no change compared to the wild-type *pDR5:GUS* expression pattern (i.e. collumella initials and collumela root cap cells). This suggests that *ARF16* is not competing with other activator ARFs to specify the *pDR5:GUS* expression pattern in the root (Wang et al., 2005). There is no data available for *pDR5*:*GUS* expression in the shoot in *pCaMV35S:MIR160c* lines.

Overall, there is inconsistency in the results of papers published regarding the nature of class C ARF proteins as either activators or repressors of transcription, and further experiments are needed to clarify this problem.

Cross talk with different phytohormones

Differences in seed germination in response to ABA were measured for *pARF10:ARF10, pARF10:mARF10, pCaMV35S:miR160* expression . It was reported *pARF10:mARF10* lines were hypersensitive to ABA. 0.2 μM of ABA inhibited radicle emergence in *pARF10:mARF10* compared to *pARF10:ARF10* and wild type lines. Conversely, *pCaMV35S:miR160* lines exhibited reduced sensitivity to ABA. Microarray analysis comparing *pARF10:mARF10* and control *pARF10:ARF10* lines showed that a series of ABA-inducible genes were overexpressed more than two-fold in *pARF10:mARF10* lines, including *LATE EMBRYOGENESIS ABUNDANT* (*LEA*), *EARLY METHIONINE-LABELED* (*EM*), *2S SEED STORAGE PROTEIS* and *OLEOSIN* genes (Liu et al., 2007). The promoters of overexpressed genes had significantly ABA-responsive element (ABRE) binding site motifs, all of which responded to exogenous ABA (Liu et al., 2007).

DISCUSSION

This chapter describes representative examples on the diverse role of *ARF* genes in patterning the sporophytic generation of *Arabidopsis*. An attempt to classify developmental effects by phylogenetic status was attempted. Several scenarios for the ancestral role of each class can be proposed, at least for the putative common ancestor of tracheophytes where the sporophyte generation is dominant. One possible scenario is that class A *ARF* genes were involved in the specification of organ fate, such as roots, cotyledons and vascular tissue. Thus, class A *ARF* genes are differentiating

ARFs, promoting the activation of genes due to the presence of free auxin in the embryo. Class B *ARF* genes are not important for embryo patterning and were possibly coopted to pattern novel structures of the shoot, and in particular, the establishment of organ polarity. Finally, it is difficult to ascribe a general function to class C *ARF* genes, although they might have a possible role as promoters of undifferentiated cell states (see chapter 7). Loss-of-function analysis of class C *ARF* genes should be analyzed in the embryo as all class C *ARFs* as well as *miR160* precursors are expressed during this stage of development. Little attention has been directed to *ARF* genes in patterning the gametophyte of angiosperms, although a single study points that they are crucial in establishing the identity of cells of the female gametophyte: in *Arabidopsis* multiple loss-of-function of class A and B *ARFs* leads to transformation of synergid cells into egg cells, reinforcing the hypothesis that class A *ARFs* as putative controllers of cell fate (Pagnussat et al., 2009). Further knowledge on the ancestral role of *ARF* genes can only be proposed after understanding the role of *ARF* orthologues in representative species of each of the main lineages of embryophytes.

The following chapter describes the components of auxin genetic toolkit in *Marchantia* as well as describing possible scenarios on the origin of *ARF* genes within the charophycean algae and embryophytes.

CHAPTER 3,

Phylogenetic analysis of the auxin genetic toolkit in land plants

INTRODUCTION

Distribution of Auxin genetic toolkit in the green branch of life.

The comparison of genomes from flowering plants (e.g. *Arabidopsis*), a lycophyte (*Selaginella moellendorffii*) and moss (*Physcomitrella patens*), show that the common ancestor of mosses and tracheophytes possessed all the gene families controlling auxin biosynthesis, transport, transcriptional responses and conjugation, suggesting an ancestral developmental role of auxin in the last common ancestor of all embryophytes (Floyd and Bowman, 2007; Rensing et al., 2008; Banks et al., 2011). Recent transcriptome analyses from two members of the sister group to land plants, the charophycean algae *Choleochaete orbicularis* and *Spirogyra pratensis*, identified incomplete sequences of homologues of *TOPLESS*, *PIN*, as well as partial sequences with homology to ARF and AUX/IAA domains 3 and 4 of protein-protein interaction, although the identity of these genes as either *AUX/IAAs* or *ARFs* was not clearly distinguished because of lack of full length transcripts (De Smet et al., 2011). These studies did not detect the presence of *TAA* and *YUCCA* in charophycean algae. Finally, most members of the embryophyte auxin genetic toolkit were not detected in Chlorophyte algae (De Smet et al., 2011). Thus, the land plant auxin kit may have been assembled by successively adding components during evolution of the grade of charophycean algae from which land plants evolved, with the full complement appearing only in the common ancestor of land plants.

There are currently no studies dealing with the structure and complexity of auxin regulation in the basal most lineage of land plants, i.e. the liverworts. Such information would allow corroborate whether the complexity of auxin regulation is correlated with an increase in morphological complexity from charophycean algae to embryophytes (Cooke et al., 2002). In this chapter I will use phylogenetic analyses to assess the identity of key components of the auxin signaling pathway in *Marchantia polymorpha*.

Previous hypothesis on Auxin Response Factor evolution

The most recent phylogenetic study of ARF evolution across major lineages of land plants using basal angiosperms, gymnosperms, lycophytes and bryophyte sequences classifies ARF genes into three main clades: clade A, composed of orthologues of *Arabidopsis ARF5-8*, which are thought to act as activators; clade B, composed of orthologues of *Arabidopsis ARF1-4* and *ARF9*, which are thought to act as repressors and clade C, composed of orthologues of *Arabidopsis ARF10*, *ARF16* and *ARF17*, which are also though to act as repressors (Finet et al., 2012). Major propositions from Finet et al. (2012) included:

1. Clade B ARF genes are not present in bryophytes and thus, they evolved after the split of lycophytes from bryophytes. The authors mention that a set of four ARF genes from the moss *Physcomitrella patens* were loosely associated with clade A and although their identity was not clearly established they were interpreted as moss-specific genes rather than putative clade B ARF genes.

2. If clade B ARF genes are not present in all land plants, the common ancestor of all land plants at least had one ARF activator (clade A) and one repressor (clade B).

3. A new set of genes was found in *Physcomitrella patens* and the lycophyte *Selaginella moellendorffii*, which lack a B3 domain but have domains 3 and 4 that are more closely related to domains 3 and 4 of ARF proteins than to those of AUX/IAA proteins. AUX/IAA domains I and II were not detected in this new type of gene. Finet et al. (2012) propose that a putative loss of the B3 domain in these genes suggests a possible mechanism for the origin of AUX/IAA genes.

4. Trans-activating short-interfering RNAs (*ta-siRNAs*) were found to have target sites in *ARF3/4* orthologues of gymnosperms and basal angiosperms, monocots and eudicots. However, no conserved target sites were found in mosses and lycophytes, suggesting that ARF regulation by *ta-siRNA*s arose in the lineage leading to seed plants. *ARF1/9* and *ARF2* (sister groups of ARF3/4) *ta-siRNA* target sites were probably lost in these genes in ancestor of flowering plants.

However, Axtell et al. (2007) previously reported that in the moss *Physcomitrella patens*, *miR390* directs cleavage of 6 *TAS3* loci targets, leading to synthesis of *tasiRNAs* that in turn direct slicing of target mRNAs *in trans*: *tasiAP2* which targets an AP2 orthologue, and *tasiARF* which targets an Auxin Response

Factor orthologue. However, the recognition sequences of *tasiRNAs* in mosses are different to that of the *tasiARF* target sequences in angiosperms (Axtell et al., 2007) .

5. *miRNA167* target sites in ARF6/8 orthologues were found only in seed plants but not bryophytes and lycophytes, agreeing with information published in previous studies (Axtell and Bartel, 2005). No orthologue of the *ARF5/7* lineage has *miR167* binding sites in *Arabidopsis*, suggesting that *miR167* regulation appeared specifically in the ancestor of the *ARF6/8* lineage. The restriction of ARF6/8 expression by miR167 in *Arabidopsis* is involved in integument development (sporophytic structures surrounding gametophytes), as missexpression of these gene causes arrested growth of ovule integuments and anther sterile tissues (Wu et al., 2006).

6. *miRNA160* target sites are present in all clade C orthologues of *ARF10*, *ARF16* and *ARF17* (including mosses and lycophytes), suggesting that *miR160* regulation was present in early in the evolution of land plants.

In this chapter I explore the auxin genetic toolkit in *Marchantia polymorpha*. By comparing the toolkit in *Marchantia* with those in other land plants as well as charophycean algae, hypotheses concerning the auxin genetic toolkit in the last common ancestor of embryophytes can be formulated.

RESULTS

A conserved Auxin Genetic toolkit across all land plants.

The availability of transcriptome assemblies provided by the Joint Genome Institute as part of the *Marchantia polymorpha* genome project allowed us to find putative orthologues of the auxin genetic toolkit reported for previously sequenced genomes of *Arabidopsis thaliana*, *Selaginella moellendorffii* and *Physcomitrella patens*. BLAST searches were performed for *ARF*, *AUX/IAA*, *TIR*, *TOPLESS*, *GH3*, *SAUR*, *YUCCA*, *TAA*, *AUX/LAX* and *PIN* orthologues. I was able to find conserved representatives of each family in *Marchantia polymorpha* (Table 1). Moreover, BLAST searches using domains 3 and 4 of protein-protein interaction allowed identification of 2 isogroups, or genes, (isogroup12370 and isogroup04655) that have domains 3 and 4 but neither ARF B3 domains, nor AUX/IAA DII of protein degradation, suggesting that they exist as an independent gene family.

In addition, BLAST searches were performed to identify microRNA loci involved in *ARF* regulation, since *miR160* is known to have putative *ARF* targets in *Physcomitrella*, and the *miR390* mediated synthesis of tasi-RNA transcripts targeting ARF transcripts is also conserved in *Physcomitrella* (Allen et al., 2005; Axtell et al., 2006; Talmor-Neiman et al., 2006). I identified putative precursor transcripts for both *MIR160* (see chapter 6 for further details) and *MIR390*. I assembled a *TAS3-like* transcript with two putative *miR390* binding sequences, however the intervening sequence did not show similarity to either *ARF* or *AP2* transcripts of *Marchantia*.

Phylogenetic analysis of Auxin Response Factors.

I performed Bayesian phylogenetic analysis to elucidate the evolutionary history of Auxin Response Factors using sequences from the angiosperm *Arabidopsis thaliana*, the gymnosperm *Pseudotsuga menziesii*, the fern *Asplenium platyneurum*, the lycophyte *Selaginella moellendorffii*, the moss *Physcomitrella patens,* the liverwort *Marchantia polymorpha*. A putative *ARF* orthologue from the streptophytic algae *Spirogyra pratensis* was also included in this analysis but this gene has not been identified as a proper ARF orthologue due to its incomplete sequence (De Smet et al., 2011; Finet et al., 2012).

Pseudotsuga and *Asplenium* sequences were obtained from the ONE KP project webpage, the *Spirogyra* sequence was obtained from transcriptome data from de Smet *et al* (2011). The putative *Spirogyra ARF* sequence is incomplete and only includes a fraction of the B3 domain, its inclusion decreased the number of comparable characters between taxa but offered an opportunity to root the tree, specially since it shows high sequence conservation with all embryophyte *ARFs*. The analysis used a matrix of 444 nucleotide characters and 45 taxa.

Three main *ARF* lineages (A, B and C) were obtained **(**Figure 1**)** in accordance with previously published analyses (Remington et al., 2004; Finet et al., 2012). However, all three *ARF* lineages had representatives from liverworts, mosses, lycophytes, gymnosperms and angiosperms. Only *Asplenium* sequences nested exclusively within lineage B, suggesting that class A and C *ARFs* were lost in this species, which we consider unlikely, or more likely class A and C *ARF* sequences have not been identified yet in *Asplenium* due to the fragmentary nature of the transcriptome data. Importantly, in comparison to Finet *et al* (2012), bryophyte orthologues were present in all three *ARF* lineages. Lineage A is a highly supported

(100%) monophyletic group containing orthologues of activating *ARF* sequences, similar to *ARF5/MONOPTEROS*. Sister to lineage A, lineage B is a highly supported monophyletic group (100%) containing *ARF* repressors orthologous to *ARF3/ETTIN.* Finally, lineage C stands as sister to both lineages A and B and is composed of putative ARF repressors orthologous to *ARF10* of *Arabidopsis.* Lineage C forms only a moderately supported (92%) monophyletic group.

An unrooted tree shows that the *Spirogyra ARF* does not nest with any of three lineages (Not shown).

In accordance with Prof. Kochi's group in Kyoto University, who is also working with *Marchantia ARF* genes, we named the *Marchantia ARF* genes in the following way: *MpARF1* belongs to lineage A, *MpARF2* belongs to lineage B and *MpARF3* belongs to lineage C.

Phylogenetic analysis of genes containing domains 3 and 4 of protein-protein interaction.

The presence of homologous domains 3 and 4 of protein-protein interaction in *ARFs* and *AUX/IAA*s provides a way to elucidate the origin of these gene families. Studies of charophycean algal transcriptomes have identified at least four sequences with striking similarities to ARF or AUX/IAA domains 3 and 4 (De Smet et al., 2011). John Alvarez (personal communication) identified a peculiar orthologue of the *Arabidopsis RAV2-like* gene family in *Marchantia* (*MpRAV2*) that has both domains 3 and 4 or protein-protein interaction as well as a B3 domain. Thus *MpRAV2* provides a way to root the domain 3 and 4 tree assuming it shares a more distant common ancestor with either ARF or IAA genes. Moreover, the identity of *Marchantia* genes possessing only domains 3 and 4, such as *isogroup12370* can be clarified.

I performed a bayesian phylogenetic analysis using a matrix of 70 homologous amino acid characters comprising domains 3 and 4 of 70 taxa including *MpRAV*, *AUX/IAA*, *ARF* orthologues of *Marchantia*, *Physcomitrella*, *Selaginella, Asplenium,* the gymnosperm *Picea glauca,* and *Arabidopsis,* as well all available streptophytic algal sequences (*Spirogyra pratensis* and *Coleochaete orbicularis*), and the D34-bearing genes of unknown identity from *Marchantia*, *Physcomitrella*, *Selaginella.*

The unrooted phylogenetic tree established *Corb_contig2131* from *Coleochaete* as well as *MpRAV2* as as sequences distantly related compared to all other sequences. Thus, we used these two sequences to root the tree (Figure 2). The

rooted tree displays *AUX/IAA* sequences as a monophyletic group with maximum support. The *AUX/IAA* clade is sister to all other sequences, however, *ARF* sequences are not a well-supported monophyletic group (50%). Thus the relative relationships between the three clades of *ARF* sequences and *AUX/IAA* sequences remains ambiguous in this tree. Class C *ARF* sequences form a well supported monophyletic lineage (98%) and both class A and B *ARF* sequences form a well supported monophyletic lineage (98%), although its not possible to see a clear division between lineages A and B, and thus this lineage is demarcated class A/B. Surprisingly, streptophytic algal members nest within the Class C ARF lineage (*spra_contig219* from *Spyrogira*), within the A/B lineage (*corb_UMD_Coleochaete_c9703*) and within the *AUX/IAA* sequences (*corb_UMD_Coleochaete_c11109*). All algal sequences have very long branches, so their positioning within a particular group could be due to long branch attraction. Finally, D34 only genes of *Marchantia, Physcomitrella* and *Selaginella* form a monophyletic group nesting within lineage A/B.

Due to the long branch present in the putative *AUX/IAA* from *Coleochaete*, I repeated this analysis without this sequence and including additional tomato sequences (Figure 3). The topology of the unrooted tree showed that class C *ARF* sequences nest as a monophyletic group (with maximum support) sister to the remaining sequences. A lineage with 90% support joins *AUX/IAAs* and class A/B *ARFs* as sister to each other, although neither of these groups have strong support as monophyletic groups, 91% for ARFs and 84% for *AUX/IAAs*.

Phylogenetic analysis of AUX/IAA repressors.

Bayesian phylogenetic analyses were performed comparing conserved domains 2, 3 and 4 of *AUX/IAAs* in *Marchantia*, *Physcomitrella*, *Selaginella*, *Asplenium*, *Pseudotsuga* and *Arabidopsis*. The matrix compared 309 nucleotide characters and 49 taxa. The tree was rooted using the *Marchantia AUX/IAA* (*MpAUX/IAA*) in accordance to the current hypothesis of land plant evolution (Figure 4). This shows a tree with low diversification outside the euphyllophytes with only a single member for *Marchantia*, and three closely related paralogues for *Physcomitrella* and three paralogues for *Selaginella*, two of which form a clade, with the third whose position is not well-supported. Euphyllophyte *AUX/IAAs* form a clade with maximum support (100%). Within the euphyllophyte sequences are three clades, Group A contains only representatives from seed plants (100% support) and groups

B1 and B2 contain representatives from both seed plants and ferns, however the B lineage is not well supported (84%). Group B in turn is subdivided into a highly supported lineage B1 (0.99%) and second not highly supported lineage B2 (75%).

Phylogenetic analysis of TOPLESS corepressors.

Bayesian phylogenetic analysis was used to construct a tree including sequences from *Marchantia*, *Physcomitrella*, *Selaginella*, *Asplenium* and *Arabidopsis*. The matrix included 3084 nucleotide characters and 13 taxa. The tree was rooted with the *Marchantia TOPLESS* (*MpTPL*), generating a tree that roughly agrees with the current hypothesis of land plant relationships (Figure 5), with two *Physcomitrella* genes as sister to all tracheophyte TPL sequences. However, within tracheophytes, *Selaginella* TPL orthologues are more closely related to *Arabidopsis* than *Asplenium* TPL genes. All branches of the tree have maximum support.

Phylogenetic analysis of TIR receptors.

This analysis resulted from a matrix comparing 1524 nucleotide characters and 28 taxa, using representatives from *Marchantia*, *Physcomitrella*, *Selaginella*, *Asplenium, Pseudotsuga* and *Arabidopsis*. As an outgroup I used 6 sequences of the COI1-like F box subfamily (Figure 6). Two monophyletic lineages with maximum support result from this analysis, the TIR1-like F box orthologues and the COI1-like F box orthologues. There is a single *Marchantia* orthologue for each lineage, corroborating the presence of a single auxin receptor in the transcriptome of *Marchantia*.

Phylogenetic analysis of TAA aminotransferases.

This analysis was performed on an alignment of 804 homologous nucleotide characters and 16 taxa using orthologues from *Marchantia*, *Physcomitrella*, *Selaginella* and *Arabidopsis*. The external group was composed of *PYRIDOXAL PHOSPHATE-DEPENDENT TRANSFERASES*, the tree shows two monophyletic clades with maximum support, one for the external group and one for the *TAA* orthologues, although within the *TAA* lineage, relationships do not recapitulate the current hypothesis of land plant evolution (Figure 7).

Phylogenetic analysis of YUCCA monoxygenases.

This analysis was performed on an alignment of 1140 homologous nucleotide characters and 23 taxa using orthologues from *Marchantia*, *Physcomitrella*, *Selaginella* and *Arabidopsis*. In *Marchantia* there are two putative *YUCCA* paralogues but one of them (*MpYUC2*) has a premature stop codon compared to other genes and it was thus excluded from the analysis to expand the number of comparable characters. The tree was rooted with the full length *Marchantia* orthologue (*MpYUC1*) and the outcome shows a tree with *Selaginella* and *Arabidopsis* sequences more closely related and *Physcomitrella* sequences as sister to tracheophytes, agreeing with the current hypothesis of land plant evolution (Figure 8).

Phylogenetic analysis of GH3 orthologues.

This analysis was performed on an alignment of 1080 homologous nucleotide characters and 46 taxa using orthologues from *Marchantia*, *Physcomitrella*, *Selaginella, Asplenium, Pseudotsuga* and *Arabidopsis*. The tree was rooted with the Marchantia orthologue (Figure 9). The tree shows two main lineages with high support, Group 1 with 99% support has sequences from all land plant representatives and Group II with maximum support has only euphylophyte sequences, unexpectedly there is a *Selaginella* lineage positioned as sister to Group I and II and its position does not agree with the current hypothesis of land plant evolution.

Phylogenetic analysis of SAUR orthologues

This analysis was performed on an alignment of 83 homologous amino acid characters among 55 taxa including orthologues from *Marchantia*, *Physcomitrella*, *Selaginella, Asplenium, Pseudotsuga.* No *Arabidopsis* genes were included as they increased the computational time required for the runs to converge. The unrooted tree resulted in several unresolved topologies (Figure 10). However, a mildly supported lineage that includes most *Marchantia SAUR* sequences as well as representatives from all land plant lineages is observed; this may represent a core *SAUR* lineage. We used this lineage to root the tree and the outcome is two *SAUR* groups, Group I which includes orthologues from *Marchantia*, *Physcomitrella*, *Selaginella* and *Asplenium* and its diversification is limited compared to group II, which is the core *SAUR* lineage and contains sequences from all land plants.

DISCUSSION

The auxin genetic toolkit of the embryophyte last common ancestor

Previous studies were able to provide approximate scenarios inferring the ancestral composition of some of the gene families involved in auxin biology. All the main components of auxin biosynthesis, response, transport and conjugation have been proposed to exist in the common ancestor of *Physcomitrella* and *Arabidopsis* (Remington et al., 2004; Rensing et al., 2008). Finet et al (2012), hypothesized that the embryophyte ancestor had only class A and class C *ARF* genes. Here we discuss the genetic composition of the common ancestor of all land plants given our phylogenetic results including a member of the most basal lineage of land plants, the liverwort *Marchantia polymorpha*.

Due to sparse phylogenetic sampling, all of the analyses suffer from random sampling errors (Yang and Rannala, 2012) resulting in trees with insufficient resolution and trees that do not conform to accepted land plant phylogeny. Much of the latter could be due to the paucity of sampling across land plants. For example, large phylogenetic gaps exist between the moss and lycophyte sequences with no hornworts sampled. Likewise, as no whole genome sequence for either a fern of a gymnosperm is available, incomplete sampling in these taxa is likely. However, due to their importance in forestry, deep transcriptome sampling is available for some conifers such that sampling in these taxa is more complete than in ferns. Furthermore, the taxa for which sequences are available for mosses (*Physcomitrella*) and lycophytes (*Selaginella*) generally have long branches and are not ideal for phylogenetic reconstruction across land plants. Despite these limitations, some broad conclusions can be postulated, even though the details will require more extensive sampling. In the following passages I will treat each of the gene families separately and formulate some general hypotheses as a conclusion.

ARF gene phylogeny.

The phylogenetic analysis robustly establishes 3 *ARF* lineages (A, B and C) for all embryophytes as Liverworts, Mosses, Lycophytes, Gymnosperms and Angiosperms all posses at least one of the three types of *ARF* genes. Only in the case of Ferns we were unable to find class A and C *ARF* genes, but this is probably due to

sampling errors, as these sequences are obtained from incomplete transcriptome data. Compared to Finet et al (2012) our phylogenetic analysis incorporates *MpARF2*, a gene that is difficult to identify in transcriptome data derived from mRNA isolated from thallus tissue. The inclusion of *MpARF2* in the analysis helps unite the four class B moss ARF genes into a monophyletic group of class B *ARF* genes. This phylogenetic analysis suggests that the common ancestor of all land plants already had all three types of *ARFs* (A. B and C), and that with a single copy of each, the *Marchantia* genome may resemble the ancestral state.

D34 phylogeny.

This phylogeny aimed to answer three questions:

1. If the embryophyte ancestor already had 3 types of *ARFs*, at what point in streptohytic algal evolution did the *ARF* gene family diversify?
2. What is the origin of the *AUX/IAA* clade and
3. What is the origin of the D34-bearing genes and do they represent a monophyletic group given their existence in at least three main lineages of land plants (Liverworts, Mosses and Lycophytes)?

With regards to the first question, with one *Spirogyra* D34 nesting within class C ARFs, one *Coleochaete* D34 nesting with class A/B *ARFs*, and one *Coleochaete* D34 nesting within *AUX/IAAs,* it is tempting to speculate that the common ancestor of *Coleochaete*, *Spirogyra* and Embryophytes had at least one type of class A activator ARF, one type of class C repressor *ARF*, and possibly an *AUX/IAA* gene, depending upon when the B3 domain was lost and degron domain 2 was acquired. The most recent phylogenetic analyses assessing land plant and streptophytic algae relationships places *Coleochaete* or *Spirogyra* (Zygnematales), as sister to land plants (Finet et al., 2010; Timme and Delwiche, 2010; Timme et al., 2012). Thus, it is possible that the *ARF* gene family arose and expanded within the charophycean algal grade. To clarify the timing and extent of gene duplications, deep transcriptomes from relevant algal species such as *Chara*, *Coleochaete* and *Spirogyra* are required.

Class B *ARF* genes could represent an invention of embryophytes as these genes were hard to amplify from gametophytic tissue (they could be patterning the sporophyte generation), and specific class B ARF D34 were not found in algal transcriptomes. Deeper sampling within the charophycean algae is required to confirm this. Since orthologues of class B *ARFs* are indirectly regulated via *miR390* and *TAS3*

in both *Physcomitrella* and *Arabidopsis*, but to our knowledge not in *Marchantia*, this mode of regulation either arose after the divergence of the liverworts or was lost in the lineage leading to *Marchantia*.

The lack of sequence data does not allow us to know whether *miR160* mediates regulation of class C *ARFs* in Charophycean algae. Answering whether *miR160* downregulation of class C *ARFs* is specific to the embryophytes would be of great interest such as in the case of other land plant specific *miRNAs* (Floyd and Bowman, 2004; Floyd et al., 2006).

With respect to the second question concerning the origin of *AUX/IAAs*, one *Choleochaete* sequence nests within the *AUX/IAA* lineage although its position is uncertain and may be due to long branch attraction. If full-length transcriptomes show the presence of a degron domain II and the EAR motif I in this gene, then the *AUX/IAAs* gene family was already present in the common ancestor of *Choleochaete* and embryophytes. This would be consistent with the presence of *TOPLESS* orthologues in both *Choleochaete* and *Spirogyra* (De Smet et al., 2011).

Finally, with respect to the third question posed, D34-only genes from *Marchantia*, *Physcomitrella* and *Selaginella* form a monophyletic lineage within the A/B *ARF* D34 lineage with close to maximum support (99%). This would imply that this type of gene evolved from an ancestral class-A/B *ARF* in the ancestor of all embryophytes, losing its B3 domain and only retaining D34 over time. Interestingly, this type of gene was probably lost in the lineage leading to euphyllophytes. The role and interacting capabilities of this type of transcript is yet to be determined although it suggests an auxin independent mechanism to regulate Class A *ARF* activity.

Tracing the evolutionary history of genes with D34.

The discovery of an additional *RAV2*-like gene with both a B3 domain and a D34 protein-protein interaction domain allowed us to root the tree to ascertain the phylogenetic relationship between the *ARF* and *AUX/IAA* gene families. It also points to putative evolutionary scenarios for the evolution of these gene families; the two considered most likely are outlined below (Figure 11).

Scenario 1. In charophycean algal ancestors, an ancestral gene with a B3 domain and domains 3 and 4 (*B3-D34*) duplicated, leading to the creation of a RAV2-like ancestor and a *protoARF-AUX/IAA* gene (Figure 11a). The *protoARF-AUX/IAA* gene duplicated giving rise to an *AUX/IAA* ancestor and a *protoARF* gene. The

protoARF gene duplicated giving rise to a class A *ARF* activator and a class C *ARF* repressor. The *AUX/IAA* ancestor lost its B3 domain and gained degron domain II and EAR domain I that allowed interaction with TIR1 and TPL. Subsequently, and perhaps on the lineage leading to embryophytes, a duplication of the class A *ARF* activator produced class B *ARF* repressors, increasing the complexity of *ARF* regulation. Before the divergence of liverworts, class A *ARFs* duplicated again, creating D34-only genes such as *Mpisogroup12370*, which must have lost the B3 domain soon after its origin. This scenario is supported by our first D34 phylogenetic analysis (**Figure 2**) as well as by the maximum likelyhood D34 phylogeny of Finet et al (2012) that positions *AUX/IAAs* as a sister lineage to all ARFs.

Scenario 2. Because of the extremely low support (50%) for the branch connecting Class A/B D34 and Class C D34 (Figure 2) it is possible to speculate a second evolutionary scenario, in *which AUX/IAAs* evolved from a class A activating ARF (Figure 11b). This is supported by the amino acid composition of the *Marchantia AUX/IAA*, which has a domain rich in Glutamines, similar to the activating domain of class A ARFs in embryophytes. In this scenario, a *protoARF* and *protoRAV2-like* genes originated from a duplication event from the ancestral *B3-D34* gene. The *protoARF* gene in turn duplicated originating a class C type ARF repressor and a *protoARF-AUX/IAA* that duplicated again leading to *AUX/IAAs* and a *protoAB ARF*. The *protoAB ARF* in turn gave rise to class A activator and class B repressor ARF genes just as in scenario 1. This second scenario is supported by our second Bayesian analysis including D34 sequences from tomato but excluding the putative *Choleochaete AUX/IAA* due to avoid long branch attraction (Figure 3). In this analysis an unrooted tree, places *AUX/IAA* sequences and class A and B *ARF* sequences as a sister group with medium support (90%) and class C *ARFs* as an outgroup (Figure 3). In this scenario the class A and class C *ARF* gene families may have diverged prior to auxin regulation, with implications for how orthologues in extant species regulate gene expression.

Unfortunately, at present it is difficult to support one scenario over the other with confidence. The limited number of shared characters between domains 3 and 4 of different gene families also reduces resolution. Perhaps only additional sequence data from D34 bearing genes resembling ancestral states in streptophytic algae will resolve this question. However, and important conclusion from my analysis is that the evolution of *ARF* sequences appears to have evolved gradual ways to keep

activator ARF proteins in check, either by evolving competitors for their targets or by evolving interacting partners that would bind them in repressive complexes such as AUX/IAAs (Figure 4).

AUX/IAA phylogeny.

This phylogenetic analysis demonstrates that the common ancestor of all land plants and possibly up to the common ancestor of vascular plants, *AUX/IAA* genes remained as a single copy gene family. For example, all paralogues observed in *Physcomitrella* result from independent duplications within the moss lineage. This is significant since this gene family has 28 paralogues in *Arabidopsis,* all with a variety of interactions mainly between IAA proteins themselves and between IAA proteins and class A ARF activators (Vernoux et al., 2011). In the ancestral land plant, a single *AUX/IAA* protein would have limited if not single interactions with itself and the class A *ARF* activator. It is possible that the *Marchantia* genome resembles this ancestral state as it has only a single *AUX/IAA*. Its functional role, as well as interacting capabilities, are currently being tested by Hirotaka Kato in Takayuki Kochi's lab.

All euphyllophyte *AUX/IAA* sequences form a monophyletic clade. This clade in turn is divided into Group A, composed of only seed plant sequences, and Groups B1 and B2, composed of fern (*Asplenium*) and seed plant sequences. It is possible that still undetected fern sequences belong to Group A or that this type of gene has been lost in ferns. In either scenario, the ancestral *AUX/IAA* gene duplicated in the common ancestor of all euphyllophytes, starting a process of complex duplication associated perhaps with *ARF* diversification. The duplication events in the common ancestor of euphyllophytes seem to be common for other loci, such as *CLASS II* and *IV HD-ZIP* genes and *PIN* genes (Zalewski *et al*, in preparation; Prigge et al. 2006; Floyd et al. 2006; Kawai et al., in preparation).

TOPLESS phylogeny.

Results from the *TPL* phylogenetic analysis show a highly conserved set of proteins that existed as a single copy in the common ancestor of all land plants. Once again, the *Marchantia* genome resembles the genetic composition of the ancestral state bearing only a single copy of *TPL*. Interestingly, at least until the common ancestor of euphyllophytes, *TPL* remained as a single copy gene and its diversification occurred possibly only after seed plants diverged. Refining the timing

of the TPL gene family diversification can be addressed by deeper sampling from gymnosperms.

TIR phylogeny.

The phylogenetic analysis of the *TIR* gene family indicates that the genome of the common ancestor of land plants possessed a single *TIR/AFB* and a single *COI1* F box gene. However, it is not possible to infer the evolutionary history of TIR genes within land plants without broader phylogenetic sampling. However, importantly, again the *Marchantia* genome likely resembles genetic composition of the ancestral land plant with only one *TIR* receptor gene.

Auxin biosynthesis genes.

Analyses of both *TAA* and *YUCCA* gene families point at a single copy of each existing in the common ancestor of land plants. Again, this suggests that the single copy orthologues for each family in *Marchantia* resemble the ancestral state. Intriguingly, neither *TAA* nor *YUCCA* orthologues have been found in incomplete transcriptome data from charophycean algae but these plants are known to respond to auxin and have putative orthologues of auxin transport and auxin response (De Smet et al., 2011). Until more complete sequence data is available it seems that Tryptophan based synthesis of auxin may be an invention of embryophytes.

GH3 phylogeny.

This phylogeny was problematic as after 5,000,000 generations the average split deviation of posterior probabilities went only down to 0.023736. However, two clades with strong support are formed when rooting the tree with the single copy *Marchantia GH3*. A single monophyletic group with 99% support, to the exclusion of the *Marchantia* gene and a clade of *Selaginella* genes, is composed of two well-supported clades: group I with representatives from all land plant lineages, including only two *Arabidopsis* genes, including JAR1 a gene associated with jasmonic acid conjugation as well as all moss *GH3*-like sequences. Group II has only euphyllophyte representatives and its *Arabidopsis* members are associated with IAA conjugation. This topology can only be explained with gene losses in group II from both *Selaginella* and *Physcomitrella*. Additionally, the external group of *Selaginella* sequences sister to both clades I and II imply a loss of genes in this lineage for all

land plants except for *Selaginella* and liverworts. Obviously these scenarios do not fit Occam's razor, and broader phylogenetic sampling is required to avoid random sampling errors in the dataset. Although the analysis was run with a long character matrix, some of the sequences might have undergone extensive independent evolution leading to long branch attraction. For example, *Selaginella* possesses a large number of GH3 paralogues not observed for other gene families. Perhaps performing phylogenetic analysis with amino acid matrixes would be best suited for the GH3 family, but the computational time for the present analysis was limited.

However, the common ancestor of all land plants likely had a single copy GH3 gene just as in the case of *Marchantia*. The simplicity of the gene family in *Marchantia* is consistent with the observation of a limited repertoire of auxin conjugates in *Marchantia* and other liverworts (Sztein et al., 1999; Sztein et al., 2000). Also of interest is the evolution of jasmonic acid conjugation as the two *P.patens* sequences have been previously been grouped in Group I (Bierfreund et al., 2004). Furthermore, biochemical tests have demonstrated that *PpGH31* and *PpGH32* can conjugate both auxin and jasmonic acid (JA) (Ludwig-Muller et al., 2009b), this has lead to the hypothesis that the ancestral *GH3* was able to form conjugates with both IAA and JA (Ludwig-Muller et al., 2009a), and that duplication event after the divergence of mosses could have resulted in PpGH3-1-like gene founded Group I and one PpGH3-2-like gene founded Group II (Ludwig-Muller et al., 2009a), the fact that both moss genes nest within Group I is not supportive of this hypothesis. The question remains as to whether the single *MpGH3* is able to actively conjugate IAA with sugars and aminoacids or if it has more affinity with JA.

SAUR phylogeny.

This is another problematic phylogeny as none of the branches have any strong support despite an analysis of 4 million generations with average standard deviation of split frequencies of 0.008141. If both poorly supported clades are real, and since both groups have members from all sampled lineages of land plants, it is plausible to hypothesize two *SAUR* genes in the common ancestor of all land plants. If that holds true, this will be the only case in which the *Marchantia* genome does not resemble the ancestral state as *Marchantia* members of clade II have diversified considerably. Clade II resolves into a polytomy that may be difficult to resolve given the limited amount of variable synapomorphies available for this gene family. One

open question for which an answer will become apparent is whether the *SAUR* genes in each linage of land plants tend to reside in tandem duplications, as is the case for flowering plant *SAUR* genes.

What was present the ancestral auxin genetic toolkit of land plants?

The availability of *Marchantia* sequences has allowed us to envision a embryophyte ancestor capable of synthesizing auxin (*YUCCA, TAA*), transporting auxin (*PIN, AUX/LAX*), conjugating auxin (*GH3*) and transcriptionally responding to it with at least two different mechanisms that would keep class A activator ARF activity tightly regulated: via target competition with class C and class B repressor ARF proteins and via recruitment to repressor complexes via AUX/IAA proteins in the absence of auxin. The role of D34-only genes as regulators of *ARF* function (e.g. forming inhibitory heterodimers with class A ARF proteins) is yet to be determined, but this type of gene most likely existed before the divergence of liverworts from the ancestral embryophytes.

The embryophyte ancestor had already a complex diversity amongst types of gene families controlling auxin biology but little diversity within each gene family. That is, not a great number of paralogues were necessary to perform genetic functions related to auxin homeostasis. Diversification within gene families first occurred prior to the origin of euphyllophytes (See phylogenetic analysis of *AUX/IAAs*), where a general pattern of gene duplication events occurred, and markedly later during seed plant and angiosperm evolution. As for streptophytic algal genetic toolkits, we await full-length and complete transcriptome data that could pinpoint the identification of embryophyte specific auxin-related gene families and perhaps connections with the origin of new body plans.

METHODS.

Bayesian phylogenetic analyses were performed using Mr.Bayes 3.1. For aminoacid matrixes, the mixed model (aamodelpr=mixed) was used to estimate the appropriate amino acid fixed-rate model. For nucleotide matrixes, I used a partitioning scheme with 3 subsets corresponding to codon positions, with the General time reversible model (lset nst =6) and site specific rates model with 3rd positions being more variable than 1st and 2 positions (ratepr=variable). The number of generations used to run each analysis is noted in each figure legend. Each analysis was run until it was sufficient for the average standard deviation of split frequencies to drop below 0.01. Phylogenetic trees were visualized with FigTree V1.3.1.

FIGURES

Gene Family	*Arabidopsis*	*Selaginella*	*Physcomitrella*	*Marchantia*
PIN	8	5	4	4
AUX/LAX	4	2	4	1
ARF	23	7	14	3
AUX/IAA	29	3	3	1
TPL	5	3	2	1
TIR	6	2	4	1
YUCCA	11	3	6	2
TAA	3	1	4	1
SAUR	78	8	15	6
GH3	19	17	2	1

Table 1. Summary of number of paralogues belonging to major gene families of the auxin genetic toolkit across land plants.

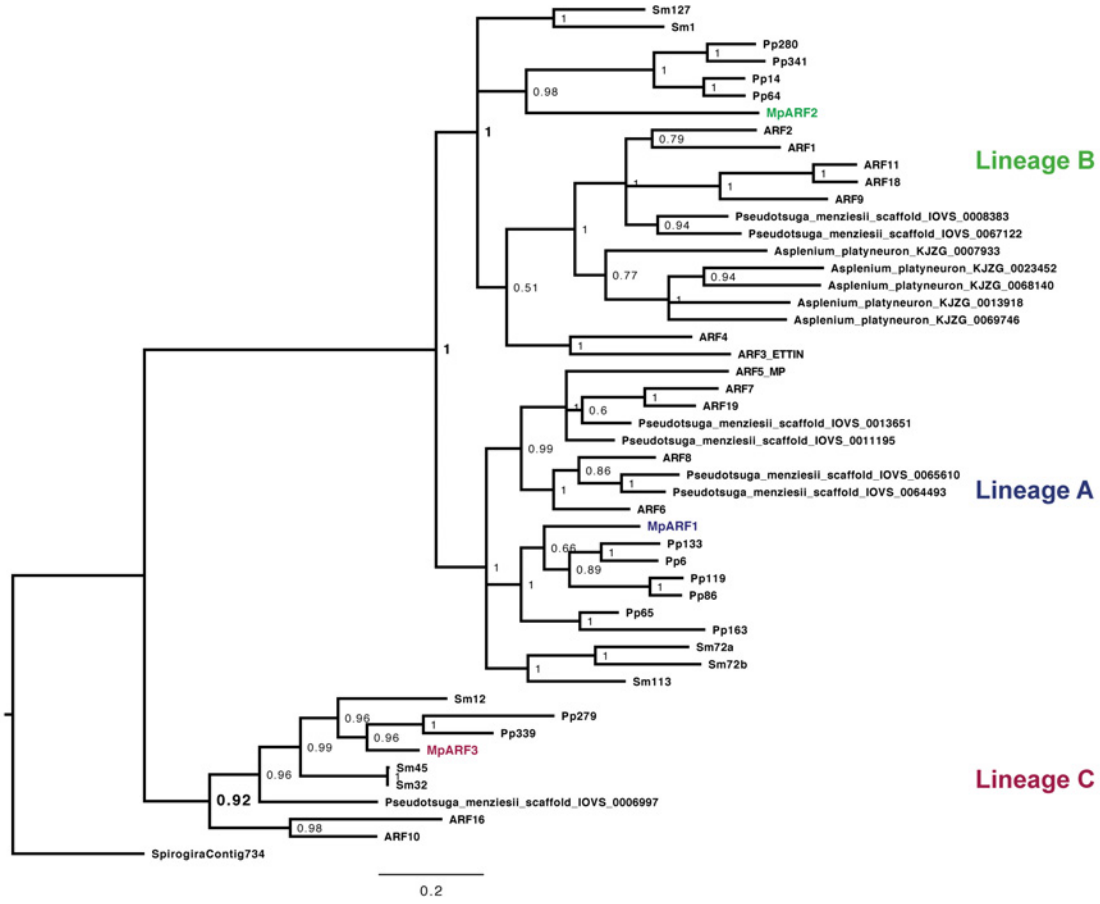

FIGURE 1. **Unrooted Bayesian phylogram of embryophyte *ARFs***. The tree shows how there are representatives from bryophyte and vascular plant sequences in each of the three main *ARF* lineages existing in embryophytes. *Marchantia ARFs* are noted in colour. Numbers above branches indicate posterior probability values. 50 taxa, 501 nucleotide characters and 5,000,000 generations. Burn trees = 5000. Average standard deviation of split frequencies = 0.004058. Scale bar indicates expected changes/ site.

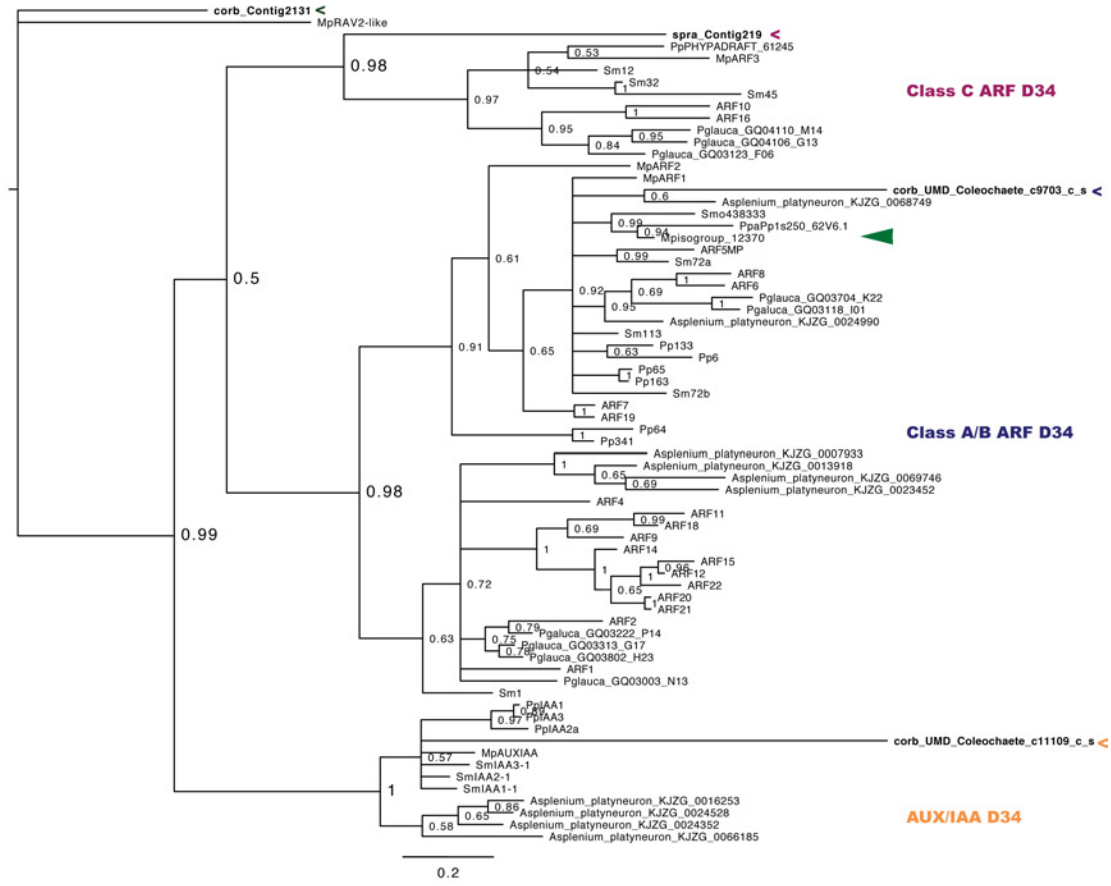

FIGURE 2. **First Unrooted bayesian phylogram of domains 3 and 4 of protein-protein interaction.** Numbers above branches indicate posterior probability values. 70 taxa. 75 aminoacid characters. 3500000 generations. Burnt trees = 10000 Average standard deviation of split frequencies = 0.009203. Scale bar indicates expected changes/ site.

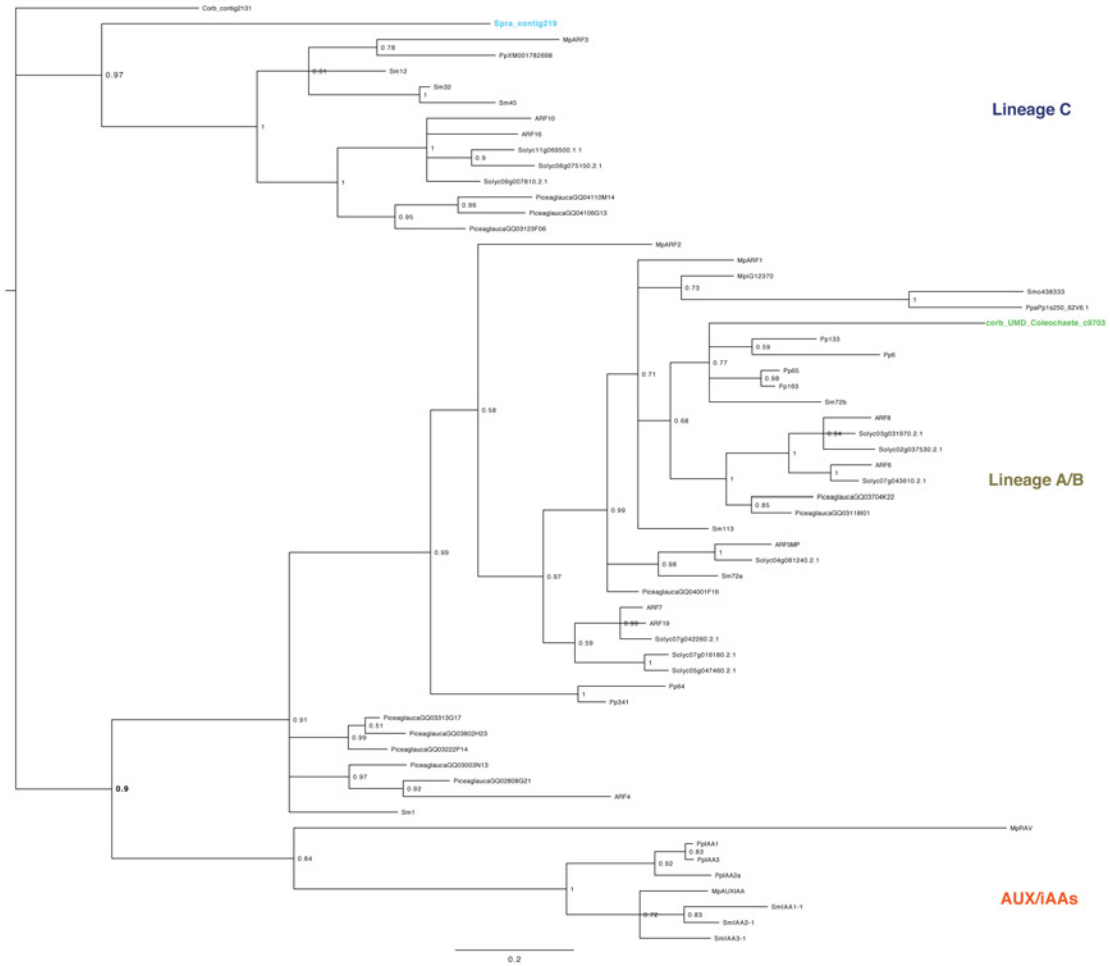

FIGURE 3. **Second Unrooted bayesian phylogenetic analyisis of domains 3 and 4 of protein-protein interaction**. Numbers above branches indicate posterior probability values. 60 taxa. 78 aminoacid characters. 3500000 generations. Burnt trees = 30000 Average standard deviation of split frequencies = 0.006866. Scale bar indicates expected changes/ site.

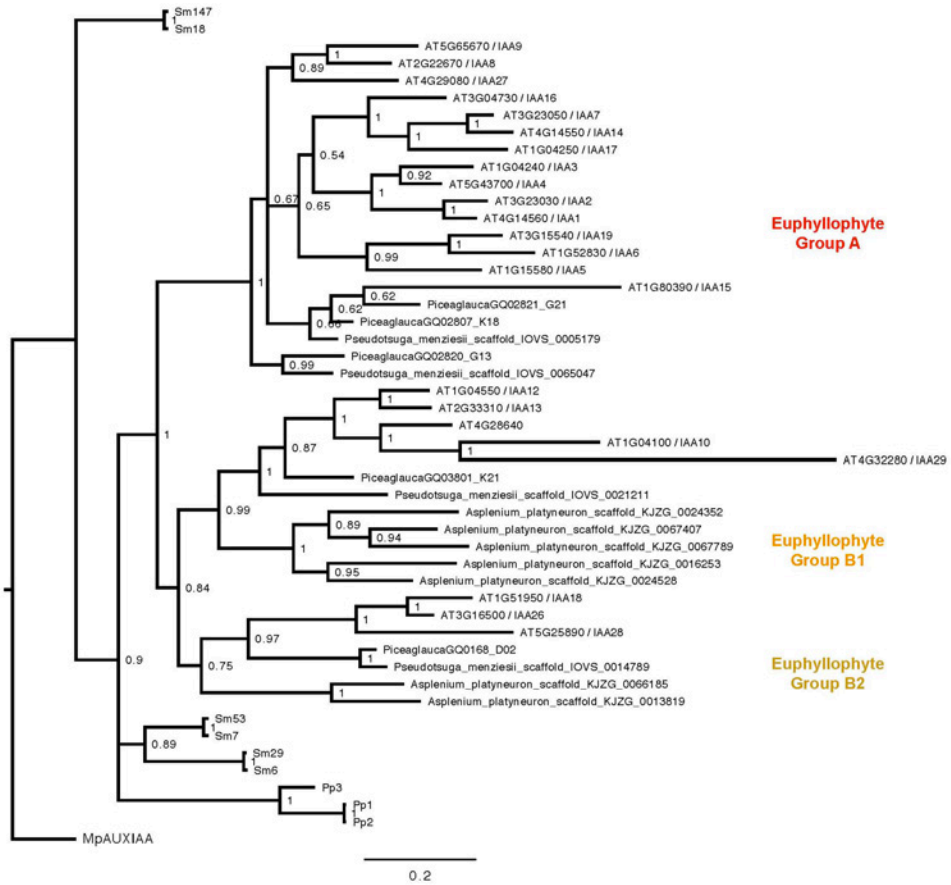

FIGURE 4. **Bayesian phylogram of *AUX/IAAs***. The tree was rooted with *MpAUX/IAA*. Numbers above branches indicate posterior probability values. 49 taxa, 309 nucleotide characters and 5,000,000 generations. Burn trees = 5000. Average standard deviation of split frequencies = 0.008575. Scale bar indicates expected changes/ site.

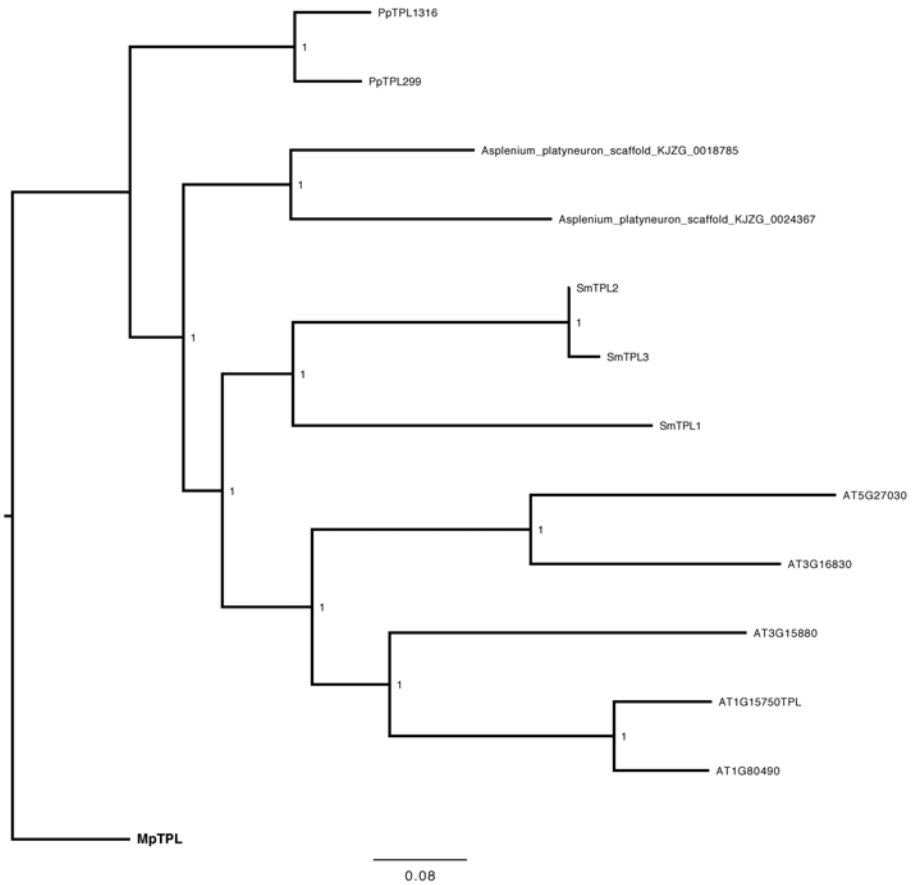

FIGURE 5. **Bayesian phylogram of *TOPLESS* orthologues**. The tree was rooted with *MpTPL*. Numbers above branches indicate posterior probability values. 13 taxa, 3084 nucleotide characters and 500,000 generations. Burn trees = 5000. Average standard deviation of split frequencies = 0.000057. Scale bar indicates expected changes/ site.

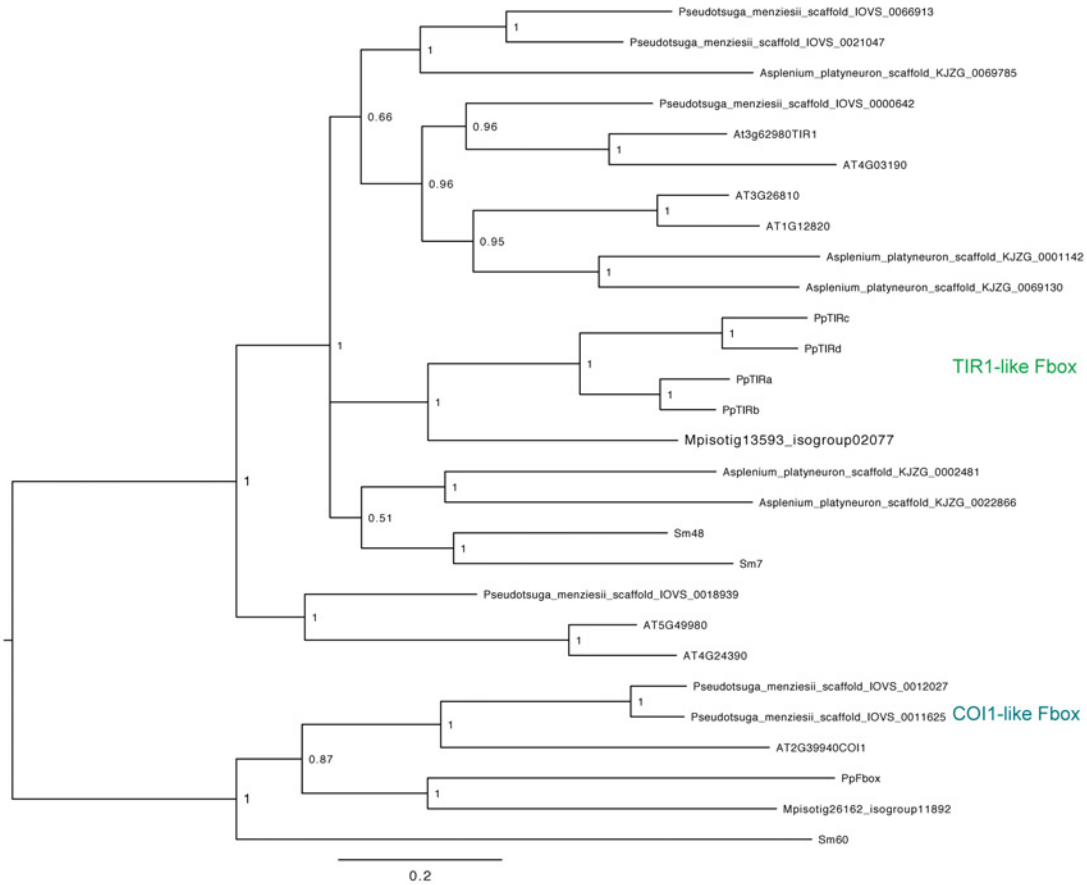

FIGURE 6. Phylogenetic tree of *TIR*-like orthologues. The tree was rooted with the COI1-like Fbox orthologues. Numbers above branches indicate posterior probability values. 28 taxa, 1524 nucleotide characters and 5,000,000 generations. Burn trees = 5000. Average standard deviation of split frequencies = 0.004495. Scale bar indicates expected changes/ site.

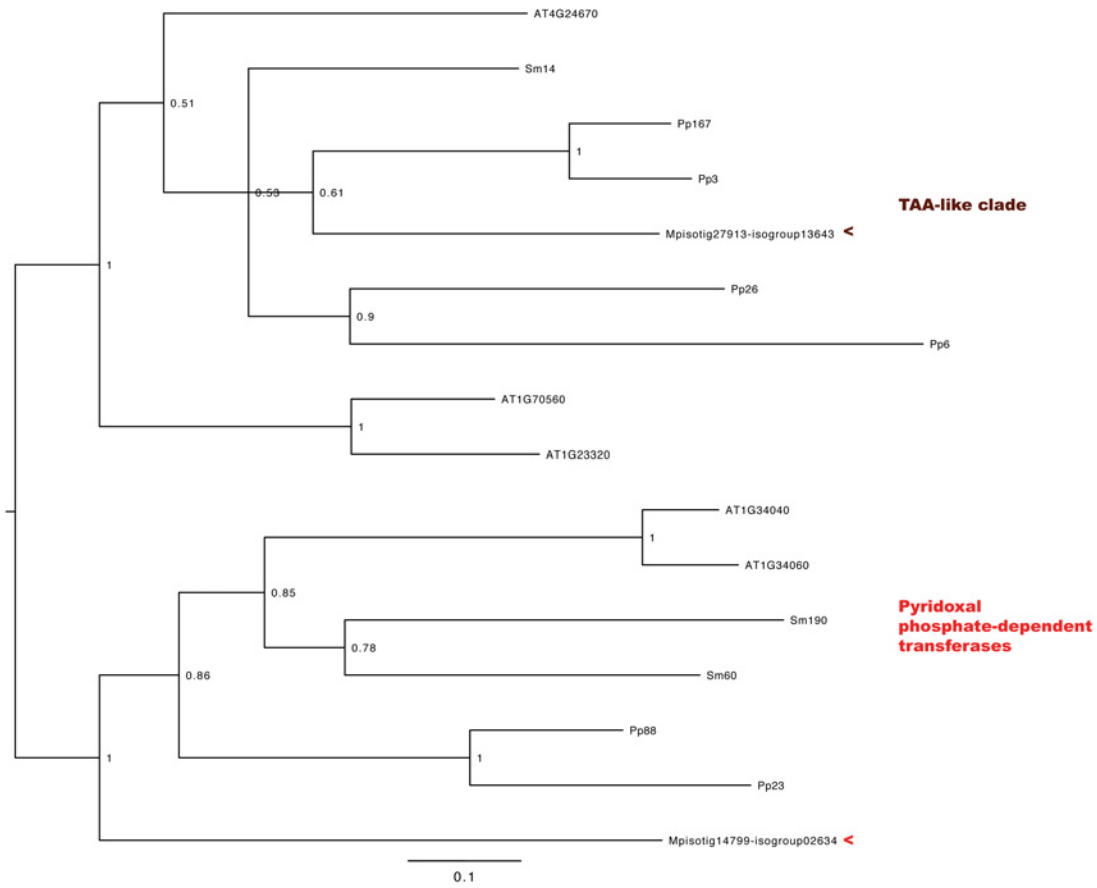

FIGURE 7. Bayesian phylogram of Tryptophane Aminotransferases. The tree was rooted with Pyridoxal phosphate-dependent transferases. Numbers above branches indicate posterior probability values. 16 taxa, 804 nucleotide characters and 1,000,000 generations. Burn trees = 1000. Average standard deviation of split frequencies = 0.009178. Scale bar indicates expected changes/ site.

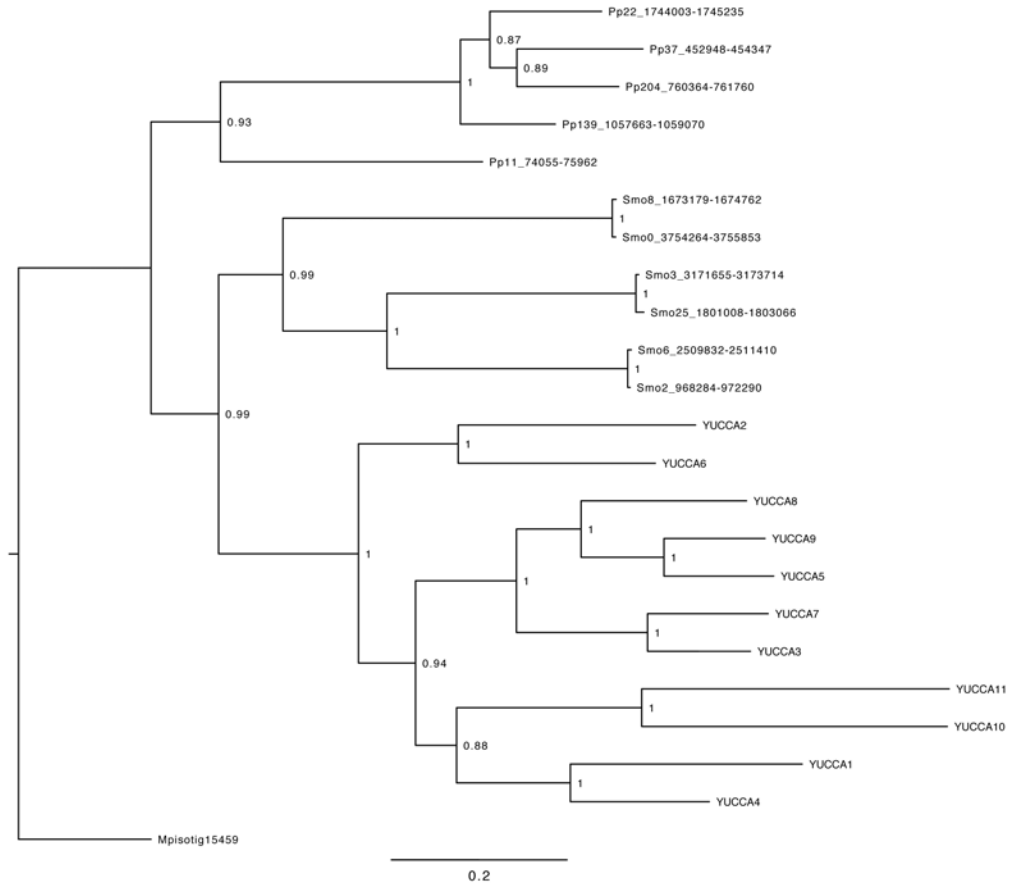

FIGURE 8. **Bayesian phylogram of *YUCCA* orthologues.** The tree was rooted with *MpYUCCA1*. Numbers above branches indicate posterior probability values. 23 taxa, 1140 nucleotide characters and 1,500,000 generations. Burn trees = 1000. Average standard deviation of split frequencies = ?. Scale bar indicates expected changes/ site.

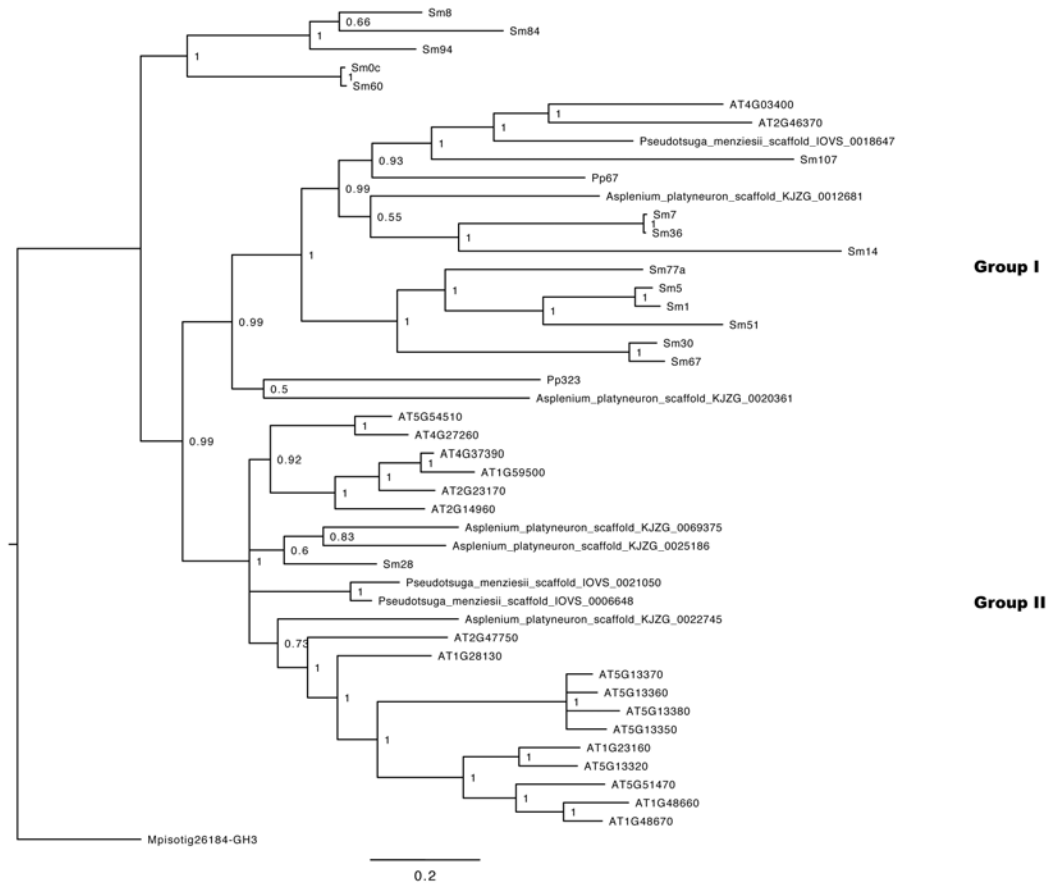

FIGURE 9. **Bayesian phylogram of *GH3* orthologues.** The tree was rooted with *MpGH3*. Numbers above branches indicate posterior probability values. 46 taxa, 1080 nucleotide characters and 5,000,000 generations. Burn trees = 5000. Average standard deviation of split frequencies = 0.023736. Scale bar indicates expected changes/ site.

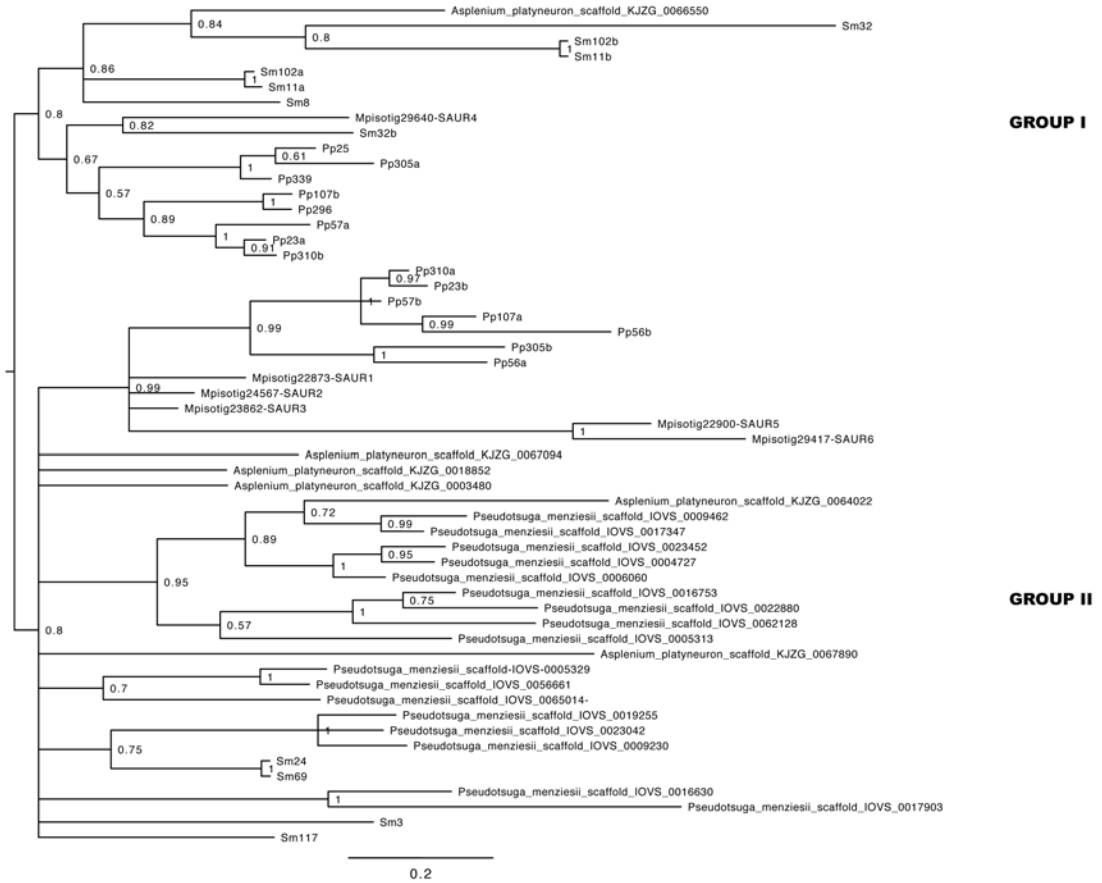

FIGURE 10. **Phylogenetic tree of *SAUR* orthologues.** The tree was rooted with *SAUR* group II. Numbers above branches indicate posterior probability values. 55 taxa, 83 amino acid characters and 4,000,000 generations. Burn trees = 4000. Average standard deviation of split frequencies = 0.008141. Scale bar indicates expected changes/ site.

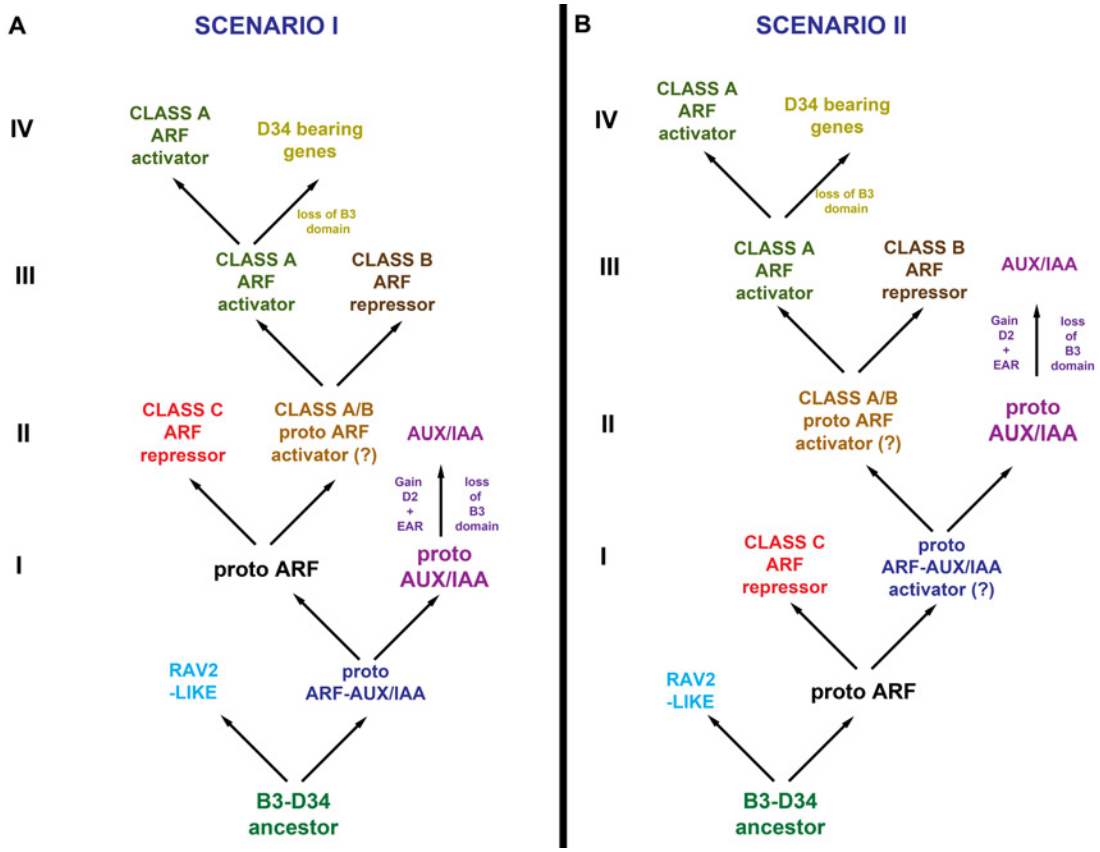

FIGURE 11. Alternative scenarios portraying *ARF* and *AUX/IAA* evolution. (A) Scenario I where *AUX/IAAs* diverged before the split of *ARFs* into Class A and Class C *ARFs*. This scenario is supported if *AUX/IAA* Domains 3 and 4 nest as sister group to all *ARF* Domains 3 and 4. **(B)** Scenario II where *AUX/IAAs* evolved from a class A proto *ARF* and ancestral versions of class C and class A *ARFs* exist prior to the evolution of *AUX/IAAs*. Roman numbers indicate the number of 'check-points' that class A activator *ARFs* would have either as target competitors (class B or C *ARFs*) or as interacting parterns that bind them to a repressing complex in the abscence of auxin (*AUX/IAAs*)

CHAPTER 4

A review of the development of the haploid thallus of *Marchantia polymorpha*

INTRODUCTION

Liverworts are members of the bryophytes and have a haploid dominant life cycle. Compared to angiosperms, where the diploid sporophyte is the only free-living generation, the gametophyte of *Marchantia polymorpha* forms a free-living thallus. In nature, *M. polymorpha* is found on rocky substrate and moist environments, as a flat green carpet of thalli growing on top of each other (Fig 1A). *M. polymorpha* is also known to colonize recently burnt habitats, forming extensive monocultures of thalli (Graff, 1936). *M. polymorpha* is dioecious, with female plants having an X chromosome and male plants a Y chromosome, and each with 8 autosomes. While male and female thalli are morphologically indistinguishable, their gametophores are sexually dimorphic.

Due to its ubiquity, *M. polymorpha* has been exploited as a model liverwort for botanical studies for more than a century and its life cycle has been described in detail (Mirbel, 1835a; Leitgeb, 1881; Kny, 1890; Goebel, 1905). Thus, the literature referenced here attempts to provide a broad view of *Marchantia* studies, but the list is not comprehensive. In the following sections I summarize the morphology, anatomy and development of the gametophyte, emphasizing several distinct stages of development during growth of the gametophyte. The specific morphologies of these stages are pertinent as disruptions to auxin perception result in developmental arrests whose morphologies resemble particular stages of wild-type development (Chapter 5 an 6).

RESULTS AND DISCUSSION

Spore germination and protonemal development

Each *M. polymorpha* sporophyte can produce more than 300,000 spores (Fig. 1B) (O'Hanlon, 1926), which readily germinate in moist light conditions. Spores will not germinate in the dark. Upon landing in a suitable environment, spores swell to approximately twice their dry size, with chlorophyll conspicuous in freshly

germinated spores. The initial growth of the sporeling produces a protonemal filament with all cell divisions occurring in the transverse orientations resulting in a short filament a few cells in length (Fig. 1C) (Kny, 1890; O'Hanlon, 1926). Subsequently, divisions occur in additional planes to produce a small group of cells at the distal end of the filament (Kny, 1890; O'Hanlon, 1926). Simultaneously, rhizoids develop from one or more proximal cells, often from the spore cell itself (Fig. 1D). The development of rhizoids presumably helps anchor the sporeling to the substrate. The change from a filamentous protonemal growth habit to one where cell division occurs in multiple planes marks the first transition in the development of the gametophyte body plan. It has been noted that this transition results in a broad diversity of morphologies at this stage of the life cycle (Mirbel, 1835a; O'Hanlon, 1926).

If spores are grown in low light conditions or exclusively under Far-Red light, the protonemal stage is prolonged, with filaments growing towards the light source, and resembling more closely the protonemal stage of mosses (O'Hanlon, 1926).

Sporeling development formation of the prothallus

The next significant step in gametophyte development is the formation of a marginal row of cells in the apical (distal) region of the sporeling, often when the plant consists of only a dozen or so cells (Kny, 1890; O'Hanlon, 1926). The marginal row of cells is conspicuous and forms the distal growing tip of the sporeling, with continued cell divisions producing a 'prothallus' - a flattened triangular or heart shaped structure that is a single cell layer thick (Fig. 1E). There is some dispute in the literature about whether a single apical cell exists in the prothallus, with some stating that there is always a two-faced apical cell (Leitgeb, 1881; Campbell, 1918; Kaul et al., 1962) whereas others have claimed otherwise (O'Hanlon, 1926). One explanation is that perhaps early during the development of the prothallus all marginal cells contribute to its growth (triangular-shaped prothalli), but that at some point a centrally located cell becomes specified as a two-faced apical cell (heart-shaped prothalli) and that this apical cell is possibly the precursor of the apical cell of the thallus that will develop from the prothallus (Fig. 1F). Regardless, the formation of an organized single cell layered prothallus marks the second major transition in the development of the gametophyte body.

From prothallus to thallus

As mentioned in the previous section, the third major transition in the development of the gametophyte body is the formation of a dorsiventral thallus consisting of multiple cell layers. The major anatomical change in this transition is the formation of an apical cell (Fig. 1F) that divides along four planes, and the major morphological event is the establishment of dorsiventrality, with specialized cells types produced both dorsally and ventrally. The earlier produced rhizoids anchor the prothallus to the substrate allowing the differentiation of a dorsal side towards the light and a ventral side towards the substrate (Fig. 1D). Light and gravity have been shown to be important for dorsiventral differentiation, and will be discussed under a later section describing development of the thallus from a gemma.

The apical cell divides along four planes, creating derivatives apically, basally and laterally (Fig. 1F) (Kny, 1865, 1890; Goebel, 1905; Campbell, 1918). The derivatives continue to divide as they are displaced from the apical meristem. The dorsal region in line with the apical meristem develops as a 'midrib' creating a proximal-distal polarity, and along which, some organs differentiate (Fig. 1G). The derivatives displaced apically differentiate into specialized dorsal tissues including air chambers with epidermal air pores (~150μm), composed of four tiers of border cells, and subepidermally derived photosynthetic filaments (20-50 μm) (Fig. 1K) (Voigt, 1879b, a; Leitgeb, 1880b; Kny, 1890; Barnes and Land, 1907; Apostolakos et al., 1982). Apical derivatives can also contribute to the formation of gemmae cups, described in more detail below (Fig. 1L-M) (Mirbel, 1835a; Kny, 1890; Barnes and Land, 1908). Ventral derivatives may contribute to the development of ventral scales, of which there are two rows on each side of the midline, or rhizoids, of which there are two types - smooth and tubercular (Fig. 1J). The scales and rhizoids differentiate a short distance behind the apical cell (Goebel, 1905; Campbell, 1918). Lateral derivatives of the apical cell contribute to the growth of the 'wings' of the thallus (Fig1H and I). In both the cases for dorsal and ventral structures, the least differentiated organs are closest to the apical meristem (Fig. 1L, 1R, 1U, 1W) and the oldest (Fig 1M, 1V, 1X), most developed organs drift away from the meristem as it produces new differentiating cells. In a mature thallus, the dorsal epidermal and subepidermal cell layers are specialized, along with the ventral epidermal layer. The cells of the other internal layers, of which there may be several, have low numbers of

chloroplasts and are largely unspecialized, with the exception of some cells that differentiate large oil bodies.

Most meristematic activity is restricted to group of cells, with a single apical cell, at the edges of the thallus in a region called the apical notch (Fig. 1F). The thallus grows by bifurcation, creating two growth centers that separate due to the growth between the apical meristems (Fig. 1G-H). In each notch there is an apical cell constituting the organizing center of the apical meristem that is protected by scales (perhaps an analogue to the stipule, Fig. 1P). During bifurcation, it is not clear whether 1. the apical cell divides creating two apical cells, 2. a second apical cell is formed at a distance from the original or 3. The original apical cell disappears and two adjacent cells acquire *de novo* apical cell identity. As long as growth conditions are suitable, this dichotomous branching of the thallus can continue, producing a plant body with multiple apical meristems growing outward from a central point where the spore germinated.

Vegetative growing thalli can produce both asexual and sexual reproductive organs. Gametophores are produced in the sexual stages and will be discussed briefly below (Fig. 1U-X). Gemma cups containing clonal asexual propagules are produced in the asexual stage. During the asexual stage, the apical meristem divides after a gemmae cup is formed in following fashion: The pattern starts with bifurcation (the production of a second apical meristem, Fig. 1H) followed by growth that creates a thallus lobe between the apical notches (Fig. 1I), and organogenesis (formation of a gemmae cup with gemmae inside), and then repeated (bifurcation > lobe growth > cup)^{n}, creating an extended fan-shaped thallus such as environmental conditions allow. As we will describe later, transgenic mutants that branch excessively rarely develop gemmae cups.

Development of gemmae within gemmae cups

In the asexual stage of the life cycle, dorsal organogenesis results in the production of gemmae cups that carry a set of asexual propagules called gemmae (Fig. 1L-M). Gemma cups develop along the midline of the thallus, at a short distance distal from the apical cell (Kny, 1890; Barnes and Land, 1908). Anatomical examination of the differentiation of the dorsal surface the thallus reveals the patterns of dorsal derivatives as they are displaced from the apical cell. Once cells are about three cells removed from the apical cell, a periclinal division produces the epidermal

and subepidermal layers, which soon separate from one another forming a gap, of an air chamber (Leitgeb, 1880b; Kny, 1890; Barnes and Land, 1907). In contrast, when gemma cups develop, the periclinal division does not occur, resulting in a small group of elongate cells that will give rise to the floor of the gemma cup (Barnes and Land, 1908). As growth continues, the elongate cells become slightly depressed relative to other cells of the epidermis, and continue to divide anticlinally producing the cells that will form the floor of the cup from which the gemmae develop. Subsequently, cells at the margin of the floor cells divide in to produce a rim of tissue that will develop into the cup itself. The basal regions of the cup develop as an extension of the dorsal surface of the thallus, complete with air pore on its outside surface. In contrast, the distal tip of the gemmae cup is only a single cell layer thick.

The cup acts as a splash cup, with raindrops propelling the gemmae over a meter from the parent plant (Brodie, 1951). Growth of thalli in lateral and inverted positions has demonstrated that the rim of the gemmae cup is negatively gravitropic, perhaps to maximize vertical positioning of cups (Miller and Voth, 1962).

Gemmae are small, flattened discs lacking dorsiventral polarity (Fig. 1N). They develop in a plane perpendicular to the parental thallus and remain dormant while inside the cup. Individual gemma develop from periclinal divisions of single cells at the floor of the cup, and thus gemma are clonal, being derived from a single cell of the parental thallus (Mirbel, 1835a; Kny, 1890; Barnes and Land, 1908). Following the initial periclinal division, the gemma primordium undergoes additional transverse divisions producing a filamentous structure. Subsequent transverse cell divisions produce a structure consisting of two cell layers, which continues to grow into flattened disc. The mature gemma is attached to the floor of the cup via a large single stalk cell. While the gemma is single cell layer thick at its margin, it is several cell layers thick in the middle regions and is thus lenticular in shape. On the two lateral sides, a row of marginal cells lies in shallow indentations, and these are the two growth centers, with apical cells. Most of the cells of the gemma contain chloroplasts, however, there are isolated cells with oil bodies instead of chloroplast, and additional superficial colorless cells in the central region that appear to be incipient rhizoids (Campbell, 1918; Smith, 1955).

In natural growth conditions physical factors such as rain would disperse gemmae beyond the maternal tissue. However, when a gemmae cup is full of gemmae, the youngest gemmae push out the oldest loosing their perpendicular

position and exposing them to environmental signals that trigger growth as described below. The production of gemma cups may be variable under different growth conditions, with light quality and humidity both influencing whether gemma cups will form (Voth, 1940; Scott, 1963; Carter and Nickell, 1967; Chopra and Sood, 1970).

Timeline of thallus development from gemma

When a gemma lands on a substrate, rhizoids develop in a central zone from both dorsal and ventral sides, likely from the colorless superficial cells visible on the mature gemma (Fig. 1N-O). The rhizoids anchor the gemma to a substrate resulting in only one side of the gemma exposed to light, which leads to polarized dorsi-ventral development (described in more detail below). The central zone exhibit much growth, with all subsequent growth of the gemma coming from the two oppositely positioned apical cells (meristems), which generate a thallus that will produce gemmae cups in approximately 20 days, completing the asexual reproduction cycle.

Two days after landing (d.a.l) on a substrate, young gemmae appear almost the same in both dorsal and ventral sides (Fig. 1N-O). Scales and very small rhizoid primordia start developing from the ventral derivative of the apical cell and scales grow to cover the apical meristems (Fig 1P) while rhizoids develop along the future midrib of the thallus (Fig. 1O), and at this stage no air chambers have yet differentiated on the dorsal sides and the ventral central rhizoids are long and prominent structures (Fig 1N). By 3-4 d.a.l., new tissue has developed due to meristematic activity of the apical notch, and this new extension of tissue is delineated by a faint ridge of cells that separate a central zone (the original central tissue of the gemma) from the newly arising tissue (Fig. 1Q). By 5-6 d.a.l., the dorsal differentiation of the first air chambers with air pores is visible just back from the apical notch. (Fig. 1R) Moreover, the original ridge delineating the central zone from the marginal and newly produced tissue protrudes vertically from the thallus (Fig. 1Q). Normally this ridge does not grow past 8-10 d.a.l. and thus becomes insignificant in size relative to growth at the apical notches. However, the ridge can continue to grow under high light conditions (Förster, 1926) in some mutant backgrounds, and in the presence of sucrose (Yuki Hirakawa, personal communication).

Between days 6 and 8 the first branching of the apical meristem is visible, creating two new apical notches, separated by as little as 400 μM. In between each apical meristem there is thallus growth, creating a third central extension of the

thallus in between each notch (Fig. 1S). Between 9-10 d.a.l., the dorsal side of the thallus is mostly covered with air chambers and the original central zone is very small compared to the rest of the thallus, although the latter still has central rhizoids as well as cells that resemble the original gemmae tissue (Fig. 1S). The first gemmae cup primordium can be seen clearly 12 days after plating, although they are immature. At this point the thallus has four apical meristems. Apical meristems will divide again about the time the first gemma cups mature (i.e. when they have a characteristic cup shape and are full of gemmae). This creates a mature thallus with 8 apical notches between days 14-16 post plating.

As early as 1835 it was noted that the rhizoids produced from growth at the apical notches (not those from the central regions) of the gemmae always developed on the side away from the light, implying light is instrumental in polarizing gemmae (Mirbel, 1835b). It is now acknowledged that an interplay between light, gravity, substrate and temperature influence polar development of gemmae, with light being the dominant force (Fitting, 1935, 1936; Halbsguth, 1936; Fitting, 1937b, a, 1938, 1939, 1942; Otto, 1976; Otto and Halbsguth, 1976). While gemmae do not usually germinate in the dark, a pretreatment with light can facilitate subsequent growth in the dark (Fitting, 1939). Strong white light from the same direction as gravity can result in the growth of upside-down thallus, even with the surface differentiating with dorsal identity in contact with the substrate (Ashihara et al., 2012). In the absence of white (blue) light, gravity may play the primary role in polarization (Ashihara et al., 2012). Polarization driven by these factors makes sense from an ecological point of view. If the gemma lands in direct sunlight, the light is used to polarize growth, whereas in a shaded condition (e.g. dominated by red light), gravity can be used to establish polarization.

Strikingly, if the effects of gravity (growth on a clinostat) and substrate are eliminated, and light is provided uniformly, an 'isolateral' gemmaling is produced, in which each apical notch develops two independent thalli with dorsal surfaces joined face to face and the top and bottom of the gemma developing as ventral (Fitting, 1936). This suggests that either two cells with the potential to become apical cells are present in each apical notch, each of which can produce a thallus if activated by a light signal, or alternatively, a single initial apical cell divides to producing two apical cells, each of which can then give rise to a thallus. Isolateral gemmalings can also be produced by alterations in auxin biology as described in a later section.

Regeneration

As with most bryophytes, *M. polymorpha* can readily regenerate if the original apical notches are damaged (Vöchting, 1885; Förster, 1926; Dickson, 1932). Adventitious growths from cut edges of thalli appear to recapitulate the growth pattern of sporeling, with an initial protonemal phase followed by prothallus and thallus growth phases (Kaul et al., 1962). In a series of experiments where thalli were cut in a variety of patterns Dickson, (Dickson, 1932) noted that regeneration tended to be from a position on the cut thallus that had been closest to the apical notch before the thallus was cut, and also tended to be from a position closest to the midline of the thallus fragment. From these results a growth substance was implied to be at highest concentrations in these positions, and later hypothesized to be auxin (see below for an elaboration of this hypothesis). Regeneration has also been observed under other environmental conditions. For example, growth of gemmalings in a hypertonic solution and subsequent transfer to a hypotonic solution caused dedifferentiation of marginal cells into protonema-like cells (Nagai, 1919). Thus, it is likely that most cells of a *Marchantia* thallus have the potential to dedifferentiate and regenerate a thallus if the apical notches are lost due to environmental perturbations.

Gametophores

The sexual cycle can be induced by an increased far-red/red ratio of light (Wann, 1925). Following induction, umbrella-like sexual organs called gametophores develop from continued growth at the apical notches, bearing either male or female gamete producing structures, antheridia (Fig1. U-V) or archegonia (Fig1. W-X), respectively (Taylor, 1837; Strasburger, 1869; Leitgeb, 1880a; Kny, 1890; Ikeno, 1903; Durand, 1908; Douin, 1920, 1921; Andersen, 1931). Gametophores initiate from apical notches as buds surrounded by scales from the apical cell (Fig 1U, W). Such buds are composed dorsally of an extension of the thallus that grows upward, and ventrally with tightly packaged rhizoids that contribute to the supporting stalks of the gametophores (Fig 1W). Cross sections of the gametophore stalks show dorsiventrality, with rhizoids only formed on one side of the filament (Kny, 1890). Fertilization depends on the presence of water for the sperm released from antheridia to swim to a distant female gametophore and reach the egg cell.

Sporophyte

The diploid or sporophytic generation (Fig. 1Y) lives attached to the female gametophore. The sporophyte is composed of foot, seta and capsule, in which spores and elaters differentiate (Mirbel, 1835a; Henfrey, 1853; Kienitz-Gerloff, 1874; Durand, 1908; Cribbs, 1918; O'Hanlon, 1926; Andersen, 1929; McNaught, 1929). Following fertilization, the zygote first divides transversely, then each of the two cells usually divides longitudinally, however, division patterns at this and later stages are variable. The apical region that will differentiate into the capsule forms a specialized epidermal layer, but all subepidermal cells will form either spore precursor cells or elaters. The spore precursor cells undergo five rounds of mitoses, before meiosis occurs, resulting in the production of haploid spores, half of which are female and half male (Fig 1B). The experimental data obtained from this thesis was not analyzed in sporophytic generation, thus this generation will not be further discussed in this thesis.

MATERIALS AND METHODS

Plant growth conditions. Australian populations of *Marchantia polymorpha* in spore production season (from November to February) were collected from field location (37°57'48.36"S, 145° 6'20.41"E) around Melbourne suburbia. Sporangia was collected using the Lumar.V12 dissecting microscope (ZEISS) and placed in eppendorff tubes with 500 µl sterile water. 500 µl of 2x sterilization solution (2% sodium hypochlorite, 0.1% TritonX100) were added to the suspended sporeangia, mixed and incubated for 1 minute, the solution was discarded and sporangia was washed with 1ml of sterile water two times, silica gel was added to dry sporangia and let sit for one hour in laminar flow before storing at 4°C for over a year.
Spore solutions diluted in 1ml of water were alicuoted in petri dishes with Gambourg's ½ B5 media.

Microscopy. Plants were observed in Lumar.V12 dissecting microscope (ZEISS) and photographed with a AxioCam HRc prior to fixation in FAA (EtOH 50%, Glacial acetic acid 5%, Formaldehyde 10%, water up to 100 ml) overnight at 4°C. Samples were dehydrated in an ethanol series from 50%, 70%, 95% and two rounds of 100% for at least 30 minutes. Samples were critical point dried with Baltec CPD 030 and sputter coated with gold using atmospheric argon in a Baltec SCD 005. Scanning

Electron Microscopy was performed with Hitachi S-570 at 10kV and photos were digitalized using SPECTRUM® Software.

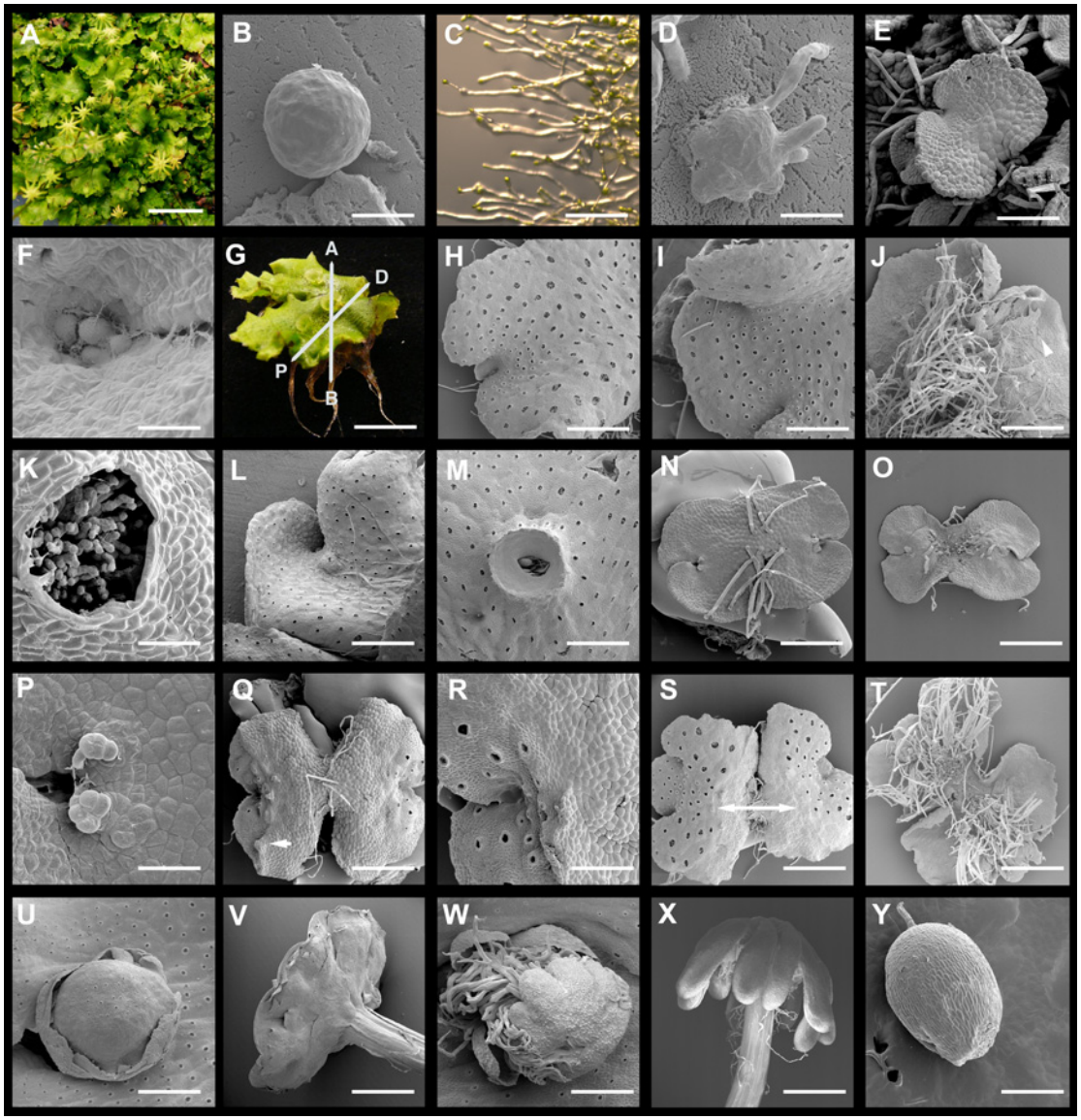

FIGURE 1. Summary of *Marchantia polymorpha* development. **(A)** General perspective on thallus growth in mature colony with female gametophores, scale bar = 1 cm. **(B)** Ungerminated spore, scale bar = 30 µm. **(C)** Induction of extended protonemal growth by Far-Red light induction of sporelings. **(D)** Germinating sporeling with initial rhizoids, scale bar = 43 µm. **(E)** Prothallus phase in sporeling after 14 days of plating, scale bar = 176 µm. **(F)** Apical notch detail showing putative meristematic cells of 18 day old sporeling, scale bar = 20 µm. **(G)** Overview of 2 different polarity axes described in the thallus: apico-basal, dividing dorsal and ventral structures; and proximo-distal running along the midrib (from the notch and away from it), scale bar =1.5 cm. **(H)** Dorsal view of 12 day old gemmaling showing

a recent bifurcation event, scale bar = 1mm. **(I)** 14 day old gemmaling showing the two apical notches drifting away by growth in intercalary thallus lobes, scale bar = 1mm. **(J)** Ventral side of thallus with rhizoids running along the midrib (produced from the apical notch) and scales scattered along the thallus wings, scale bar = 1 mm. **(K)** Air pore showing the inside of air chambers full of photosynthetic filaments, scale bar = 86 μm **(L)** Young gemmae cup primordia arising from apical notch, scale bar = 1.36 mm. **(M)** Mature gemmae cup with dormant gemmae inside, scale bar = 1mm. **(N)** 2 day old gemmaling dorsal view with central rhizoids and two apical notches, scale bar = .38 mm. **(O)** 2 day old gemmaling ventral view, with newly arising rhizoid primordia close to the apical notch, scale bar = 60mm. (P) Dorsal side of apical notch of 2 day old gemmaling with two scale primordia, scale bar = 50 μm. **(Q)** 5 day old gemmaling dorsal side, arrowhead points at ridge dividing central zone from newly developed tissue, scale bar = 0.6 mm. **(R)** Detail of transition zone with differentiating photosynthetic tissue (left) and the original juvenile tissue of the central zone of gemmalings (right), scale bar = 250 μm. **(S)** Dorsal view of 7 day old gemmalings with most of the thallus covered with air chambers, central zones lies between arrowheads, scale bar = 1 mm. **(T)** Ventral side of 7 day old gemmaling with rhizoids covering the entire midrib, scale bar = 1mm. **(U)** Young antheridiophore primordia surrounded by scales, scale bar = 0.6 mm. **(V)** Mature antheridiophore, scale bar = 1.2 mm. **(W)** Young archegoniophore primordia surrounded by scales and rhizoids protruding from ventral side, scale bar = 0.3 mm. **(X)** mature archegoniophore, scale bar = 1.2 mm. **(Y)** Young sporophyte before spore maturation, scale bar = 0.27 mm. Photos (C) and (Y) were taken by Tom Dierschke.

CHAPTER 5
The role of auxin in Bryophytes

While most studies have focused on the role of auxin in flowering plants, there is a wealth of information, a combination of genetics and pharmacological experiments, on auxin biology in bryophytes, and in particular mosses and liverworts. Here I briefly describe the current understanding of the roles of auxin in moss development, and in the following section, provide a more detailed discussion of auxin biology in *Marchantia* in conjunction with a description of my own pharmacological observations on the role of exogenous auxin and auxin biosynthesis inhibitors in patterning different developmental stages of the thallus of *Marchantia*.

AUXIN IN MOSSES

Auxin transcriptional Responses are conserved in Physcomitrella patens

In the moss *Physcomitrella patens,* a land plant with a gametophyte dominant life cycle, key features of the auxin signaling pathway are conserved with flowering plants: Degradation of AUX/IAA repressors is necessary to activate auxin transcriptional responses, interaction between AUX/IAAs and TIR1 occurs in yeast in the presence of IAA or NAA, and *AUX*/*IAA* transcripts are rapidly induced by auxin application (after 1 hour) (Prigge et al., 2010).

A genetic screen for NAA insensitive mutants identified seven *naa-resistant* (*nar*) alleles: substitutions in degron domain II in one or other of the three *Physcomitrella* AUX/IAAs conferred them with resistance to TIR-mediated proteolysis in the presence of auxin (Ashton et al., 1979; Prigge et al., 2010). *Physcomitrella*, like most mosses but unlike most other bryophytes, has an extended protonemal phase in its life cycle, initially producing photosynthetic chloronemal filaments and subsequently producing caulonemal filaments, from which gametophore buds arise. Growth in media with exogenous auxin accelerates the transition from caulonema to chloronema developmental stages (Johri and Desai, 1973) and triggers formation of ectopic rhizoids from leafy gametophore shoots (Ashton et al., 1979). Auxin resistant, *nar* mutants fail to make the transition from chloronema to caulonema developmental stages. Silencing of all four *TIR* orthologues

(*PpAFB1-4*) resulted in a similar phenotype to those of *nar* mutants confirming the conservation of the TIR mediated auxin perception and ARF de-repression between mosses and angiosperms.

Prigge *et al*. (2010) suggest that an ancestral auxin signaling module has been co-opted to pattern novel morphological structures in highly divergent lineages such as *Arabidopsis* and *Physcomitrella*. Because auxin promotes rhizoid formation in streptophytic algae (Klambt et al., 1992), liverworts (Kaul et al, 1962) and mosses (Ashton et al., 1979), and also promotes formation of root hairs in tracheophytes it has been postulated that rhizoids and root hairs can be interpreted as analogous structures determined by homologous genetic pathways (Prigge et al., 2010). This is supported by studies demonstrating that homologous genes direct the growth of rhizoids and root hairs (Menand et al., 2007; Jang et al., 2011; Jones and Dolan, 2012) .

Polar auxin transport in Physcomitrella patens

Studies measuring auxin distribution in moss gametophytic shoots did not detect polar auxin transport (PAT) in leafy gametophores. Fujita *et al* (2008) fed mosses with radioactive auxin and failed to detect basipetal polar auxin transport in haploid shoots, but detected transport in sporophytes of several species of mosses (Fujita et al., 2008). However, a survey of expression patterns of the *Physcomitrella* PIN genes indicates that at least some of the PIN genes whose gene products are predicted to be plasma membrane localized are expressed in the gametophyte stage of the life cycle (K. Sakakibara and J. Bowman, unpublished data). This may suggest that a failure to observe PAT in this generation is due to the crudeness of the assay, and that finer scale PAT may occur during development of the moss gametophyte.

Auxin distribution was measured indirectly in moss by using the auxin inducible soybean *GH3* promoter fused to *GUS* (*pGH3:GUS*). *GUS* signal was detected in the base of the gametophore stem, rhizoids, axillary hairs (which originate in leaf axils), and at the base of the leaves (Bierfreund et al., 2003). As in *Arabidopsis, GUS* activity in *GH3:GUS* lines was enhanced after a 24 h incubation period with 10 μM NAA, which also causes stem elongation. Treatment of leafy gametophores with 50 μM auxin transport inhibitor NPA for 7 days did not cause changes in morphology or *GH3:GUS* expression. In young moss sporophytes, *GH3:GUS* is expressed in the apical part more than the basal part. In mature sporophytes, *GUS* expression is stronger in the basal part, with the signal confined to

the seta and foot, suggesting an active mechanism that shifts the distribution of auxin during sporophyte development. 50 μM NPA treatment for 7 days produced abnormal sporophytes with possible axis duplication, resulting in multiple sporangia, as well as mis-positioning of the sporophyte within the archegonium (Fujita et al., 2008).

These experiments suggests several scenarios: First, PAT may be less critical for the growth of haploid shoots in mosses compared to angiosperm shoots and thus independently evolved mechanisms pattern haploid and diploid shoots. Second, auxin polar transport is present in sporophytic generations of both mosses and angiosperms. This shared character could have evolved independently or alternatively, the common ancestor of mosses and angiosperms used PAT to pattern its sporophyte and perhaps its gametophyte (Fujita et al., 2008). Refined versions of these scenarios will depend on the elucidation of the role of PIN proteins in haploid and diploid stages of moss development.

Recent studies with streptophytic algae *Chara corallina* confirm NPA inhibited PAT in this species (Boot et al., 2012). Furthermore, the presence of PIN orthologues have been reported for another streptophytic algae, *Spirogyra pratensis* (De Smet et al., 2011), suggesting that auxin transport was present in the common ancestor of land plants. Given that PAT occurs in the gametophyte of liverworts (se below), PAT may have been lost in the moss haploid shoots but was preserved to pattern moss protonemata and rhizoids (Rose and Bopp, 1983; Rose et al., 1983).

Auxin biosynthesis regulators in Physcomitrella patens

The *SHI/STY* gene family has been characterized in *Arabidopsis* as positive regulators of auxin biosynthesis by transcriptional activation of YUCCA genes (Eklund et al., 2010a). Two *SHI/STY* orthologues have been identified in *Physcomitrella* and they share transcriptional activator characteristics with *SHI/STY* genes in *Arabidopsis* such as Q-rich sequences and nuclear localization (Eklund et al., 2010b). Expression patterns obtained by transcriptional fusions with GUS reporter genes show SHI expression in caulonemal filaments but not in chloronemal cells in *Physcomitrella*. In the leafy gametophores, *PpSHI* expression is specific to axilliary hairs in the shoot apex and young rhizoids (Eklund et al., 2010b). *PpSHI* expression patterns are highly similar to *GH3:GUS* expression patterns. Consistent with phenotypes obtained by application of exogenous auxin, *PpSHI* overexpression using the 35S promoter promoted the transition of chloronemal to caulonemal cells. Bud

formation and leafy gametophores were induced earlier in *35Spro:PpSHI* lines and free IAA levels were increased dramatically compared to the wild type. Conversely, single knockout lines of either of the two *PpSHI* genes resulted in decreased levels of free auxin, and reduced levels of caulonemal cells compared to chloronemal cells, and reduced elongation of the stems in the leafy gametophores (Eklund et al., 2010b). Compared to the yet controversial role of PAT, these results suggest a prominent role for auxin biosynthesis in patterning the haploid generation of mosses and hint that the genetic programs controlling auxin biosynthesis already existed in the common ancestor of mosses and angiosperms.

AUXIN IN LIVERWORTS

Liverworts compose the most basal lineage of land plants and have either thalloid or "leafy" gametophytes that differ from the axial gametophytes of mosses. Since the 1930's several studies have been published dealing with the morphological effects of a variety of chemicals in liverworts, these chemicals include phytohormones such as auxin and cytokinin but also substances such as acenaphthene, actidione, caffeine, colchicine, naphthalene, chromic acid, parathion, picric acid and socium cacodylate, all of which cause morphological effects (Kaul et al., 1961a). I will focus on studies dealing with auxin analogues and antagonists that are known to cause developmental effects in angiosperms. In the results section I will describe my own observations of developmental effects of exogenous auxin application as well as auxin biosynthesis inhibitors and I propose novel, previously undescribed, roles of auxin in *Marchantia* morphogenesis.

INTRODUCTION

Detection of auxin in Marchantia

In 1926, a Dutch PhD student, Fritz Went (Went, 1926) reported a method for the isolation of a growth substance, later to be confirmed as auxin, that mediated the phototropic bending of coleoptiles extending the observations first made by Darwin (Darwin, 1880). Went developed a quantification assay based on the ability of substances to induce growth, the Avena curvature test, that facilitated the identification of the presence of auxin in a variety of plants (Went, 1928). The extensive literature on the growth behavior of *Marchantia* stimulated interest in whether auxin was responsible for growth in this species. However, early attempts at identifying the growth hormone in *Marchantia* were unsuccessful, leading some to question whether auxin stimulated thallus growth (Goedecke, 1935). Soon after, experiments with exogenous application of auxin and auxin analogs led to profound morphological and growth alterations in *Marchantia* indicating that auxin could act as a growth substance in *Marchantia* (Fitting, 1939)**.** Finally in 1967, improvements in

biochemical techniques facilitated the isolation from *M. polymorpha* thalli of IAA that induced coleoptile growth in the Avena curvature test (Schneider et al., 1967).

Auxin response reporter GH3 in Marchantia polymorpha

The soybean *GH3* promoter and the artificial *DR5* promoter were used to drive *GUS* expression in *Marchantia polymorpha* as putative markers of auxin responses in development. Notably, *pDR5:GUS* lines did not show any staining with or without exogenous auxin, whereas *pGH3:GUS* showed increased activity in response to exogenous NAA in a dose dependent manner (Ishizaki et al., 2012). Sites of expression of un-induced *pGH3:GUS* lines included incipient rhizoids on the surface of 7-10 day old gemmae and the base of mature and developing gemmae cups in the thallus. No expression was detected in the apical notches or along the midrib. Young archegoniophores lacked any *pGH3*:*GUS* activity, but staining was observed in elongating stalks and the lobes of mature archegoniophores. Staining was observed in young antheridiophores and at the base of antheridia in mature stages. In the diploid generation, *GUS* activity was detected throughout the sporophyte in early stages which was later restricted to the foot and seta in mature stages (Ishizaki et al., 2012).

Results obtained from this study do not account for previous observations of polar auxin transport from the apex along the midrib, excision studies dealing with thallus regeneration or rhizoid production (see below). Furthermore, if the meristem is a source of auxin, as it is in flowering plants, the *pGH3:GUS* reporter fails to report this source. If the *GH3* promoter is recognized by some of the endogenous Auxin Response Factors of *Marchantia*, it is not known whether it represents the summary of all *ARF* activity in *Marchantia* or just a fraction of their activity. Thus, the use of alternative reporters, such as promoters of endogenous auxin response genes or *DII-VENUS* should be considered.

Polar auxin transport in Marchantia

As described by (Vöchting, 1885; Douin, 1923; Dickson, 1932; Voth, 1940), excised thalli from *Marchantia polymorpha* exhibited two behaviors: (1) thalli preserving sections of the midrib regenerated a new apical notch from the zone where the old midrib existed; and (2) excised pieces without midrib took longer time to regenerate and developed regenerating buds and apical notches in all directions,

although with a tendency for regeneration to occur from tissues that were originally towards the excised apex. Furthermore, notch formation in midrib-less thalli was enhanced by addition of 10^{-4} g/liter IAA (Binns and Maravolo, 1972). When radioactive auxin (C^{14}-IAA) was fed to the excised thalli and regenerated for seven days, auxin accumulated in the midrib and regenerating tissues suggesting a possible gradient (Binns and Maravolo, 1972). The direction of transport was determined by placing donor blocks of C^{14}-IAA in top, middle and bottom sides of the midrib of the excised notch-less thalli and by measuring radioactivity after a few hours. Such experiments showed that C^{14}-IAA placed in the apical region moved downwards from the apical region, corroborating basipetal gradient. Furthermore, triiodobenzoic acid (TIBA) inhibited basipetal transport just as in angiosperm model systems (Maravolo, 1976). Later studies confirmed basipetal transport but also detected acropetal transport although its strength is considerably less than basipetal, and it was hypothesized that acropetal transport is a result of overwhelming any endogenous transport system with excessive exogenous auxin (Gaal et al., 1982).

Effects of auxin in liverwort growth

Germination and dormancy

While spores do not normally germinate in the dark, treatment with IAA stimulated germination of dark grown spores. Likewise, while gemmae usually do not begin their growth, e.g. produce rhizoids, in the dark, growth on media containing IAA induced them do so (Fitting, 1939).

As described for *Marchantia* (Vöchting, 1885; Douin, 1923; Dickson, 1932; Voth, 1940), in *Lunularia,* excision of an apical notch causes growth of adventitious thalli exclusively from the midrib of the original thallus (Vöchting, 1885; LaRue and Narayanaswami, 1957). This suggests that the midrib of the thallus carries information, perhaps in the form of a hormone, which allows it to regenerate meristematic cells. When excisions disconnected an apical notch from the gemmae cups of *Lunularia,* germination of gemmae within cups was observed. “Germination” was defined as growth of gemmae into a short thallus from at least one of its notches. Germination was inhibited as soon as new adventitious thalli with an apical notch regenerated. It was thus hypothesized that apical notches exert a basipetal gradient of an inhibitory substance that restrict gemmae growth in *Lunularia* (LaRue and

Narayanaswami, 1957). When applying a lanolin paste with NAA, IAA and IBA (5mg/ml) to the apical midrib regions of cut thalli, gemmae germination was inhibited as well regeneration of adventitious thalli. This suggested that in *Lunularia,* auxin plays the role of the proposed inhibitor of gemmae germination and growth (LaRue and Narayanaswami, 1957). When auxin was applied to the basal part of excised thalli (thalli that retained its apical notch), ectopic rhizoid growth was observed as well as the formation of a new thallus from the apical notch, suggesting alternative role for the hormone depending on site of application.

In contrast to *Lunularia*, in *Marchantia polymorpha,* addition of IAA (0.01%) to the top of gemmae cups induce rhizoid production in gemmae although their growth is still slow, suggesting that auxin breaks a part of gemmae dormancy. An inhibitor of germination is thought to exist in *Marchantia,* possibly secreted from gemmae cups themselves as gemmae inside isolated cups did not produce rhizoids until the gemmae cups degenerated (Tarén, 1958). Returning germinated gemmae to their original cup did not stop growth, suggesting that the inhibitory substance does not have an effect after dormancy is initially broken (Tarén, 1958).

Patterns of regeneration and apical dominance

The patterns of regeneration observed by Vöching, Douin, Dickson, and others (Vöchting, 1885; Douin, 1923; Dickson, 1932; Voth, 1940) can be interpreted in light of postulated polar auxin transport. Vöchting noted that in transverse pieces of *Lulularia* thallus regeneration was always polar, in that it occurred from the end that was nearer the excised apical notch. However, if the lateral lobes were removed, but the apical notch remained intact, no regeneration from the cut ends was observed, implying that the apical notch exerts apical dominance over the regeneration process. Subsequent experiments demonstrated that many, if not most, of the cells of the thallus retain the potential to dedifferentiate into totipotent cells. Careful analysis or the regeneration process revealed that regenerants formed towards the ventral side of the cut thallus, implicating a second inherent polarity of the thallus in the regeneration process. One interpretation of this data is that the apical meristem exerts apical dominance during thallus growth, in a manner similar to shot apical meristem dominance over axillary bud growth observed in flowering plants. Furthermore, if auxin is transported basipetally from the apical notch, regeneration might occur at the point in thallus fragments with the highest concentration of auxin.

Apical dominance has also been reported in *Marchantia* in a difference in lobe growth following branching, with the lobe closest to the midrib growing faster than its sister lobe, creating separate unequal lobes. An early separation of the two lobes by thallus excision, releases the smaller lobe from inhibition and conversely, inhibition of lobe growth is restored by addition of IAA (Davidonis and Munroe, 1972).

Auxin has also been reported to cause coiling (extra dorsal growth) of the *Riccia fluitans* thallus, an aquatic liverwort that curls naturally in dry conditions (Prior and Riggs, 1963).

Gemma development and growth

The effects of exogenous IAA, NAA and 2,4-D on gemmae growth have been reported in several studies. As with most studies in which exogenous auxin is applied, the phenotype observed depends upon the concentration of auxin perceived. Furthermore, it is likely that different cell types respond differently due to variations in qualitative and quantitative expression of genes encoding auxin response and transport machinery. This is exemplified in the studies by Rousseau where application of a high level of auxin resulted in stimulation of dorsal rhizoid growth, a cessation of cell division at the apices, and cell elongation of the cells flanking the apices (Rousseau, 1950, 1951b, a, 1952b). Nonetheless, some generalizations of the effects of exogenous auxin in young gemmae can be made as follows: in low concentrations auxin increases the size of the thallus (Ishizaki et al., 2012), breaks gemmae dormancy (Tarén, 1958), produces formation of extra notches in dormant gemmae (Kaul et al., 1962), and restores apical dominance (Davidonis and Munroe, 1972). At higher concentrations auxin promotes the formation of numerous rhizoids on the dorsal side of the gemmae (a dorsiventral patterning defect), and further increases in concentration produce a callus-like tissue with stunted growth (Fitting, 1939; Rousseau, 1950, 1951b, a; Halbsguth and KOHLENBACH, 1953; Rousseau, 1954; Tarén, 1958; Kaul et al., 1961b, 1962; Maravolo and Voth, 1966; Otto and Halbsguth, 1976; Ishizaki et al., 2012).

IAA seems to be more readily metabolized than NAA or 2,4-D by *Marchantia* as plants grown in high concentrations of IAA are able to produce a thallus after going through a callus stage (Kaul et al., 1961b, 1962). However, compared to other land plants *Marchantia* has slow rate of metabolizing IAA to an amide or ester conjugate (Sztein et al., 1999).

Patterning and growth of the thallus

The available data can be synthesized into a model of early patterning and growth of gemmalings. The anchoring of sporelings via differentiation of centrally located rhizoids is the initial step for the formation of a dorsiventral thallus. These rhizoids may behave differently physiologically than the subsequently produced rhizoids that normally form only on the ventral surface. Anchoring results in white light illumination only on one side, which will differentiate as the dorsal side of the plant.

Several lines of evidence suggest that light, gravity and auxin are involved in this polarization. That spores and gemmae do not normally germinate in the dark, and that auxin can substitute for light to induce germination in these circumstances, suggest that auxin synthesis or action is activated by light. Furthermore, that spore germination in liverworts usually requires blue light (Chopra and Kumra, 1988) suggest that it is light in this part of the spectrum that may activate auxin action. Other parts of the light spectrum may also contribute to patterning. For example, red light has been postulated to be required for the development of rhizoids, with far-red light inhibiting rhizoid production (Ninnemann and Halbsguth, 1965; Valio and Schwabe, 1969; Otto and Halbsguth, 1976), implicating involvement of phytochrome signaling. That excess auxin induces dorsal rhizoids suggest that the initial light signal would induce a morphogenetic factor -such as the phytohormone auxin- to accumulate in the ventral side of the sporeling, perhaps by polarizing auxin efflux carriers, or by promoting its synthesis ventrally.

One simplistic model is that light (blue) induces auxin synthesis on the side of the gemmaling towards the light and that auxin is then transported ventrally to induce rhizoid development and ventral identity. Indeed this model has been explicitly stated by Otto and Halbsguth: 'It is conceivable that light causes the production or activation of a rhizoid growth-inducing substance which is then transported away from the irradiated surface' (Otto and Halbsguth, 1976). Note that this model is very similar to that proposed for blue light induced photomorphogenic growth in flowering plants, completing a cycle back to Darwin and Went. Other factors, such as gravity and red light, can also influence establishment of dorsiventrality, but these factors may only become important under conditions of low light levels. Finally, light may also promote the activity of genetic programs, e.g. Class III HD-Zip gene expression

(Sandra Floyd and John Bowman, unpublished observations), involved in the differentiation of air chambers composed of photosynthetic filaments and air pores that antagonize with the formation of rhizoids.

The influence of auxin on thallus growth patterns following establishment of dorsiventrality has not been as intensively investigated since most experiments have been performed by germinating spores or gemmae directly on IAA containing media. However, again some general conclusions may be drawn. First, increases in thallus size and the formation of extra apical notches in IAA treated gemmae suggest that auxin influences branching of the thallus (Kaul et al., 1962; Ishizaki et al., 2012). Second, Rousseau (Rousseau, 1952a, 1953) reported irregular patterns of air chamber development and an upward elongation of gemma cups, indicating that auxin contributes to multiple growth and patterning events during thallus development.

In this following section I explore the effects of exogenous auxin and newly described inhibitors of auxin biosynthetic enzymes on the growth and development of gemmalings.

RESULTS

Application of exogenous auxin and auxin analogues

To address the role of auxin in the gametophyte of *Marchantia polymorpha,* I grew clonal gemmae in the presence of exogenous synthetic auxin analogues naphthalene-1-acetic acid (NAA) and dichlorophenoxyactetic acid (2,4-D). Because auxin also influences the formation of a variety of structures in angiosperms (i.e. roots, leaves, flowers, cotyledons and vascular tissue), I examined whether any additional tissues of the thallus or developmental processes affected by exogenous auxin. I applied auxin to young undifferentiated gemmae and also to established dorsi-ventral thalli. For application to established thalli, gemmae were grown on Gambourg's B5 media and later transferred to 10 μM NAA or 10 μM 2,4-D plates.

Exogenous synthetic auxin analogue application to gemmae between days 0 to 6 post plating triggered ectopic rhizoid formation on the dorsal surface of the thallus (Fig. 1A-B), from regions that would not normally produce rhizoids, e.g. the regions that would normally give rise to the wings. There is no development of air chambers/air pores or gemmae cups, but plants are not completely ventralized as there

is no dorsal scale formation. However, neither do plants develop normally into a lobed thallus with clear distinctions between apical notches and midribs. This might be due to meristem activity inhibition, making all developmental pathways converge exclusively to rhizoid formation such that little other growth/differentiation is observed.

Application of auxin analogues after growing 6 to 10 days in B5 media caused the development of a thallus with excessive rhizoids, although only restricted to the original central zones of the gemmae and mostly from the ventral side of the thallus. Thus, the meristematic cells composing the apical notch no longer respond to exogenous auxin by producing rhizoids, but the cells of the central zone of the gemmae can still respond in this manner. This indicates that by day 6 of growth, most dorsal cells have lost the capacity to produce rhizoids in response to auxin. However, dorsal defects are seen, with the dorsal side of the thallus having poorly developed air pores (Fig. 1C-D) that are not clearly open or are just partially formed, air chambers that are asymmetric and disorganized, and the dorsal epidermis forms an uneven surface with air pores protruding upwards (Fig. 1D). No gemmae cup development is observed.

Application of auxin analogues to thallus after 12 to 18 days of growth in B5 media caused previously produced gemmae cups to continue to grow resulting in a tubular elongate appearance (Fig. 1E-F). The gemmae cups grew as if they exhibited a gravitropic response. Likewise, the growing tips of the thallus bend downwards, a growth pattern reminiscent of epinastic growth of leaves of seed plants in response to high levels of auxin,. Again, the shapes of the air chambers were asymmetric, spatially disorganized and protruding upwards (Fig. 1F).

In contrast to synthetic auxins, application of 10 μM indole acetic acid (IAA) to gemmae failed to induce ectopic rhizoids or tubular cups, suggesting the *Marchantia* is able to metabolize IAA more efficiently than other auxin analogues**,** consistent with earlier studies. Similar experiments as describe above were not performed for IAA 10 μM.

Application of an inhibitor of auxin biosynthesis

As a complementary approach I tested the effect of the auxin biosynthesis inhibitor L-Kyneurenine (L-Kyn) on gemmae development. L-Kyn acts as an alternative substrate and competitive inhibitor, for the *TRYPTOPHAN*

AMINOTRANSFARASE OF ARABIDOPSIS1 (*TAA1*) and *TRYPTOPHAN AMINOTRANSFERASE RELATED1* (*TAR1*) enzymes, thereby inhibiting the transition of Tryptophan (Trp) to indole-3-pyruvic acid (IPyA), a key step in auxin biosynthesis (Stepanova et al., 2008; Tao et al., 2008; He et al., 2011). In *Arabidopsis*, the phenotype of plants grown in the presence of 100 µM L-Kyn resembles the phenotype of the *wei8 tar2* double mutant (the *weak ethylene insensitive8* mutant is a null loss-of-function allele of *TAA1*) (He et al., 2011).

I applied 100 µM L-Kyn to wild type gemmae and established thalli, early and late developmental stages, respectively, as described above for the application of exogenous auxin. When gemmae are grown in the presence of L-Kyn from day 0 a slight decrease in ventral rhizoid numbers is observed. Thalli grew and branched in a manner similar to control thalli grown in standard B5 media. However, thalli grown in the presence of L-Kyn from day 0 are unable to produce normal gemmae cups, with gemmae cup rims failing to fully develop and very small propagules inside a depression (Fig. 1I-J).

Application of L-Kyn to established thalli that had grown for 7 days in B5 Media caused gemmae cups derived from different apical notches to become fused into a single structure (Fig. 1K-L). The extent of fusion varied, with some cups less fused than others, possibly because they had already been established before transferring the plants to L-Kyn. Gemma cup development occurs after a new apical meristem is formed. After branching, there is a growth phase that separates the apical notches prior to a new round of gemmae cup formation. By inhibiting auxin synthesis, we observed reduction of the growth phase that separates the notches before gemmae cups are produced, this could explain the fusion of adjacent cups.

Ectopic expression of DII-VENUS reporter line.

I tested a putative auxin maxima reporter line based on *DII-VENUS* of *Arabidopsis* (Brunoud et al., 2012) by translationally fusing the degron domain 2 of the endogenous MpAUX/IAA to the amino-terminal end of a triple tandem repeat of YFP with a carboxy-terminal Nuclear localization signal (*3X-VENUS-N7*) (Heisler et al., 2005). This chimeric gene was driven by the *MpEF1* promoter (to be described in more detail in Chapter 6), which drives expression essentially constitutively. Interestingly, sporelings transformed with *MpDII-VENUS* exhibit dramatic phenotypic defects. Primary transformants have strong, intermediate or weak

phenotypes. Strong (Fig. 2B) and intermediate (Fig. 2C) phenotypes are similar to each other and I classified then in terms of their size, with strong phenotypes having excessively dwarfed thalli. Both strong and intermediate types have a reduction in lamina expansion, delayed bifurcation and no gemmae cup production. They are able to form dorsal air chambers and ventral rhizoids and thus dorsiventrality is not affected. From a population of 74 primary transformants, 39 plants had strong (Fig. 2B), and 17 intermediate (Fig. 2C) phenotypes after 3 weeks of growth in 2 rounds of selective media (i.e. 75% of the lines have phenotypic effects). Weak lines had a phenotype similar to that of wild type. When observing fluorescence, most lines had very weak signals throughout the thallus (Fig 2D). Unfortunately, I was not able to detect a robust and constant spatio-temporal fluorescence pattern among several independent transformants.

DISCUSSION.

Novel roles of Auxin in patterning the thallus of Marchantia.

Our series of pharmacological studies differed from previous reports as they were able to test the role of exogenous auxin and auxin inhibitors in different stages of gemmaling development. We classified gemmae development into three main phases depending on their capacity to respond to exogenous auxin: An early phase up to day 4 of gemmaling development with "weak" developmental robustness, where exogenous auxin application channels all meristematic activity into rhizoid differentiation. At some point in this period a robust dorsiventral polarity must be established in gemmalings. In a second intermediate phase, up to day 10 of gemmaling development, exogenous auxin application no longer disrupts dorsiventral polarity but it sill has a strong effect on ventral rhizoid elongation and production. Most importantly dorsal cells do not differentiate into rhizoids and plants are able to form a lobed thallus, air chambers are the most affected structures in this phase and it might be plausible to hypothesize that auxin is required for proper air pore development. In a third phase, from day 12 of gemmaling development, plants are more resilient to exogenous auxin application. One hypothesis is that excess auxin may be transported into gemmae cups, this in turn could be explained by the action of polar auxin transport. Alternatively, auxin conjugating enzymes (such as *GH3*) could be metabolizing auxin in all regions except the gemmae cups. Interestingly, this late

response shows a gravitropic response, consistent with the notion that auxin is a hormone that transduces a gravity stimulus.

While my pharmacological studies using auxin biosynthesis inhibitors (L-Kyn) did not induce polarity defects, different developmental effects on thallus development were observed and some of these were complementary to defects induced by excess exogenous auxin. In early stages of development, auxin biosynthesis inhibition disrupted gemmae cup and gemmae formation, as well as rhizoid formation (although rhizoid formation was difficult to analyze quantitatively). In later stages of development L-Kyn application disrupted the growth phase (branching) that spatially separates notches before they start producing gemmae cups, resulting in gemmae cups produced by two adjacent apexes fusing into a single structure. This fusion suggests that fields of cells are communicating to act coordinately in the development of a single gemmae cup, indicating *Marchantia* exhibits plasticity during organogenesis. A question that remains unanswered is whether L-Kyn application affects also the rates of bifurcation, as this could be linked with phenotypes seen in the following chapters. Magnus Eklund has grown gemmae in higher concentrations of L-Kyn (up to 500 μM), showing that individuals loose their capacity to grow, with amorphous patterning and lack of dorsiventrality establishment, suggesting a prominent role for auxin biosynthesis in patterning the thallus (see next chapter for a description of auxin insensitive plants). All of these chemicals could also be analyzed in the sporophyte generation to get an introductory idea on the role of auxin in this stage of development.

Combining information gathered from the extensive body of literature and our pharmacological experiments, I can say that the role of auxin in thallus development is just as varied as it is in angiosperms. Recapitulating, auxin is involved in rhizoid determination (establishment of dorsiventral polarity), polar thallus regeneration, gemma and apical cell dormancy, gemmae cup development, air pore development, and spacing of organs during branching. This suggests that the common ancestor of embryophytes may have used auxin in a variety of processes. Although the precise morphology and anatomy influenced by auxin in this common ancestor is as yet unclear, the antagonisms with light reported by Fitting, Halbsguth, and others, as well as the convergences between auxin transport inhibition and klinostat treatments

suggest that auxin was a key player in linking the key environmental cues shaping embryophyte morphology outside an aquatic medium.

Development of Auxin maxima reporters is challenging in Marchantia.

The development of auxin maxima or auxin response reporters is another useful tool to link developmental processes and specific genetic pathways to auxin metabolism. As reported in the introduction, the lack of signal of the soybean *GH3:GUS* reporter in apical notches and midribs suggests an incomplete picture of auxin responsiveness in *Marchantia*. As described in chapter 1, synthetic auxin reporters are based on transcriptional fusions of artificial tandem copies of auxin response elements with reporter genes or on degradation of reporter genes in response to auxin. In an organism with a simple genomic structure, where most of the auxin genetic toolkit is represented by single genes, introducing such reporter constructs could affect transcriptional homoestasis. This appears to be the case observed using *MpDII-VENUS*, where plants harboring the construct have growth and differentiation defects. In this particular case, introducing additional *TIR* targets might compromise degradation of *AUX/IAA* proteins by *TIR*. This would in turn create additional copies of functional *AUX/IAA* repressors even in the presence of auxin, generating a putative *ARF* loss-of-function phenotype. Consistent with the hypothesis that such reporters interfere with auxin homeostasis, Sandra Floyd (personal communication) tested variations of *DR5*-type constructs, where multiple copies of AuxREs are positioned in several tandem repeats upstream of a reporter gene. These constructs also create phenotypic defects, such as disorganized rhizoid production and short stature, consistent with perturbations in auxin hemostasis. In this case, *ARF* loss-of-function phenotypes are potentially created by ARF sequestration into targeting transgenic constructs. Transcriptional analysis and phenotypic comparisons between *MpARF* loss-of-function and “auxin maxima reporters” will lead to understanding the effects of this type of construct in the plant. The pathway to creating a stable auxin maxima/response reporter in *Marchantia* requires perhaps the use of endogenous auxin responsive promoters.

MATERIALS AND METHODS

Exogenous auxin assays. Dormant gemmae were plated on ½ Gambourgs B5 media with 10 µM 2,4-D or NAA (SIGMA). Several assays were performed to test developmental effects of auxin in different gemmaling developmental stages. Gemma were grown or transferred to auxin media after the following periods in Gambourgs B5 media: 0, 2, 4, 6, 8, 10, 12, 14 and 16 days. 3 main phenotypic classes were obtained and figure 1 shows representatives of each class: class I contains plants grown from 0 to 4 days in B5 media prior to transfer to auxin media; class II, plants grown 6 to 10 days prior to transfer and class III, plants grown 12 to 16 prior to transfer.

Auxin biosynthesis inhibitor. L-Kyneurenine was obtained from SIGMA and diluted in DMSO for a 50mM stock. 100 µM working solutions were tested in a similar fashion to exogenous auxin assays. Only two phenotypic classes were obtained, those plants grown 0 to 10 days in B5 media prior to transfer to auxin media and plants grown 12 to 16 days in B5 prior to transfer to auxin media. The latter show the fusion in gemmae *cup primordia.*

Microscopy. Plants were observed in Lumar.V12 dissecting microscope (ZEISS) and photographed with a AxioCam HRc prior to fixation in FAA (EtOH 50%, Glacial acetic acid 5%, Formaldehyde 10%, water up to 100 ml) overnight at 4°C. Samples were dehydrated in an ethanol series from 50%, 70%, 95% and two rounds of 100% for at least 30 minutes. Samples were critical point dried with Baltec CPD 030 and sputter coated with gold using atmospheric argon in a Baltec SCD 005. Scanning Electron Microscopy was performed with Hitachi S-570 at 10kV and photos were digitalized using SPECTRUM® Software.

MpD2VENUS construction. A 467 bp fragment was amplified with KOD polymerase from MpAUX/IAA containing proteolysis domain II and upstream sequence but not the EAR domain, using primers longD2MpIAAKpnI-F and D2-MpIAA-R-BamHI-AUXmaxV2. The fragment was cloned in pCRII and sequenced. KpnI and BamHI were used to subclone into *pEF1* 3XVENUSN7 in BJ36 a shuttle vector with the EF1 promoter driving three tandem copies of reporter gene VENUS

fused to a NLS in the C-terminal end. The resulting construct was in turn subcloned into HART binary vector using NotI. HART is a binary vector with a double CamV35S promoter driving *Hyg* resistance gene.

Plant transformation and culture. *Marchantia* transformation was based as directed in (Ishizaki et al., 2008). Growth prior *Agrobacterium* infection was made in liquid 0M51C media sucrose 2% in 100 ml flasks for 9-11 days. *Agrobacterium* strain GV3001 was transformed with binary vectors and cultured for 2 days at 28°C in LB media and culture for 2-4 hours in 10ml of 0M51C media with 1µl of 100 µM Acetorsyringone prior to co-cultivation with *Marchantia* spores for a period of 48-60 hours. Transformants were selected in Hygromicin (10 µg/ml) Gambourg's B5 ½ media plates. After 10-15 days, survivors were re-plated to a second round of selection in fresh Gambourg's B5 ½ Hyg plates for 1 week, and later transferred to Gambourg's B5 media or stored at 4°C for storage and subsequent use.

Primers

Primer Name	Sequence
longD2MpIAAKpnI-F	**GGTACC**ATGAGCTCCAGCAACAGCCCCTCGTCCGAGG
D2-MpIAA-R-BamHI-AUXmaxV2	A**GGATCC**CAAGTTCTTCCGGAACGATCGAATGGG

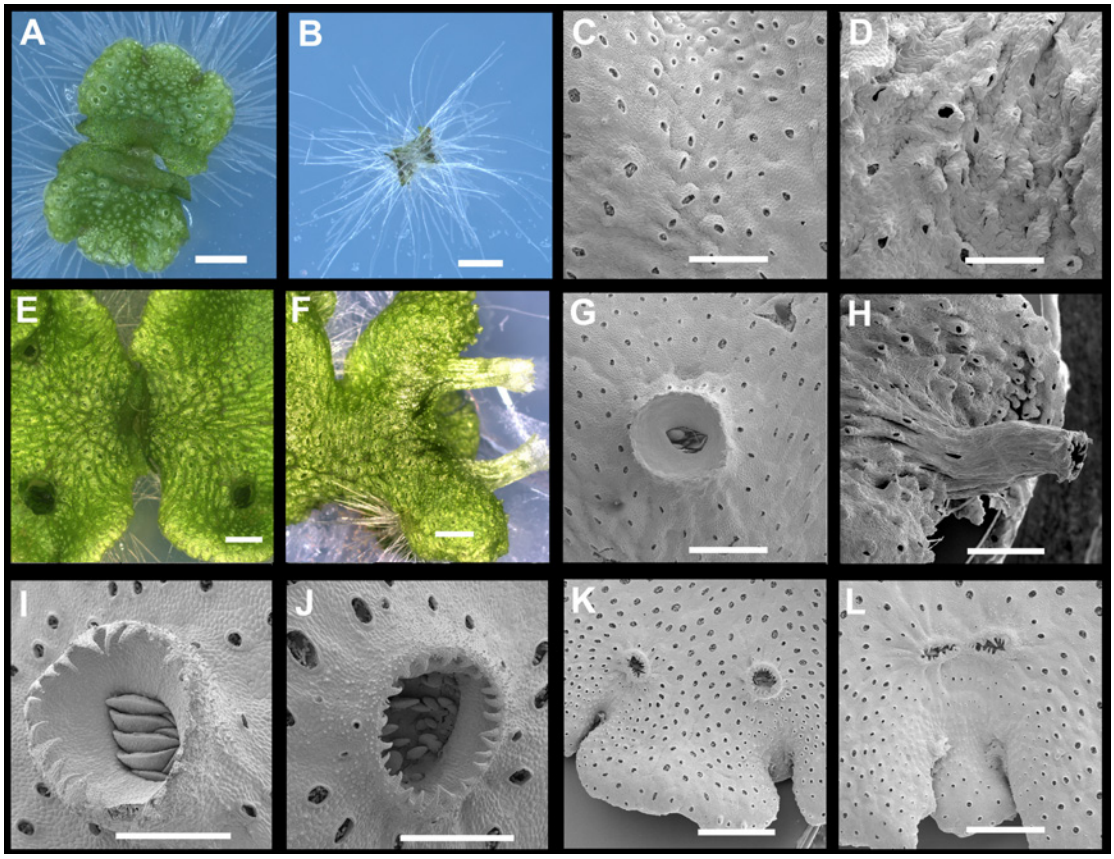

FIGURE 1. Developmental effects of auxin in the *Marchantia* thallus. (A) Wild type gemma after 10 days of growth in B5 media, scale bar = 1mm **(B)** Wild type gemmae grown for 10 days in 10 µM NAA B5 media, scale = 1 mm **(C)** Wild type epidermis 15 day old thallus, scale bar = 0.6 mm **(D)** Wild type epidermis of 15 day old thallus, transferred on day 6 from B5 media to 10 µM 2,4-D media, scale bar = 0.6 mm **(E)** 23 day old wild type thallus, scale bar = 1mm **(F)** 23 day old wild type thallus transferred to 10 µM NAA media after 16 days in B5 media, scale bar = 1 mm **(G)** Wild type mature gemmae cup grown in B5 media, scale bar = 1 mm **(H)** Wild type mature gemmae cup of 17 day old gemmaling transferred to 10 µM 2,4-D media after 12 days in B5 media, scale bar = 1 mm **(I)** Wild type mature gemmae cup, scale bar = 0.5 mm **(J)** Wild type mature gemmae cup of plants grown on L-Kyn 100 µM from day 0 **(K)** Mature thallus grown in B5 media showing thallus lobe separating bifurcated apical notches, scale bar = 1.2 mm **(L)** Mature thallus of plants grown in B5 media for 7 days and later transferred to L-Kyn 100 µM, showing a smaller lobe spacing apical notches and fused gemmae cup primordia, scale bar = 0.75 mm.

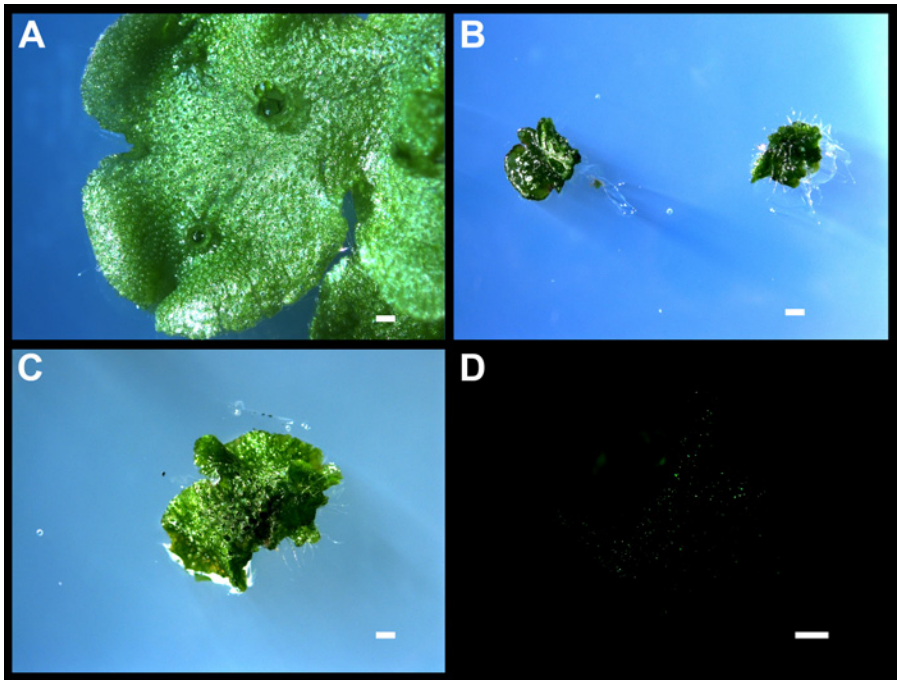

FIGURE 2. *MpD2VENUS* causes developmental effects in *Marchantia.* (A) Reporter line (*C1HDZIP:GUS*) transformed at the same time as *MpD2VENUS* with a wild type phenotype, scale bar = 1mm **(B)** Strongest phenotype of *MpD2VENUS* lines with same age as in A**,** scale bar = 1mm **(C)** Intermediate phenotype of MpD2VENUS lines, scale bar = 1mm **(D)** Intermediate *MpD2VENUS* lines have limited fluorescence, scale bar = 1mm**.**

CHAPTER 6

Dominant versions of the *MpTOPLESS* co-repressor disrupt auxin response signaling in *Marchantia*.

INTRODUCTION.

In this chapter I focus in disrupting the transcriptional output of the auxin-signaling pathway by creating transgenic plants expressing dominant alleles of endogenous *Marchantia* orthologue of *TOPLESS* (*MpTPL*). *Arabidopsis* experiments have shown that TPL with domains 3 and 4 derived from an AUX/IAA can recruit class A ARF proteins into a repressor complex. Chimeric TPL-BDL fusions mimic a loss-of-function ARF allele by constitutively binding to ARF proteins via domains 3 and 4 in an auxin insensitive fashion (Szemenyei et al., 2008). Conversely, a loss-of-function TPL allele using the dominant negative allele TPL^{N176H} creates a protein that is unable to appropriately keep activator ARF proteins in check in the absence of auxin and phenocopies the loss-of-function pentuple *tpl* mutant where TPL and all its paralogues have been inactivated (Long et al., 2006; Szemenyei et al., 2008). In either of these cases, it is not clear whether repressor ARF proteins (class B or C) are affected as the repressor ARF proteins do not appear to interact with AUX/IAAs in *Arabidopsis* (Vernoux et al., 2011).

RESULTS

MpTPL expression pattern

To characterize the expression pattern of *MpTPL* and therefore its potential role in development we fused a genomic region 3.6kb upstream of the start codon of *MpTPL* with the fluorescent reporter gene *3xVENUSN7* and analyzed fluorescence in different developmental stages of the gametophyte. The length of the promoter region was chosen after identifying the next open reading frame upstream of the *MpTPL* loci. The expression pattern presented is a consensus of more than 10 independent lines. Reporter gene expression in ungerminated gemmae (Fig. 1A), 5 day old gemmae (Fig. 1B) and in mature 25 day old thallus (Fig. 1D) it is highly concentrated in the meristematic regions although it is possible to see signal throughout the thallus (Fig. 1C). *pTPL:3xVENUS* lines have the strongest signals in mature thalli, apical notches,

gemmae cup primordia, as well as mature gemmae cups (Fig. 1A-D). *pTPL:3xVENUS* plants have high *VENUS* expression in both archegonoiophores (Fig. 1F) and antheridiophores (Fig. 1G), particularly in the dorsal umbrella-like caps but not in the putative archegonial notches (archegonia are extensions of the thallus and could have meristematic cells). Transfer of mature *pTPL:3xVENUS* plants to 10 μM 2,4-D plates resulted in a decreased level of expression of reporter genes, suggesting a possible regulatory feedback between auxin and *TPL* expression (Fig. 1E).

EF1 promoter

As a tool for ectopic expression we used the 1.7 kb promoter region of the *Translation Elongation Factor 1* (EF1) from *Marchantia.* This promoter was first identified in Prof. Takayuki Kohchi's lab in a screen searching for useful promoters to constitutively drive transgene expression. The EF1 promoter (pEF1) was chosen over the 35S Cauliflower Mosaic Virus (pCaMV35S) promoter for its ability to drive strong gene expression in the apical notch. Because most developmental processes take place in the apical notch, it was essential to choose a promoter driving gene expression in this region. In contrast, the pCaMV35S promoter drives high levels of expression in the differentiated regions of thalli and does not drive expression at high levels in the meristematic regions (Ishizaki et al., 2008). To examine the temporal and spatial pattern of gene expression driven by pEF1, I created *pEF1:citrine* plants. In *pEF1:citrine* plants, fluorescence can be detected throughout the thallus (with higher intensity than the TPL promoter), with the highest levels in the apical notch and both developing and mature gemmae cups (Fig. 2A). Within gemmae cups, fluorescence signal in *pEF1:citrine* plants is detected in dormant gemmae (Fig. 2B). Although it might not drive expression in all cell types of *Marchantia*, the pEF1 represents a useful tool for 'constitutive' temporal and spatial over-expression analyses.

MpTOPLESS gain-of-function alleles

Part 1: pEF1:MpTPL

I first ectopically expressed the wild-type MpTPL protein driven by the EF1 promoter (*pEF1:MpTPL*). Haploid organisms may be potentially more sensitive to changes in gene expression conferred by transgenes, especially for those genes that act in a dose dependent fashion, as observed in the case of *TPL* in *Arabidopsis* (Long

et al., 2006). Therefore, I anticipated that developmental defects might be observed in *TPL* overexpression in *Marchantia*.

Thallus size in *pEF1:MpTPL* plants is diminished compared to that of wild-type plants (Fig. 2C-D), plants are slightly compact, with thallus wings being less flat than the wild type and with an inner depression along the midribs (Fig. 2D). The epidermal tissue is rather dark green, reminiscent of early developing air chambers (Fig. 2D). Most notably, gemmae cup formation is disrupted, with gemmae cups entirely absent in some cases, (Fig. 2E-F). The loss of gemmae cups did not impair the formation of gemmae, as it is possible to see naked gemmae and gemmae primordia formed in isolated spots at the positions where gemmae cup would normally develop along the midrib (Fig. 2F).

Part 2: pEF1:MpTPL-D34 and pMpTPL:MpTPL-D34

I next designed experiments based on fusions of MpTPL with domains 3 and 4, the protein-protein interaction domains of AUX/IAA and ARF proteins. The protein generated, MpTPL-D34, should be able to interact with endogenous ARF proteins through domains 3 and 4 ameliorating their response to auxin, and thus, mimicking loss-of-function ARF phenotypes (Szemenyei et al., 2008). We translationally fused MpTPL to domains 3 and 4 of each of the three *Marchantia* ARFs, the endogenous *Marchantia* AUX/IAA, the *Arabidopsis* BDL/IAA12 protein, and two genes (*isogroups12370* and *04655*) of unknown function that possess domains 3 and 4 but no ARF3 B3 or AUX/IAA dII domains (Figure 3 and See chapter 3 for more details). All fusions were driven by the EF1 promoter (e.g. *pEF1:MpTPL-D34*^{MpIAA}).

pEF1:MpTPL-D34^{MpBDL} plants failed to develop a clear dorsiventral thallus, instead remaining an unorganized tissue mostly composed of a cluster of cells without any organization (Fig. 4A). It was possible to detect a few rhizoids, scales and air chambers but none of these structures were organized in a particular manner, and they did not compose the main tissue of the plant. Since no organized thallus developed, no gemmae cups were formed. Similar phenotypes were obtained with *pEF1:MpTPL-D34*^{MpARF1} (Fig. 4B), *pEF1:MpTPL-D34*^{MpARF2} (Fig. 4C), *pEF1:MpTPL-D34*^{04655} (Fig. 4D), *pEF1:MpTPL-D34*^{12370} (Fig. 4E) and *pEF1:MpTPL-D34*^{MpIAA} (Fig. 4H-I). In contrast, *pEF1:MpTPL-D34*^{MpARF3} (Fig. 4F) was also tested but it did not cause the same effect as other domains 3 and 4 and it will be described in later paragraphs.

One prediction of constitutively expressing MpTPL-D34 proteins is that activator ARF activity should be downregulated, even if MpAUX/IAA proteins are degraded due to the presence of auxin - i.e. the transgenic plants should be largely auxin insensitive. Therefore we transferred *pEF1:MpTPL-D34*^{MpIAA} plants to auxin media and analyzed their capacity to develop previously described phenotypes induced by exogenous auxin. *pEF1:MpTPL-D34*^{MpIAA} plants exhibited development of ectopic rhizoids in the presence of auxin (Fig 4I-J), leading us to conclude that either rhizoid development is independent of ARF activity, or alternatively, that the auxin transcriptional response is not entirely eliminated in *pEF1:MpTPL-D34*^{MpIAA} plants.

One possibility is that the pEF1 does not drive expression at high enough levels in all auxin responsive cells. Thus, we used the 3.6 kb endogenous *MpTPL* promoter to drive expression of *MpTPL-D34*^{MpIAA} *(pMpTPL:MpTPL-D34*^{MpIAA}). *pMpTPL:MpTPL-D34*^{MpIAA} lines had a similar but slightly weaker phenotype than *pEF1:MpTPL-D34*^{MpIAA}: plants failed to pattern a flattened thallus and also formed a cluster of unorganized cells similar to wild type prothalli, but some plants were able to form a single gemmae cup that produced gemmae (Fig. 4K, M and N). The gemmae from these cups have a disorganized shape with multiple extensions and a thin and sharp morphology, and the two apical notches conspicuous on wild-type gemmae are not apparent (Fig. 4N and P). Weak *pTPL:MpTPL-D34*^{MpIAA} lines were able to form a thallus, although the lamina did not extend beyond the midrib, forming a very narrow and elongated thallus with aberrant gemmae cups in which gemmae have developed rhizoids while inside the cup. Importantly, when strong transgenic lines are grown in the presence of 10 μM 2,4-D for 12 days, they were auxin insensitive as assayed by the lack of ectopic rhizoids (Fig. 4K-L). These results suggest that the chimeric MpTPL-D34 protein is capable of creating auxin insensitive plants if expressed in the appropriate cells at appropriate levels.

As described in a previous section, MpTPL fusion experiments with domains 3 and 4 of *MpAUX/IAA, AtIAA12, MpARF1, MpARF2, Mpig04655* and *Mpig12370* driven with the *EF1* promoter generated very similar strong phenotypes. However, the fusion using domains 3 and 4 of *MpARF3* failed to disrupt patterning in a manner comparable to domains 3 and 4 from other genes tested. *pEF1:MpTPL-D34*^{MpARF3} plants were able to form a dorsi-ventral thallus as ventral rhizoids, dorsal air chambers and gemmae cups were formed. However, although the thalli have a

convoluted surface (Fig. 4F), with a depression along the midrib and with folded lobes into the apical notches, creating more compact thalli compared to the wild type (Fig. 4F). The implications of this experiment will be elaborated in the discussion.

MpTOPLESS loss-of-function alleles

In *Arabidopsis*, a missense mutation in *TOPLESS* substituting Asparagine 176 with Histidine, creates a dominant negative allele that results in a similar effect to creating a pentuple *tpl tpr* loss-of-function phenotype. (Long et al., 2006). The dominant negative protein specifically affects the auxin response machinery, despite the involvement of *TOPLESS* with other hormonal signaling pathways (Braun et al., 2011). We generated an analogous mutant version of *MpTPL* substituting the conserved Asparagine 176 by a Histidine ($MpTPL^{N176H}$) and drove its expression with pEF1.

$pEF1{:}MpTPL^{N176H}$ plants exhibit an aberrant phenotype consistent with a disruption in auxin response. The most noticeable phenotype of $pEF1{:}MpTPL^{N176H}$ plants is an increased frequency of bifurcation of the thallus compared to the wild-type and the control *pEF1:MpTPL* plants (Fig. 5A-B). The result is a highly branched compact thallus that has 6 or 7 apical notches in the space in which the wild type would normally have one apical notch (Fig. 5B). Perhaps as a consequence of this, the production of gemmae cups was delayed up to a month after plating. As described before, after a bifurcation of the apical notch wild-type plants produce a new gemmae cup. It seems that $pEF1{:}MpTPL^{N176H}$ plants remain in the bifurcation program compromising the production of gemmae cups. When produced, $pEF1{:}MpTPL^{N176H}$ gemmae cups are aberrant , being narrow and having a slight tubular structure reminiscent of gemmae cup phenotypes that develop in the presence of exogenous auxin (Fig. 5C and D). Gametophore development is also affected in $pEF1{:}MpTPL^{N176H}$ plants. $pEF1{:}MpTPL^{N176H}$ gametophores are short in stature as they do not elongate upwards as do gametophore in wild type (Fig. 5E and F). Although short in stature, more gametophores are produced in $pEF1{:}MpTPL^{N176H}$ lines as a consequence of having more apical notches (Fig. 5E and F). $pEF1{:}MpTPL^{N176H}$ archegoniophores have ectopic single filaments protruding from large than normal apertures in the epidermis of dorsal caps (Fig. 5G and H).

If $pEF1{:}MpTPL^{N176H}$ is creating a dominant negative allele, one expectation is that phenotypes observed may be similar to those generated by gain-of-function

alleles of some *MpARF* genes, in particular those of activator ARF genes. To test whether *pEF1:MpTPL*^{N176H} creates a phenotype similar to a gain-of-function *MpARF* phenotype, we generated *pEF1:MpARF1* plants. While *pEF1:MpARF1* plants did not present the same phenotype as *pEF1:MpTPL*^{N176H}, a slight increase in the rate of bifurcation compared to wild type was noted. Statistical quantification of the rate of branching may be required as the phenotype is not obvious (Fig. 6 A and B). Alternatively, ectopic expression of *MpARF1* lacking domains 3 and 4 may generate stronger *AUX/IAA* insensitive phenotypes as shown in *Arabidopsis* (Krogan et al., 2012).

DISCUSSION

TOPLESS corepressor can be used to disrupt auxin responses in Marchantia.

MpTPL overexpression. I used the highly conserved *TPL* corepressor in *Marchantia* to disrupt auxin responses assuming this function would be conserved throughout embryophytes. There are no over-expression experiments of *TPL* in *Arabidopsis* reported, and given there are five paralogues, it is not clear whether it would result in aberrant phenotypic effects. However, in *Marchantia*, with a single paralogue, a dosage effect is observed. The lack of gemmae cups in *EF1:MpTPL* lines can be interpreted as a complementary phenotype compared to the elongation of cups observed when mature thalli are plated on media containing auxin, i.e *TPL* represses gene activity involved in cup production. These results support the hypotheses that *MpTPL* interacts with components of the auxin signaling pathway in gemmae cup primordia and that *MpTPL* acts in dose dependent manner. Furthermore, the phenotypes are consistent with the idea of gemmae cup primordia as sources or sinks of auxin maxima (see chapter 5), and that gemmae cup development is one of the most sensitive tissues to disruptions in auxin homeostasis.

MpTPL-D34 Fusions. The rationale behind these experiments is that the translational fusion of domains 3 and 4 with TPL should result in a transcriptional corepressor that can interact with ARF proteins through domains 3 and 4 and this interaction would be insensitive to auxin. I used all domains 3 and 4 found in genes in the *Marchantia* genome, except for the domains associated with the NGA homologue. Variations in

phenotypes between the various constructs would most likely reflect the differential interaction capabilities of the domains 3 and 4 from different genes.

Constitutively expressing the fusion protein *MpTPL-D34*^{MpIAA}, creates auxin insensitive plants, whose phenotype possibly mimics that of multiple loss-of-function ARF proteins capable of interacting with AUX/IAA proteins. These phenotypes show that auxin response plays a general role in the establishment of essential internal cues for organized patterning, cell growth and differentiation. However, due to the severity of the phenotypes, it is not possible to dissect specific patterning roles of auxin, such as those observed by pharmacological experiments (chapter 5). Driving the fusion proteins with tissue or cell type specific promoters is required to dissect these roles further. Although many *MpTPL-D34* lines had a general unorganized growth, several lines are able to produce limited growth (Fig 3C), and may phenotypically resemble early stages of development where sporelings transition through a prothallus stage before acquiring a lobed thallus with multiple cell layers. I will return to this theme in my final conclusions.

Similar phenotypic effects were obtained using MpTPL-D34^{MpIAA}, MpTPL-D34^{MpBDL}, MpTPL-D34^{MpARF1} and MpTPL-D34^{MpARF2} fusion proteins. This suggests that ARF1 can homodimerize, that ARF1 and ARF2 can heterodimerize and that AUX/IAAs and MpARF1 and MpARF2 are able to heterodimerize. This latter scenario may not occur in the thallus, as *MpARF2* is not detectably expressed in this developmental stage.

The fact that similar results to the previously mentioned fusions also occur with the overexpression of MpTPL-D34^{Mp04655} and MpTPL-D34^{Mp12370}, suggests a putative auxin independent mechanism of regulating ARF complex formation. The role of these novel genes as positive or negative regulators of auxin signaling is yet unknown. However, they might act by mechanisms similar to those seen in small interfering peptides in *Arabidopsis* (Wenkel et al., 2007; Seo et al., 2011; Seo et al., 2012).

Finally, the *EF1:MpTPL-D34*^{MpARF3} lines have stunted growth but are able to produce a dorsiventral thallus with distinctive apical notches, air chambers and gemmae cups along a mid-rib. This suggests that MpARF3 interacts with a different affinity compared to MpARF1 and AUX/IAA proteins, and thus its regulation might be independent of the auxin signaling pathway.

Different promoters show that auxin response is involved in patterning different structures.

My initial experiments with *MpTPL-D34* fusions were performed with the *EF1* promoter. Surprisingly, these lines were able to morphologically respond to auxin despite the drastic phenotypes disrupting general patterning, growth and dorsiventrality. This could be explained by three possibilities: 1. *EF1:MpTPL-D34* fusions do not disrupt auxin response, at least with respect to rhizoid induction; or 2. Rhizoid production is a auxin dependent ARF independent developmental process; or 3. A lack of expression of the TPL-D34 chimeric proteins in all auxin responsive tissues could account for ectopic rhizoid production. The availability of the *TOPLESS* promoter allowed me to test these alternative scenarios, with my results supporting the second possibility. Interestingly, both *EF1* and *TPL* promoters have similar expression patterns at least at a macroscopic level. However, the fact that *pTPL:TPL-D34*^{MpIAA} in auxin media do not form ectopic rhizoids, suggests that *pTPL* drives stronger expression in rhizoid initials that *pEF1*. With respect to dorsal tissues, *pTPL:TPL-D34*^{MpIAA} lines sometimes develop gemmae cups with gemmae while *pEF1:TPL-D34*^{MpIAA} plants never develop gemmae cups. Therefore, *pEF1* has stronger expression levels in gemmae cup primordia than *pTPL*. This experiment shows the importance of using the promoters of the genes being studied in order to make proper statements about their function.

Dominant negative alleles of TPL.

The conserved asparagine in amino acid 176 in across all TPL embryophyte orthologues allowed testing the dominant negative *tpl-1* mutation (caused by a substitution of Asparagine 176 for Histidine) in *Marchantia*. In *Arabidopsis* strong *tpl-1* phenotypes the shoot meristem is transformed into a root meristem and in plants exhibiting weaker phenotypes, the shoot meristem fails to form and embryos have fused cotyledons (Long et al., 2002). In *Arabidopsis*, a single amino acid substitution phenocopies the pentuple mutant of all *TOPLESS* related genes (Long et al., 2006). Furthermore, translational fusions of the TPL^{N176H} protein fused to GFP in a wild-type background recreate the *tpl-1* phenotype despite the presence of 5 wild type proteins, suggesting this experiment was feasible in *Marchantia*.

I was able to observe a robust consistent phenotype in multiple *EF1:MpTPL*^{N176H} plants with the increase in branching rates the most obvious effect,

followed by aberrant gemmae cups (when formed) and short archegoniophore stature. I was unable to determine if these effects are a result of ectopic *ARF* expression as they could be caused by mis-regulation of other genes repressed by *MpTPL*. The partial convergence with auxin phenotypes, such as branching defects and aberrant gemmae cup development, suggests that at least some of the phenotypes are due to alterations in auxin signaling. However, overexpression of the class A *MpARF1* activator using p*EF1* did not recapitulate the *EF1:MpTPL*^{N176H} phenotype. This suggests that additional de-repressed factors might be behind some of the phenotypic effects in a *EF1:MpTPL*^{N176H} background. Furthermore, the effects of the *MpTPL*^{N176H} allele should be tested using the *MpTPL* promoter to drive its expression.

In *Arabidopsis,* TPL is necessary for proper BDL mediated ARF repression (Szemenyei et al., 2008). However, no reported ARF mis-regulation converts shoots into roots. The only genes causally linked to the shoot to root conversion are the master root meristem determinant *PLETHORA* (PLT) genes: *PLT1*/*2* are mis-expressed in the SAM in *tpl-1* embryos and triple *tpl-1 plt1-5 plt2-1* embryos do not develop double roots, making *PLT* genes necessary for the shoot to root conversion in *tpl-1* (Smith and Long, 2010; Prasad et al., 2011). Chromatin immunoprecipitation expriments also suggest that *TPL* directly represses *PLT* expression in the apical region of the embryo (Smith and Long, 2010). Furthermore, *PLT* expression disappears in single *mp-T470* and double *nph4-1 mp-G12* loss-of-function class A ARF mutants (Aida et al., 2004). A possible scenario to involve ARFs in this network would require class A ARF Activators as positive regulator of PLT genes in the presence of auxin (Aida et al., 2004).

Intriguingly, in *Marchantia,* bifurcation rates can be increased by mis-expression of class C ARFs in the apical notch (see following chapter), and class C ARFs can produce conversions of cotyledons into roots if mis-expressed in *Arabidopsis* (John Alvarez, unpublished data). These results are intriguing as there is no evidence that class C ARFs interact with TPL via AUX/IAAs (Vernoux et al., 2011). Protein interaction screens of ARFs, TPL and IAAs in *Marchantia* will be necessary to further address these questions.

MATERIALS AND METHODS

Cloning of MpTOPLESS. MpTPL was cloned using cDNA from wild type *Marchantia* thallus using *extaq* (TAKARA) and degenerate primers TPL-F1 and TPL-R1 that flanked a conserved region in the MpTPL transcript. A nested PCR using a second set of degenerate primers TPL-F2 and TPL-R2 internal to the initial region amplified a 1kb fragment that was cloned in pCRII and sequenced. New gene specific primers were designed based on the partial cDNA fragment of MpTPL and used in 5'RACE ready cDNA synthesized with the GAGA primer and a 5'RACE adaptor. For 5'RACE experiments UPM and TPLR4 primers were used using touchdown PCR changing the alignment temperature from 70°C to 60°C. A second nested PCR was performed using primers NUP and TPLR3 with similar PCR conditions. For 3'RACE, an external PCR performed using TPLF3 and the GAGA primer and a nested PCR was used using primers TPLF4 and GAGA. All fragments were cloned in pCRII and sequenced. A full-length transcript was finally amplified with proofreading KOD polymerase using primers MpTPL-SalI-F and MpTPL-EagI-R and cloned and sequenced in pCRII, this clone was named 1416G.

MpTPL^{N176H}. PCR based mutagenesis using "assembly PCR" was used to create *MpTPL*^{N176H}. An initial set of two PCR fragments were KOD amplified using primers M13F and MpTPL(N176H)-R (fragment1) and primers MpTPL(N176H)-F and M13R (fragment 2) and using 1:50 *MpTPL* in pcRII (1416G) as template. Both fragments 1 and 2 were used as templates in a subsequent PCR reaction and amplified with primers M13F and M13R. This final PCR product (named 1626) was cloned in pCRII and sequenced to corroborate a successful mutagenesis.

Vector engineering. The EF1 promoter was amplified with primers MpEF1-NdeI-F and MpEF1-SalI-R, cloned into pCRII and sequenced. It was subcloned into the shuttle vector BJ36 using NdeI and SalI sites. This new plasmid was called EF1proBJ36 V2.0 and it is used to create constituve expression constructs. MpTPL was cut from pcRII with EcoRI and inserted in EF1proBJ36V2.0, several clones were obtained and checked for orientation. Subsequently EF1:MpTPL BJ36 was subcloned into binary vector HART using Not I. HART is a binary vector created by Sandra Floyd based on BART (used for *Arabidopsis* transformation). In contrast to BART

that confers BASTA resistance to plants, HART has two CamV35S promoters in tandem driving a Hygromicin Resistance gene (*hptII*).
MpTPL^{N176H} was cloned into entry Gateway vector pE2B using EcoRI sites (inserting in place of the ccdB gene), checked for orientation and used to perform an LR reaction to recombine into PKIGWB2 (a Gateway based binary vector provided by Kimizune Ishizaki of Takayuki Kohchi's lab).

Reporter construct. The 3.6Kb fragment of the MpTPL promoter was amplified using primer MpTPLproF5-NdeI and MpTPLproR1-SalI cloned and sequenced in pCRII (3685). The *MpTPL* promoter was subcloned into *3XVENUSN7BJ36* using NdeI and SalI. *3XVENUSN7* has 3 copies of YFP Venus with a C-terminal Nuclear localized sequence Plasmid and was kindly provided by Marcus Heisler and David Smyth (Heisler et al., 2005). *MpTPLpro*:*3xVENUSN7* BJ36 was subcloned into HART using NotI sites. Promoter sequences were obtained by assemblying partial 454 reads from the first *Marchantia* genome drafts provided by JGI. Once a putative assembly was made, experimental corroboration of promoters were performed using PCR and a number of forward nested primers (based on the putative promoter) and a reverse primer sitting in the start codon of the *MpTPL* transcript.

MpTPL-D34 fusions. A *MpTPL* transcript without a stop codon was amplified using primers MluI-MpTPL-ATG-F and EcoRI-MpTPL-NoSTOP-R and cloned into EF1-BJ36V2.0 using MluI and EcoRI sites. Subsequently domains 3 and 4 of MpAUX/IAA(EcoRI/HindIII), MpARF1(EcoRI/EcoRI), MpARF2 (EcoRI/HindIII), MpARF3 (EcoRI/HindIII), Mpisotig04655(HindIII/HindIII), Mpisotig12370 (HindIII/HindIII) were amplified from WT thallus cDNA with primers adding restriction enzymes and cloned and sequenced in pCRII. Each D34 was subcloned into *EF1pro:MpTPLNoSTOP* BJ36 and orientation checks were performed in the cases where directional cloning was not possible. All constructs were subcloned into HART using NotI.
Fusions using the endogenous *MpTPL* promoter were made by subcloning the MpTPL promoter with Nde and MluI and subcloning into *EF1:MpTPL-D34*^{MpIAA} BJ36 and subsequently subcloning into HART using NotI.

Plant transformation and culture. *Marchantia* transformation was based as directed in (Ishizaki et al., 2008). Growth prior *Agrobacterium* infection was made in liquid 0M51C media sucrose 2% in 100 ml flasks for 9-11 days. *Agrobacterium* strain GV3001 was transformed with binary vectors and cultured for 2 days at 28°C in LB media and culture for 2-4 hours in 10ml of 0M51C media with 1µl of 100 µM Acetorsyringone prior to co-cultivation with *Marchantia* spores for a period of 48-60 hours. Transformants were selected in Hygromicin (10 µg/ml) Gambourg's B5 ½ media plates. After 10-15 days, survivors were re-plated to a second round of selection in fresh Gambourg's B5 ½ Hyg plates for 1 week, and later transferred to Gambourg's B5 media or stored at 4°C for storage and subsequent use.

Microscopy. Light and electron microscopy were performed as described in chapter 4.

Primer Name	**Sequence (5' to 3')**
TPL-F1	GTNGAYGACAAYCGCTAYTCMATG
TPL-F2	CTKATYAAYCARAGYCTCAATTGG
TPL-R1	ATWGCNCCTTCRCTYTCATTCCT
TPL-R2	TCCCAMACCTTGATNGTYTTRTCATC
MpTPLF3	AGCTGCTCTTACTCCCTCTCCGAATCCAGC
MpTPLF4	GAATGTTGCCAGGACTCTTCATCAGGGCTC
MpTPLR3	AAGCTGGATTCGGAGAGGGAGTAAGAGCAG
MpTPLR4	GAGCCCTGATGAAGAGTCCTGGCAACATTC
MpTPL-SalI-F	ATGTCGACAGACAGGGGCGATAGGAACAGCGTACAATG
MpTPL-EagI-R	ATCGGCCGTTGTATACACTGGCTTTCAAGCAGCCACGG
MpTPL(N176H)-F	GGACCCTTATCCACCAAAGCCTGAATTGG
MpTPL(N176H)-R	CCAATTCAGGCTTTCGTGGATAAGGGTCC
MpEF1-NdeI-F	ATCATATGCAAATGAGTCACACACATTGTTGAG
MpEF1-SalI-R	ATGTCGACCAACCTTTCTGCAGGCACATCAATACTG
MpTPL pro F5-NdeI	ATCATATGTCTTGTTCCGGGAAATACCGGGATATAGTCC
MpTPL pro R1-SalI	ATGTCGACTGTACGCTGTTCCTATCGCCCCTGTCTATCGAATGG
MpTPL pro F1 int	TCGTGCGTGCGCGCTTCGGGTCGGTGCGCTTCTCC
MpTPL pro R1	TGTACGCTGTTCCTATCGCCCCTGTCTATCGAATGG
MpTPL pro F2-CORR	AGAACATTCAACGCGCGACGACTTCCTCAGCC
MpTPL pro F3-COR	ATCACCTGGTTCCAGTGCCGGGTAGTTAACC
MpTPL pro F4-COR	ACTTGAACACGAACCGGCTAGTTTTGCAACC
MpTPL pro F5-COR	TCTTGTTCCGGGAAATACCGGGATATAGTCC
EcoRI-MpIAA-DIII/IV-F	**taGAATTC**GCTGTTCAGTCAAACTCCTGGTTTGTG
HindIII-MpIAA-DIII/IV-R	**taAAGCTT**TCACACGTTCGGTTGAGTCGTCTTGTTTG
EcoRI-MpARF1-DIII/IV-F	TA**GAATTC**CCCGTATCTTCTCCCCAGCGGAGC
EcoRI-MpARF1-DIII/IV-R	TA**GAATTC**TCAGGGGCACCCCCGCTGGGCATC
EcoRI-MpARF2-	**GAATTC**TTCCAACAAGGTCCAGTTCGTAGCTACACG

DIII/IV-F	
HindIII-MpARF2-DIII/IV-R	AT**AAGCTT**CTACATGTCGTCGCCGCGCGCCCCGCC
MpARF3-D34REAL-EcoRI	A**GAATTC**GGTGAGTCCTTCTCGCACTGCAAAG
MpARF3-D34REAL-HindIII	A**AAGCTT**CTACTGCGACCGCGTTTTGCCGTTG
HindIII-ig12370-DIII/IV-F	**taAAGCTT**TCCACCAAAACCTTTGAGGACCTAC
HindIII-ig12370-DIII/IV-R	**taAAGCTT**TTAGTACTGTTTCAAAGTTCCAGTTC

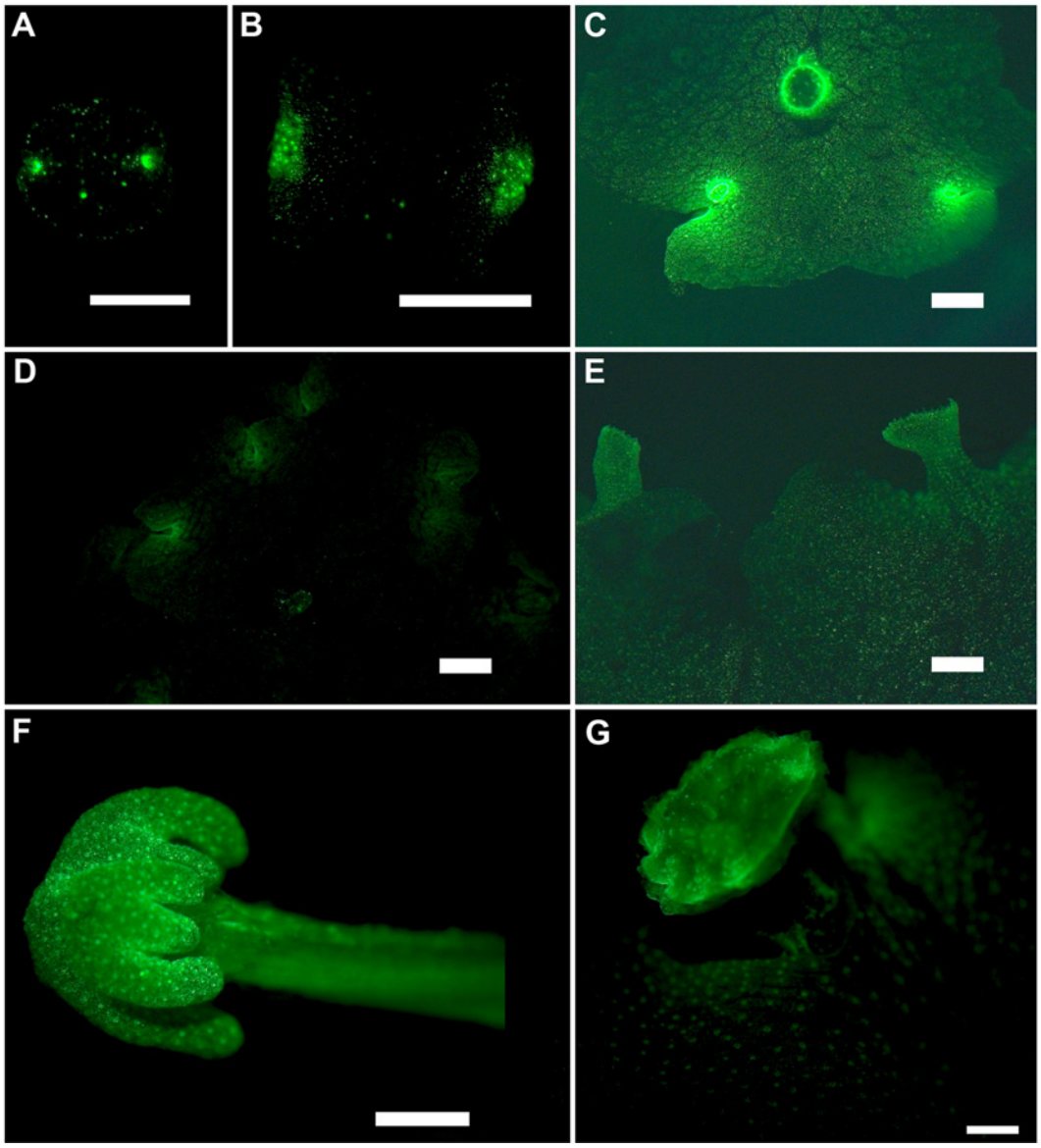

FIGURE 1. *MpTPL* expression patterns. (A) Day 0 un-germinated Gemma **of** *pTPL:3xVENUSN7* with expression in 2 apical cells, scale bar = 0.250 mm **(B)** 5 day old gemmae of *pTPL:3xVENUSN7*, scale bar = 0.5 mm **(C)** Mature *pTPL:3xVENUSN7* line with expression in young and old gemmae cups, scale bar = 1 mm **(D)** Mature *pTPL:3xVENUSN7* line, 25 days old with expression in apical notches, scale bar = 1 mm **(E)** *pTPL:3xVENUSN7* plants grown in 2,4-D 10µM B5 ½ after 16 days of growth in B5 ½ media **(F)** Archegoniophores of *pTPL:3xVENUSN7* plants **(G)** Young antheridiophores of *pTPL:3xVENUSN7* plants.

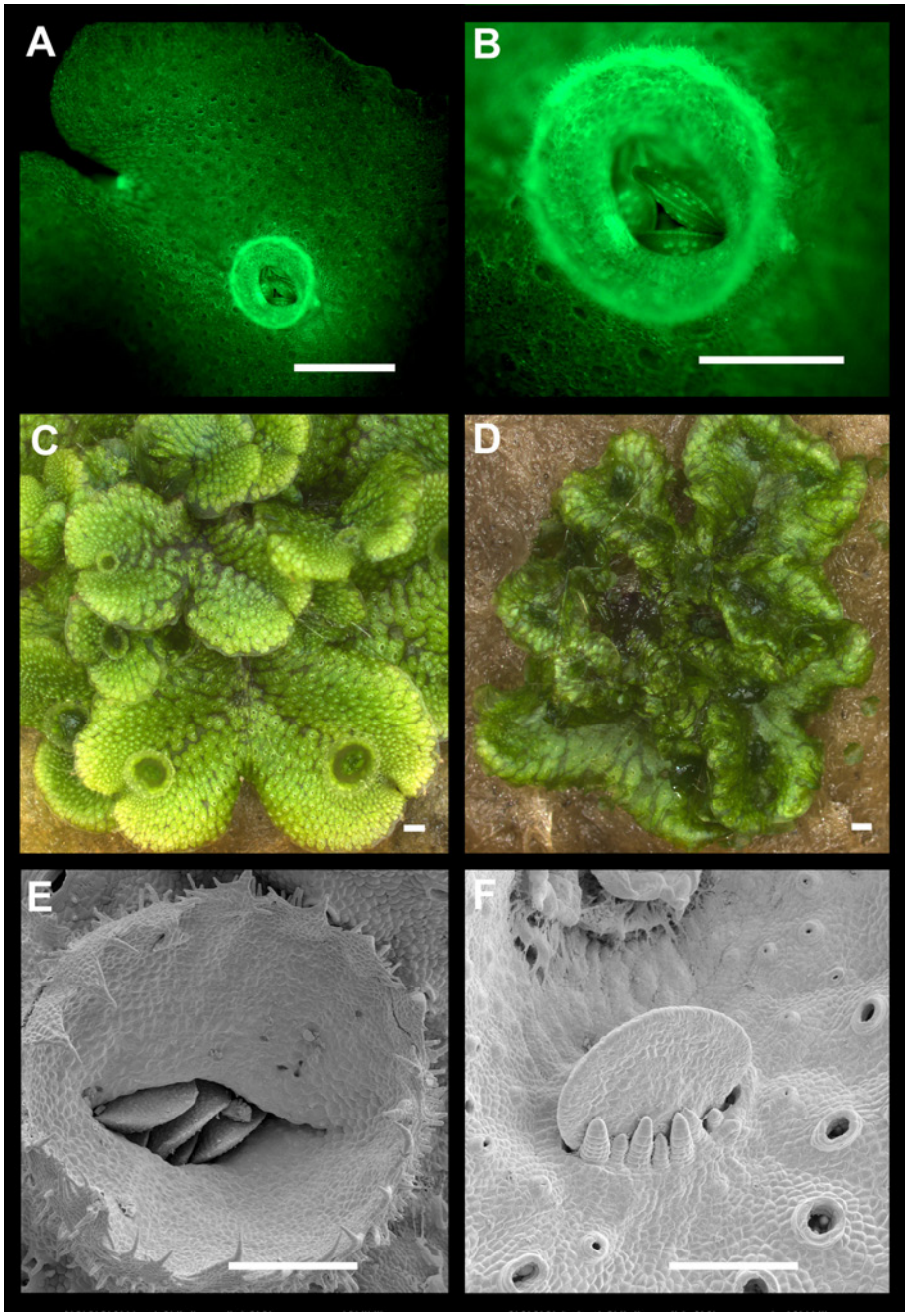

FIGURE 2. Developmental effects of *MpTPL* overexpression. (A) *pEF1:citrine* overview of thallus development with strong expression in apical and gemmae cup rims, scale = 1mm. **(B)** *pEF1:citrine* also drives expression in dormant gemmae, scale bar = 0.5 mm. **(C)** Wild type mature thallus, scale bar = 1 mm. **(D)** *pEF1:MpTPL* representative line, showing decresed wing expansion and thallus depressions along the midrib as well as dark green air chambers that resemble juvenile tissue, scale bar = 1mm. **(E)**. Wild type mature gemmae cup with dormant gemmae inside, scale bar = 300 µm. **(F)** *pEF1:MpTPL* plants have no geamme cups, repsentative line with naked

mature dormant gemmae and gemmae primordia with filaments growing by transversal cell divisions, scale bar = 150 µm.

FIGURE 3. Amino acid alignment of domains 3 and 4 of protein-protein interaction. *Marchantia* has 6 proteins that potentially interact with each other via domians 3 and 4. All domain were tested in this study by fusions with the C-terminal end of MpTPL, except for D34 of ARF5/MP and MpRAV2-like. Alignment shows only the most conserved regions of both domains. Note how MpARF3 and MpRAV2-like have the least conserved domains 3 and 4.

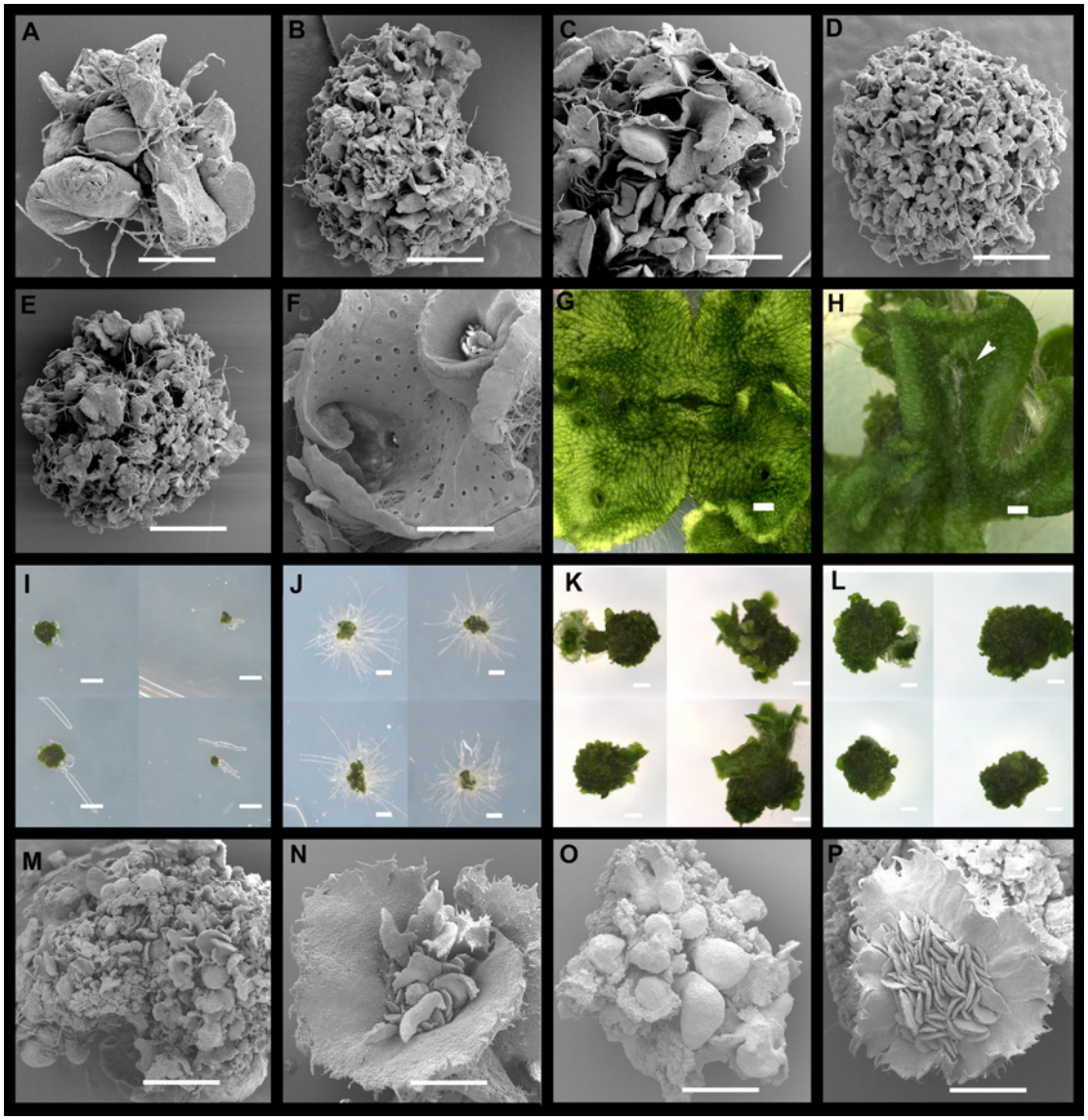

FIGURE 4. Creation of auxin insensitive plants by disrupting auxin response in *Marchantia*. (A) Strong *pEF1:MpTPL-D34*^{AtBDL} line showing a lack of organized patterning, dorsiventral polarity and a limited degree of differentiation. Scales, air pores and rhizoids are visible in random places. No thallus expansion is observed and growth is severely affected, scale bar = 430 µm. **(B)** *pEF1:MpTPL-D34*^{MpARF1} line showing a disorganized undifferentiated thallus similar to the prothallus stage of wild-type development, scale bar = 1 mm. **(C)** *pEF1:MpTPL-D34*^{MpARF2} line showing wider thallus wings but still undifferentiated, perhaps with a weaker phenotype than other fusion constructs, scale bar = 1 mm. **(D)** *pEF1:MpTPL-D34*^{Mpig04655} line, scale bar = 1mm. **(E)** *pEF1:MpTPL-D34*^{Mpig12370} line, scale bar = 1.36 mm. **(F)** *pEF1:MpTPL-D34*^{MpARF3} lines are able to differentiate into mature stage of development with gemmae cups and a more clearly established dorsi-ventral polarity

with dorsal air chambers and ventral rhizoids, thallus is not expanded and flat and rather folded along the margins so there is a depression along the midrib, scale bar = 860 µm. **(G)** Wild type mature thallus, scale bar = 1mm. **(H)** Weak *pTPL:MpTPL*^{MpIAA} are able to form a mature thallus although the depression along the midrib resemble *EF1:MpTPL* lines. Arrowhead point at gemmae cups with rhizoids, possibly protruding from inside gemmae as a sign of dormancy disruption. **(I)** Compound image with four representative *pEF1:MpTPL-D34*^{MpIAA} lines grown in B5 ½ media for 15 days as a control for auxin response experiment, scale bars = 1mm. **(J)** Compound image with four representative *pEF1:MpTPL-D34*^{MpIAA} lines grown in 2,4-D 10µM B5 ½ media for 15 days, these plants remain with its characteristic morphology but are able to produce ectopic rhizoids in respone to auxin. **(K)** Compound image with four representative *pTPL:MpTPL-D34*^{MpIAA} lines grown in B5 ½ media for 12 days as a control for auxin response experiment, scale bars = 1mm. **(L)** Compound image with four representative *pTPL:MpTPL-D34*^{MpIAA} lines grown in 2,4-D 10µM B5 ½ media for 12 days do not produce or elongate ectopic rhizoids, scale bars = 1mm. **(M)** Representative *pTPL:MpTPL-D34*^{MpIAA} line grown in B5 ½ media with characteristic prothalli like appearance, scale bars = 0.86 mm. **(N)** *pTPL:MpTPL-D34*^{MpIAA} lines occasionally produce gemmae cups with aberrant gemmae inside, scale bar = 0.5 mm. **(O)** *pTPL:MpTPL-D34*^{MpIAA} lines grown in 2,4-D 10µM B5 ½ media do not produce ectopic rhizoids, scale bar = 0.86 mm. **(P)** *pTPL:MpTPL-D34*^{MpIAA} gemmae cups grown in 2,4-D 10µM B5 ½, scale bar = 0.6 mm.

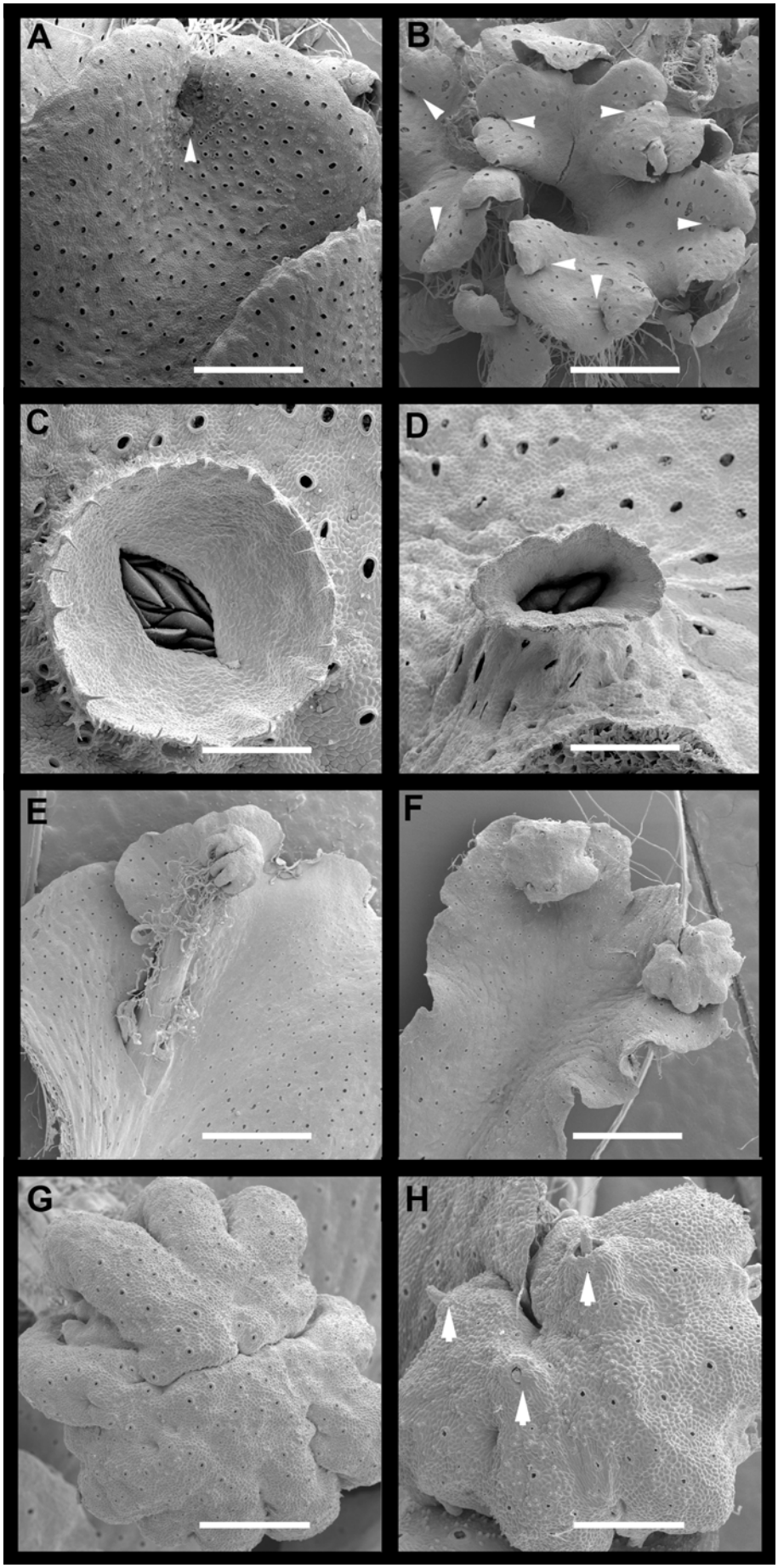
A
B
C
D
E
F
G
H

FIGURE 5. Developmental effects of dominant negative *MpTPL*^{N176H} protein.
(A) Wild type thallus with arrow head pointing at single apical notch, scale bar = 1.36 mm. **(B)** *pEF1:MpTPL*^{N176H} lines with compact and multibifurcated thalli with at least 7 apical notches (arrowheads) produced in a similar area compared to A, scale bar = 1.5 mm. **(C)** Wild type mature gemma cup, scale bar = 0.5 mm. **(D)** *pEF1:MpTPL*^{N176H} gemmae cups are elongated and narrow, similar to developmental effects produced by exogenous auxin application in the wild type, scale bar = 0.6 mm. **(E)** Wild type thallus with young archegoniophore elongating upwards form the apical notch, scale bar = 1.2 mm. (F) *pEF1:MpTPL*^{N176H} archegoniophores do not elongate and remain short and close to the original apical notch, scale bar = 1.2 mm. **(G)** Wild type archegoniophore dorsal surface, scale bar = 0.43 mm. **(H)** *pEF1:MpTPL*^{N176H} archegoniophores produce exposed protrusions in dorsal side and do not elongate the 9 lobes that compose the gametophore, scale bar =0.3 mm.

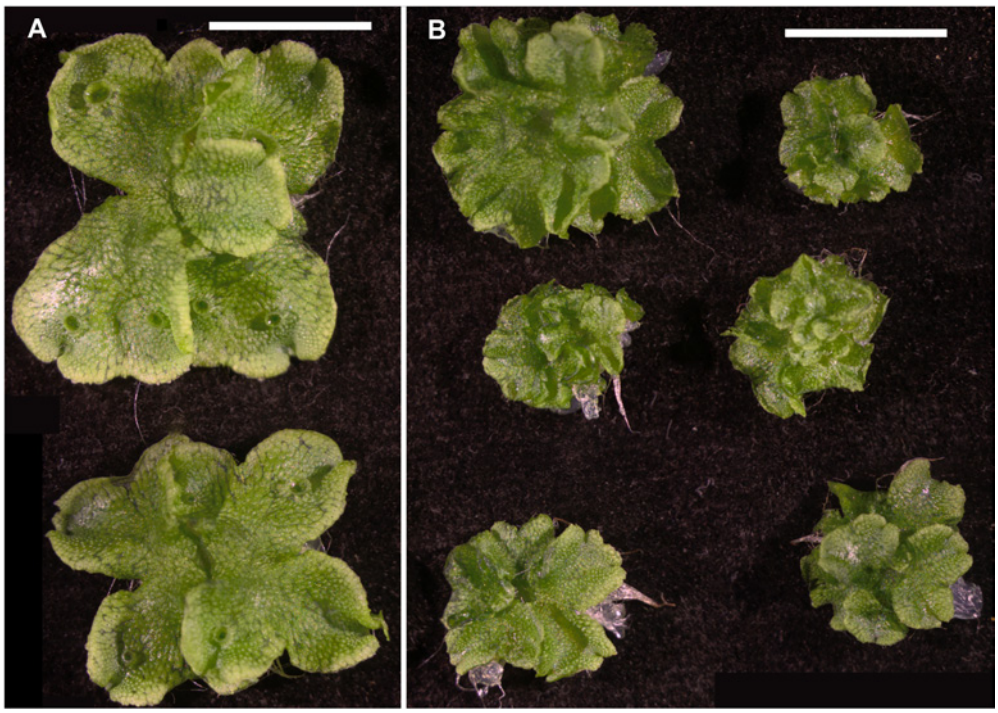

FIGURE 6. *MpARF1* overexpression. (A) Wild type mature thallus **(B)** *pEF1:MpARF1* showing 6 independent lines that do not show any strong phenotype but it is possible to see an slight increase in notch production, both lines were grown simultaneously from gemmae.

CHAPTER 7

Analysis of *MpARF3:* A putative promoter of undifferentiated cell states.

As reported in Chapter 1, Bayesian phylogenetic trees place *MpARF3* within class C *ARFs*, a lineage sister to class A and B *ARFs*. The phylogenetic tree indicates class C *ARFs* have experienced fewer gene duplications than the other two ARF lineages within the embryophytes. In *Arabidopsis*, orthologues of *MpARF3* are thought to act as transcriptional repressors that do not heterodimerize with AUX/IAA proteins (Vernoux et al., 2011). In this regard, they can be considered auxin independent transcriptional regulators in *Arabidopsis*. As mentioned in the previous chapter, the only protein-protein interaction domain 3 and 4 of that did not produce aberrant phenotypes in chimeric fusions with *MpTPL* was that of MpARF3, suggesting its interactions with MpARF1 are limited. Through the analysis of gain- and loss-of-function alleles of *MpARF3* we addressed the specific roles of *MpARF3* in *Marchantia* development.

RESULTS

MpARF3 is regulated by MpmiR160

Class C ARF orthologues are regulated by miR160 in *Arabidopsis* (Mallory et al., 2005; Wang et al., 2005; Liu et al., 2007). It has been postulated that miR160 regulation is conserved in mosses and lycophytes due to presence of *MIR160* transcripts and *miR160* target sites in *Selaginella moellendorffii* and *Physcomitrella patens* (Axtell et al., 2007; Finet et al., 2012). In *Marchantia*, a putative *miR160* binding site in *MpARF3* is conserved and resides in a similar position with the transcript (Fig. 1A), suggesting that *MpARF3* is also regulated by *miR160*.

I assembled the endogenous *MpMIR160* locus by using the highly conserved 14 nucleotide region of the microRNA binding site of *MpARF3* (Fig1A) as a BLAST query against unassembled genomic sequences provided by JGI. A non-coding locus possessing the complementary 14 nucleotides that was not the genomic sequence of *MpARF3* was assembled. However, this locus is not identified as an isogroup in the transcriptome data, suggesting it is expressed at low levels or the primary transcript is unstable, the latter being a common feature of microRNA transcripts. When this

sequence was analyzed for potential secondary structure with m-fold (*http://mfold.rna.albany.edu/?q=mfold/RNA-Folding-Form*), a stem-loop structure with potential miR and miR* sequences was obtained (Fig. 1B). The predicted secondary structure resembles that of *MIR160* loci encoded in the *Arabidopsis* genome, although different mismatches between miR and miR* sequences are noted, and these differences might be important for species-specific recognition by DICER to produce a functional microRNA (Fig. 1C).

Expression pattern of MpARF3 in the thallus

Genomic sequence 3.6kb upstream of the *MpARF3* coding sequence was transcriptionally fused with the *GUS* coding sequence (*pMpARF3:GUS*) to provide insight into endogenous *MpARF3* gene expression. The length of the putative promoter was decided because the next ORF upstream of *MpARF3* is approximately 3.6 kb away. This putative promoter of *MpARF3* directs expression of *GUS* in the apical notch and along the midrib of the thallus (Fig. 2A-C). In young 3-day-old gemmae, expression is detected in the apical notches cells and in scattered cells throughout the central zone (Fig. 2A). In 9-day-old gemmae expression extends from the apical notches along the midrib but the expression in cells of the central zone has disappeared (Fig. 2B). In mature thalli, expression remains restricted to regions around the apical notches, along the midrib, and in both developing and mature gemmae cups (Fig. 2C). Expression was also detected in mature female gametophores but male gametophores and sporophytes were not examined in *pMpARF3:GUS* lines (Fig. 2D).

To explore the role of *miR160* in regulating *pMpARF3:GUS* reporter gene expression, I fused the *miR160* binding site in-frame to the C-terminal end of the GUS gene, transcriptionally fused with the endogenous *MpARF3* promoter (*pMpARF3:GUSmiR160*). Surprisingly, 10 independent plants showed an expansion in the spatial domain of *GUS* expression rather than the decrease expected due to cleavage of GUS transcripts by *MpmiR160* (Fig. 2E and F). To clarify this enigma, I generated an additional sequence where the *miR160* binding site was incorporated into the 3'UTR region of the transcript (*pMpARF3:GUS-3'UTRmiR160*). I observed again in 10 independent lines an expansion in the spatial domain of expression patterns (Fig. 2G and H).

Reduction of MpARF3 function results in pleiotropic effects

To reduce the activity of *MpARF3,* I constitutively expressed both *Arabidopsis* (*AtMIR160*) and *Marchantia* (*MpMIR160*) *miR160* precursors, as either gene should potentially target *MpARF3* transcripts. Expressing the minimal (220 bp) *AtMIR160a* precursor under the control of the EF1 promoter (*pEF1:AtmiR160a*) in *Marchantia* does not produce any aberrant phenotypes, suggesting that there may be specific information lacking in the minimal *AtMIR160a* stem loop that prevents it from being functional in *Marchantia*. This is especially intriguing as this short *AtMIR160a* precursor is functional in *Arabidopsis*.

I cloned the stem loop of the putative *MpmiR160* gene, with approximately 200 additional bases flanking each side of the stem loop (total of 511 bp) and constructed a transcriptional fusion with the EF1 promoter in *Marchantia* (*pEF1:MpmiR160*). Approximately 85% of *pEF1:MpmiR160* plants (N=79) displayed a similar phenotype that differs considerably from that of the wild type. First, *pEF1:MpmiR160* plants bifurcate less frequently such that the lobes between apical notches are bulkier and not as flat as in wild-type thalli (Fig. 3A-D). Second, while the thallus lobes appear larger, individual cell size is decreased relative to that of the wild type (Fig. 3E and F). Third, perhaps as a consequence of the slower rate of branching, fewer gemmae cups develop (Fig. 3C and D). Fourth, while the gemmae cups that develop appear relatively normal, in most lines gemmae either fail to develop within the cups, or gemmae develop but their growth is slowed downed significantly, so that mature plants have very small propagules within the cups (Fig. 3G and H).

To quantitatively analyze bifurcation rates in *EF1:MpmiR160* lines, I used simultaneously transformed *EF1*:*MpmiR160* and a control line that expresses a reporter gene (*pC1HDZIP*:*GUS*) that would have a wild-type bifurcation pattern. In addition, I included a line created by Magnus Eklund, where an apical notch specific promoter (pSHI) drives expression of *MpmiR160 (pSHI:MpmiR160)*. After 20 days of growth, control lines (*pC1HDZIP:GUS*) bifurcated 3 times faster than *pEF1:MpmiR160* lines (*t test* $P=1.04^{-22}$) (Fig. 4A and Table 1). The control lines bifurcated approximately 1.25 times faster than *pSHI*:*MpmiR160* (t test P=0.005) lines, although in this latter difference, standard deviations overlap between control and *pSHI:MpmiR160* bifurcation averages (Fig. 4A and Table 1). I counted apical notches in these lines after an 8 day period, observing that the number of apical

notches in each of the genotypes doubled: control *pC1HDZIP:GUS* lines went from 8 to 16 apical notches, while *pSHI:MpmiR160* plants grew slightly less, from having 6 to 11 notches, and *pEF1:MpmiR160* lines from having an average of 2 in the first measurement to and average of 4 apical notches in the second measurement (Fig. 4B and Table 2).

When induced to produce reproductive structures, *pEF1:MpmiR160* plants displayed phenotypic defects, most conspicuously in antheridiophores (male gametophores). In the wild type, antheridia are embedded internally in the antheridiophore. In contrast, antheridiophores of *pEF1:MpmiR160* plants produce ectopic growths of putative antheridia externally on dorsal surfaces (Fig. 3I and J). In the wild type, sperm is dispatched by small pores in the dorsal surface of antheridiophores whereas in *pEF1:MpmiR160* plants such pores are mostly absent (Fig. 3I and J). In addition, *pEF1:MpmiR160* antheridiophores have a reduction in air pore number and extra growth of rhizoids from their edges suggesting that epidermal development is compromised (Fig. 3I and J). Archegenoiophores (female gametophores) in *pEF1:MpmiR160* lines were not as severely affected, although it is possible to see a degree of organ fusion, with two archegoniophores fusing to form a single structure (Fig. 3K and L).

Gain-of-function MpARF3 alleles

To generate gain-of-function *MpARF3* alleles, we drove the wild-type *MpARF3* coding sequence and a mutant version of the *MpARF3* coding sequence incorporating 7 silent mutations in the microRNA binding site (*MpARF3*^{m}), with either the *MpEF1* or the *MpARF3* promoters (Fig. 1D). All transgenes resulted in aberrant phenotypes. Driving expression with the *EF1* promoter resulted in more severe phenotypes than with the *MpARF3* promoter, and the microRNA resistant transcripts induced stronger phenotypes than those of the wild-type coding sequence. The broad expression pattern of the *MpEF1* promoter provides information on the potential of the MpARF3 protein, while expression with the endogenous *MpARF3* promoter provides information on the endogenous role of *MpmiR160* in regulating *MpARF3*.

pEF1:MpARF3 plants developed dwarfed thalli with a reduction in the extent of differentiated tissues (Fig. 5A and B). *pEF1:MpARF3* plants are characterized by a small thallus without air pores or gemmae cups, and an increase in branching.

pEF1:MpARF3^{m} lines exhibited a dramatic phenotype where most cells of the plant did not differentiate into mature flat thallus and rather remained as clumps of cells without any particular a cellular identity reminiscent of wild-type sporelings (Fig. 5C and D).

pMpARF3:MpARF3 plants showed a range of phenotypes with approximately 50% not differing phenotypically from the wild type (Fig. 5F) and 50% having a phenotype reminiscent (although not as strong) of that of *pMpARF3:MpARF3*^{m} lines (N=100) (Table 3). Approximately 90% of *pMpARF3:MpARF3*^{m} lines (N=100) (Table 3) showed drastic transformations of the thallus with a smaller and compact collection of thalli that mostly resemble *pEF1:MpARF3*^{m} lines (Fig. 5G): increased branching and a general lack of differentiation of specialized dorsal cell types, resembling a very early stage of sporeling development (Fig. 5G), weaker lines showed a slight degree of thallus expansion and differentiation with scattered rhizoids but no air chambers or scales (Fig. 5H).

To further evaluate MpARF3 in the context of its capacity to interact with other ARF proteins, we drove expression of truncated versions of *MpARF3* without domains 3 and 4 of protein-protein interaction. In *Arabidopsis*, similar experiments constitutively expressing truncated versions of *MP/ARF5* generate more aberrant phenotypes than expressing wild type versions of the gene (Krogan et al., 2012). *pMpARF3:MpARF3*$^{m}\Delta$ plants exhibited slightly less severe albeit similar phenotypes as *pMpARF3:MpARF3*^{m} mutants. In *pMpARF3:MpARF3*$^{m}\Delta$ plants there is a slight growth into compact lobed thalli, with lack of differentiation of dorsal tissues as no gemmae cups or air pores are observed (Fig. 5K). Rhizoids were present developing from the ventral sides and thus the plants maintain a degree of dorsiventral polarity. The shape of the thalli suggested a similitude with the prothallus stage of wild type development (Fig. 5L)**.**

Because of the variability of phenotypes observed for gain-of-function *MpARF3* alleles when driven with the two different promoters, an apical notch specific promoter (*pSHI*), cloned by Magnus Eklund, was used to drive both *MpARF3* and *MpARF3*^{m} in a tissue specific fashion. These constructs were cloned by Magnus Eklund and are added to this thesis due to their relevance in explaining *MpARF3* function. *pSHI:MpARF3* and *pSHI:MpARF3*^{m} plants did not differ from one another phenotypically (Fig. 5N and O), suggesting an absence of *MpmiR160*-mediated regulation in the apical notch. *pSHI:MpARF3* and *pSHI:MpARF3*^{m} plants both

exhibited an increase in branching rates compared to the wild type (Fig. 5M-O), but similar to that observed in *pEF1:MpTPLN176H* plants. Although *pSHI:MpARF3* and *pSHI:MpARF3*^{m} thalli can form dorsal air chambers, no gemmae cups are observed (Fig. 5P).

DISCUSSION

Conserved miR160 regulation existed in the common ancestor of embryophytes.

Several miRNA families are prominent regulators of transcription factors involved in developmental processes in angiosperms. Moreover, a few studies were able to trace the origin of orthologues of developmentally significant *miRs* including *miR156*, *miR160*, *miR165/166*, *miR170/171 miR319* and *miR390* to the common ancestor of *Physcomitrella* and *Arabidopsis* (Axtell et al., 2007), suggesting an ancient and indispensable role for *miRNAs* in patterning developmental processes. In particular, *miR165/166* is the only *miRNA* known to date back to the common ancestor of all embryophytes as it is present in *Marchantia* (Floyd and Bowman, 2004). *miR165/166* regulation is thought to be embryophyte specific, since the *Chara C3HDZIP* lacks a conserved *miR165/166* binding site (Floyd et al., 2006). This points at an important role for *miR165/166* regulation in specifying embryophtye body plans. Functional characterization of conserved miRNAs in bryophytes has been so far limited, with the exception of *miR156* and *miR390* in *Physcomitrella*. Loss of function of the *miR156* targets, the *SBP* orthologues of *Physcomitrella*, promotes the formation of leafy gametophores from filamentous protonemata (Cho et al., 2012). In contrast, overexpression of SBPs as well as overexpression of *miR390* delays the formation of leafy gametophores, relating *miR156* and *miR390* in gene regulatory network controlling developmental transitions (Arazi et al., 2005; Talmor-Neiman et al., 2006; Cho et al., 2012).

This study provides a novel description of the developmental role of another ancient microRNA: *miR160*, which targets the single class C *ARF* (*MpARF3*) in *Marchantia*. Furthermore, as explained in the following section, it might also be involved in developmental transitions, as its target is a promoter of undifferentiated stages of development.

Although the data presented did not explicitly demonstrate the expression of *miR160* RNA in the thallus of *Marchantia*, the following lines of evidence corroborate its existence: 1. The presence of *miR160* binding sites in *MpARF3*; 2. Annotation of a genomic locus that forms a functional stem loop with a putative 21 nucleotide miR with complementary to *MpARF3*; 3. The overexpression of this locus creates a robust phenotype that's replicated in more than 80% transformants; 4. Plants expressing *MpARF3 miR160* resistant lines show drastic phenotypes compared to

wild type *MpARF3* controls; and 5. The gain-of-function MpARF3 lines show opposite phenotypes to *miR160* overexpression lines.

Unfortunately, we are so far unable to tell if *miR160* mediated regulation of *MpARF3* is exclusive to embryophytes. Our phylogenetic analysis in chapter 3 points at the existence of a putative class C ARF orthologue detected in *Spirogyra* (De Smet et al., 2011), opening the possibility of *miR160* regulation, but this question will be solved once full length transcripts are available for charophycean algae.

MpARF3 and class C ARFs may have an ancestral role in promoting undifferentiated cell states.

Increasing the levels of expression of *MpARF3* in the *Marchantia* thallus created a strong phenotype that was initially hard to interpret. However, by comparison with parallel SEM analyses of the development of wild-type spores and sporelings, I was able to hypothesize that *MpARF3* lines were groups of cells unable to make the transition to a differentiated cell state, with a morphology similar to 10 to 14 day old sporelings. *pEF1:MpARF3^{m}* and *pMpARF3:MpARF3^{m}* lines which potentially have the highest levels of expression show the strongest transformations to a sporeling-like stage of development, without no visible sign of differentiation of cells into any particular tissue type. However, cell division does not seem to be affected as cells continue to divide in 1 month old *pEF1:MpARF3m* and *pMpARF3:MpARF3^{m}* lines. Lines with potentially lower levels of activity, such as *pMpARF3:MpARF3$^{m}\Delta$* or weak *pMpARF3:MpARF3^{m}* lines show milder reversions to a juvenile stage. One interpretation of the morphology in these lines is that development is unable to transition past the prothalli-like stage of development: no dorsal air chambers or gemmae cups differentiate but ventral rhizoids are formed and cells form a collection of flat single layered bodies, with a slight formation of lobes and potential apical notch initials. Finally, the phenotypically weakest lines, using the apical notch specific promoter *pSHI*, produce a multibifurcated thallus as a result of high rates of branching. These lines have the greatest degree of dorsal differentiation, as they are able to produce air chambers but still do not produce gemmae cups. Interestingly, both *pSHI:MpARF3* and *pSHI:MpARF3^{m}* plants have no striking phenotypic differences, suggesting that *miR160* is not expressed in the spatial domains close to the apical notch.

Conversely, loss-of-function *MpARF3* lines have pleiotropic developmental defects. Some of these phenotypes can also be interpreted as disruptions in the promotion of undifferentiated cell states. Firstly, *EF1:MpmiR160* lines bifurcate 3 times less frequently than the wild type, suggesting that *MpARF3* facilitates the production of *de novo* meristematic apical cells. It's absence does not completely disrupt *de novo* formation of apical cells so additional factors are able to produce the formation of new meristems. Secondly, the production of undifferentiated asexual gemmae is disrupted in *EF1:MpmiR160* lines. *MpARF3* may be necessary to reprogram the thallus into producing an undifferentiated gemmae precursor from a more differentiated cell.

EF1:MpmiR160 lines have a strong phenotype in sexual development as antheridiophores have exposed antheridia, perhaps as a failure to develop an epidermis covering these structures. *MpARF3* could have been co-opted to pattern this specific structure in the ancestor of the order Marchantiales, as umbrella-like gametophores are specific to this particular order of liverworts. Therefore this is a derived and not an ancestral function of class C ARFs in *Marchantia*. The identity of the putative antheridia still needs to be confirmed by additional morphological analyses.

Fusion of archegoniophores observed in female *EF1:MpmiR160* lines could be explained by a delay in branching. During sexual development, an apical notch splits and one of the daughter apical notches produces a gametophore, which is in fact an extension of the thallus. While this notch is differentiating into a gametophore, the sister notch continues to produce thallus by vegetative growth. This sister apical notch then recapitulates the growth pattern of the 'mother notch', bifurcating, with one daughter being reproductive. If growth during branching is retarded, gametophore production could be triggered before branching is complete, leading to fused gametophores observed in *EF1:MpmiR160* lines.

Finally, expression pattern of the putative *pARF3* promoter is along the thallus mid-rib, including the apical notch, gemmae cup and gemmae precursors. This zone of the thallus is perhaps the most active site of dedifferentiation, producing new apical cells and gemmae primordia.

These functional interpretations, if correct, allow the inference of ancestral developmental roles for these genes if similar roles are shared in other land plant lineages. The role of angiosperm class C ARFs has been studied in less detail

compared to class A or B ARFs due to the difficulty in interpreting complex pleiotropic phenotypes associated with gain-of-function phenotypes (Mallory et al., 2005; Wang et al., 2005; Liu et al., 2007; Liu et al., 2010; Hendelman et al., 2012). The analysis of the single class C ARF orthologue in *Marchantia* may explain several of these developmental phenotypes in a context of the extent of differentiation states of various cells and tissues. For example, leaf serration observed in all *Arabidopsis* class C gain of function phenotypes suggest a promotion of ectopic meristematic zones in each serration, such as that observed in *KNOX* gain-of-function phenotypes (Mallory et al., 2005; Wang et al., 2005; Liu et al., 2007). Likewise, production of inflorescences from siliques in loss-of-function *miR160* lines in *Arabidopsis*, points at a loss of determinacy, and consequential reprogramming to produce a new inflorescence meristem due to increased class C *ARF* activity (Liu et al., 2010). Recently, *miR160* has been found to be a repressor of totipotency in tissue cultures of *Arabidopsis* since overexpression of *miR160* (*p35S:MIR160a*) compromised the ability of calli to produce shoot meristems – i.e. loss of totipotency (Qiao et al., 2012). Conversely, overexpression of miR-resistant *ARF10* in *Arabidopsis* calli produced high levels of shoot regeneration as well as elevated expression of genes, such as *CUC1/2, WUSCHEL* and *CLAVATA3,* involved in maintaining the shoot apical meristem totipotency (Qiao et al., 2012). Additional transcriptomic profiles in gain-of-function *MpARF3* lines are needed to determine the similarities and differences compared with the expression profiles of young sporelings in the pre-prothallus and prothallus stages of development.

Class C ARFs may not interact with, but rather compete with class A ARF activators.

Expression of a truncated MpARF3 protein without protein interaction domains 3 and 4 did not create a effect similar to that observed for other truncated versions of class A ARFs in *Arabidopsis*, that is, gain-of-function phenotypes are enhanced due to lack of regulation by AUX/IAA proteins (Krogan et al., 2012). This suggests that class C ARFs are not co-opted into a repressor complex by AUX/IAAs as they may already putative repressors of transcription. Secondly, as described in the previous chapter, *MpTPL-D34*^{MpARF3} fusions did not produce the aberrant lack of growth and patterning seen with fusions between TPL and other D34s, suggesting that class C ARFs do not physically interact with either class A and B ARFs and likely

AUX/IAAs. This in turn suggests that the only putative connection between *MpARF1* and *MpARF3* in a gene regulatory network is their capacity to compete for similar targets. Given that one is an activator and one a repressor of transcription, it is tempting to speculate that *MpARF1* would have an antagonistic role to *MpARF3*, i.e. *MpARF1* would promote differentiation rather than totipotency. However, there is no strong line of evidence supporting this scenario as *pEF1:MpARF1* lines have an almost wild type phenotype with a weak tendency to increase branching, similar to gain of function *MpARF3* lines. Furthermore, lines overexpressing dominant negative versions of TPL, where class A ARF function is putatively released from a repressive complex also shows an increase in branching. In this case, there is a striking similarity between *pSHI:MpARF3/pSHI:MpARF3*^{m} lines and *pEF1:MpTPL*^{N176H} lines. This is difficult to explain given that AUX/IAA proteins have limited interaction with class C ARFs in *Arabidopsis*.

Expression of truncated versions of *MpARF1* as well as loss-of-function alleles of *MpARF1* would perhaps help in the elucidation of these apparently contradictory phenotypes.

Additional miR160 binding sites affect the expression pattern of pMpARF3 in an unexpected fashion.

An unexpected result in the elucidation of the role of *miR160* in controlling the expression pattern of *MpARF3* came from the testing of two types of *pMpARF3* transcriptional fusions with the *GUS* reporter gene. In the first type, an artificial *miR160*-binding site was translationally fused in frame with the reporter gene, and in the second case, the artificial miR-binding site was embedded in the 3'UTR downstream of the *GUS* reporter. In both cases, the addition of the *miR160*-binding site resulted in an expansion of the spatial domain of *GUS* activity compared to the controls. This type of experiment is a routine technique in *Arabidopsis* with the addition of the *miR* binding site usually restricting the spatial domain of 'constitutive' promoters such as the CaMV35S promoter (Carlsbecker et al., 2010). Because *Marchantia* has mostly single copy representatives for a variety of gene families (including *MIR* precursors, *miRNA* processing genes and targets), additional *MpmiR160* binding sites could release *miR160* targets from repression. However this was not observed, as there is no phenotype in transgenic plants harboring these types of construct. In contrast, it seems that this phenomenon might be specific for the

miR160 and *MpARF3* genetic network and that extra *miR160* binding sites could reveal that *MpARF3* is auto-regulated. Additional experiments, such as detection of cleavage of GUS transcripts with miR160 binding sites, addition of a different miR binding site to GUS and expression of these constructs with a different promoter are necessary to elucidate this strange behavior. If *MpARF3* is auto-regulated, then *MpARF3:GUS* lines in *EF1:MpmiR160* or *MpARF3* overexpression backgrounds should have different expression patterns to the wild type.

Evolutionary hypothesis on the importance of control of totipotency.

Taken together, the information obtained from *Marchantia* and *Arabidopsis* indicates that a class C ARF existed in the common ancestor of all land plants and that the ancestral gene was involved in promoting totipotent (undifferentiated) cell states. This ancestral function could be of importance for the construction of multicellular bodies if regulated in very specific spatio-temporal patterns. In the gametophytes of streptophytic algae, such as *Coleochaete,* there is no clear division of meristematic and non-meristematic cells along the periphery of the colony and thus *Coleochaete* disc-shaped gametophytes grow in a bi-dimensional plane in all directions, *i.e.* each cell is equally totipotent. In comparison, an ancestral embrophyte could have evolved mechanisms that localized totipotency-promoting genes in specific spatio-temporal pattern, creating more complex developmental patterning, leading to evolution of complex developmental processes such as branching. The role of *MpARF3* however is not absolutely necessary to produce new apical cells so a complex regulatory network must be considered in this type of evolutionary scenario.

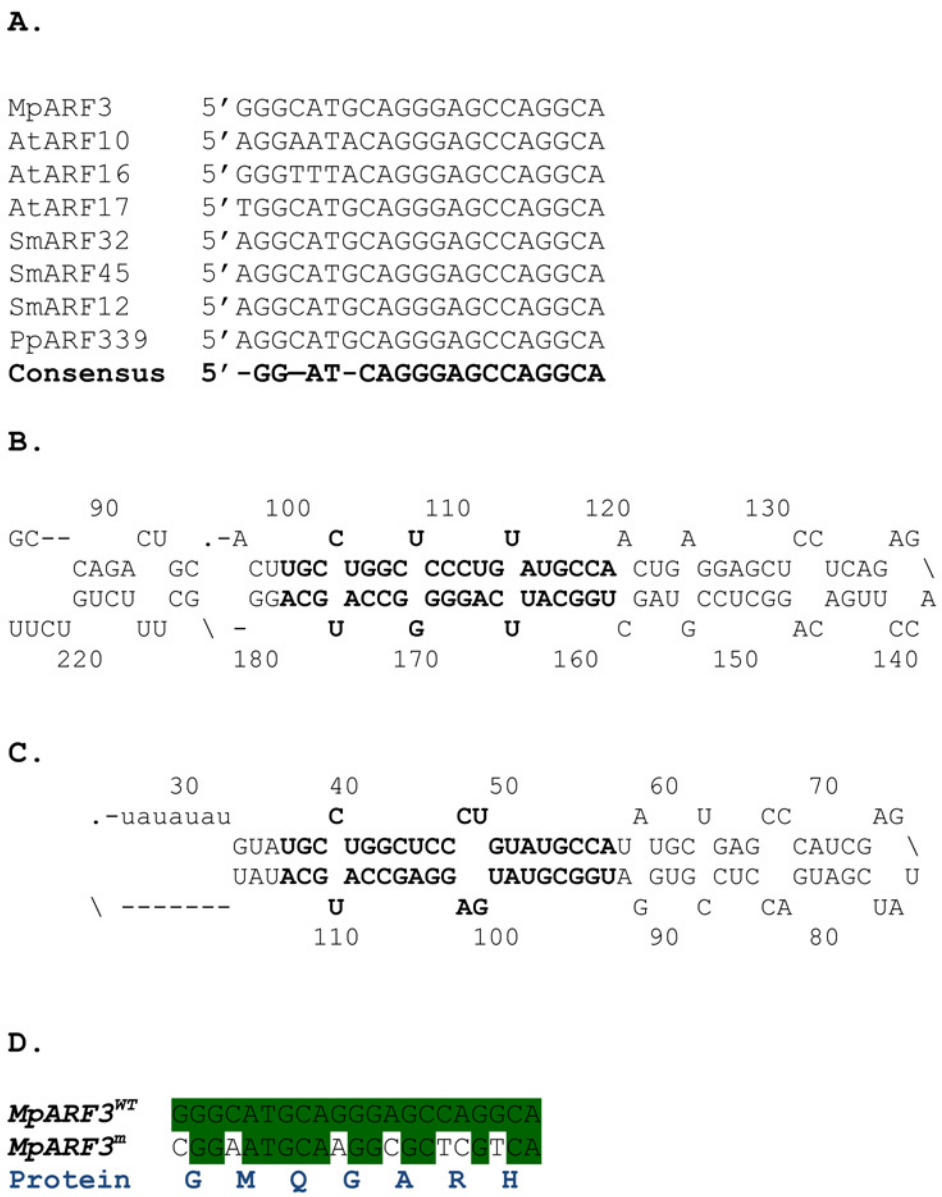

FIGURE 1. ***miR160* post-transcriptional regulation is conserved in *Marchantia polymorpha***. **(A)** Conserved miR160 binding sites in *Marchantia, Arabidopsis, Selaginella and Physcomitrella* suggesting the presence of miR160 regulation in all embryophytes. **(B)** Stem loop of the *MIR160* gene in *Marchantia polymorpha* forms a putative DICER recognized sequence. **(C)** Stem loop of the *MIR160A* gene in *Arabidopsis thaliana*, expressing this MIR gene under the EF1 promoter in *Marchantia* does not produce any phenotypic effects. **(D)** Mismatches introduced to produce silent mutations that disrupt the *miR160* binding site of the *MpARF3* transcript, sequences in blue are unaffected amino-acids sequences in both constructs.

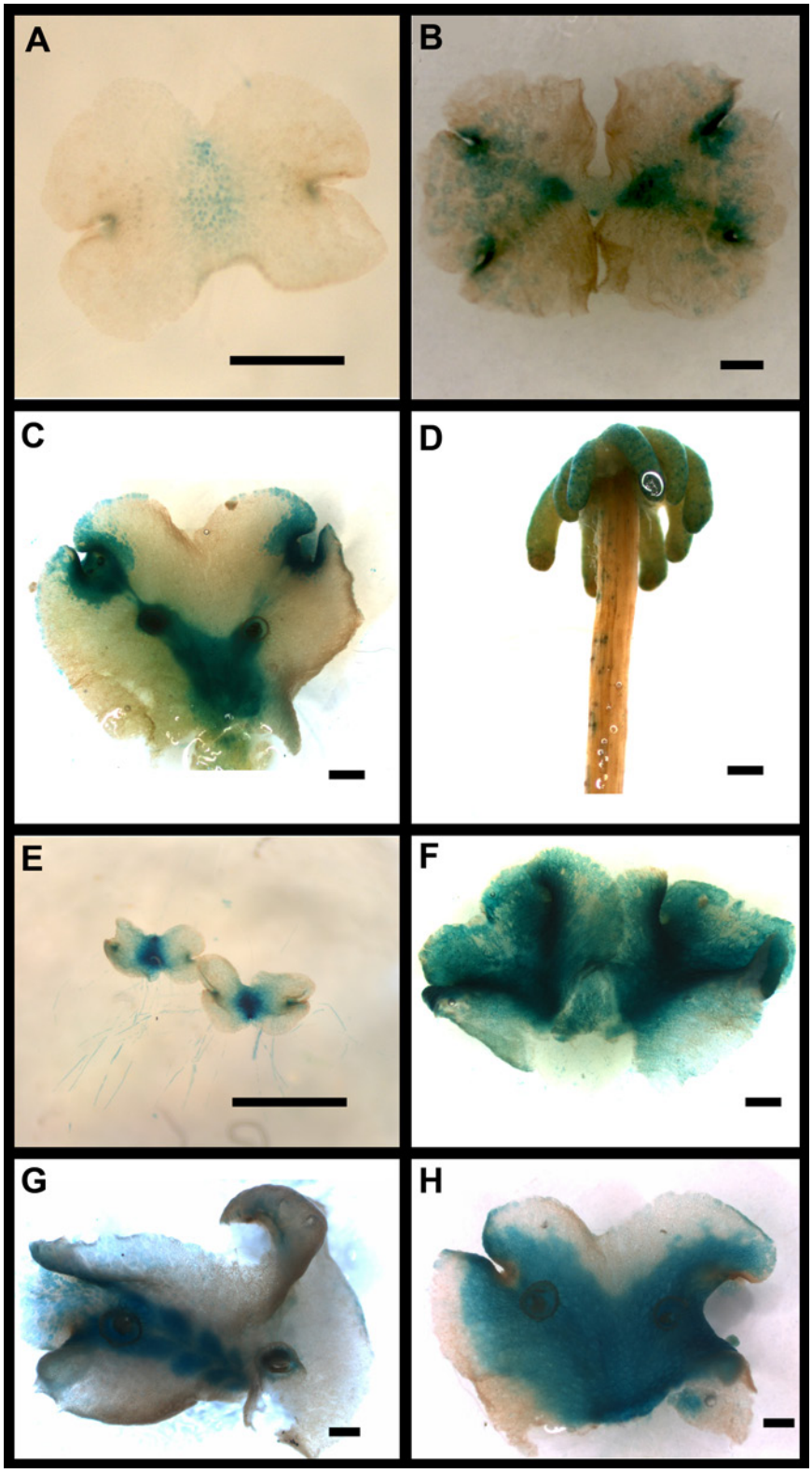

FIGURE 2. Expression patterns of *MpARF3*. (A) *MpARF3:GUS* 3-day old gemmalings with faint expression in central zones and apical meristem. **(B)** 9-day old *MpARF3:GUS* gemmalings start to show expansion of expression from the apical

notch throughout the mid-rib as well as faint expression in lobes separating notches. **(C)** *pMpARF3:GUS* mature plants showing further expression in cups, ungerminated gemmae and throught the mid-rib. **(D)** *pMpARF3:GUS* expression in archegoniophores. **(E)** Ver1 of *pMpARF3:GUS-miR160* (in which miR160 binding site is fused to the GUS protein), in 3 day old gemmalings shows strong expression in central zone and apical notches. **(F)** *pMpARF3:GUS-miR160* lines show expanded expression in mature plants compared to control lines. **(G)** Ver2 of *pMpARF3:GUS:3'UTR* including extra 800bp of 3'UTR of the *MpARF3* transcript shows a similar expression pattern to *pMpARF3:GUS*. **(H)** Ver2 of *pMpARF3:GUS:3'UTRmiR160* in which the miR160 binding site was added to the 3'UTR of *MpARF3* also shows an expansion of GUS expression. All scale bars equal 1mm, except for A which equals 0.5 mm.

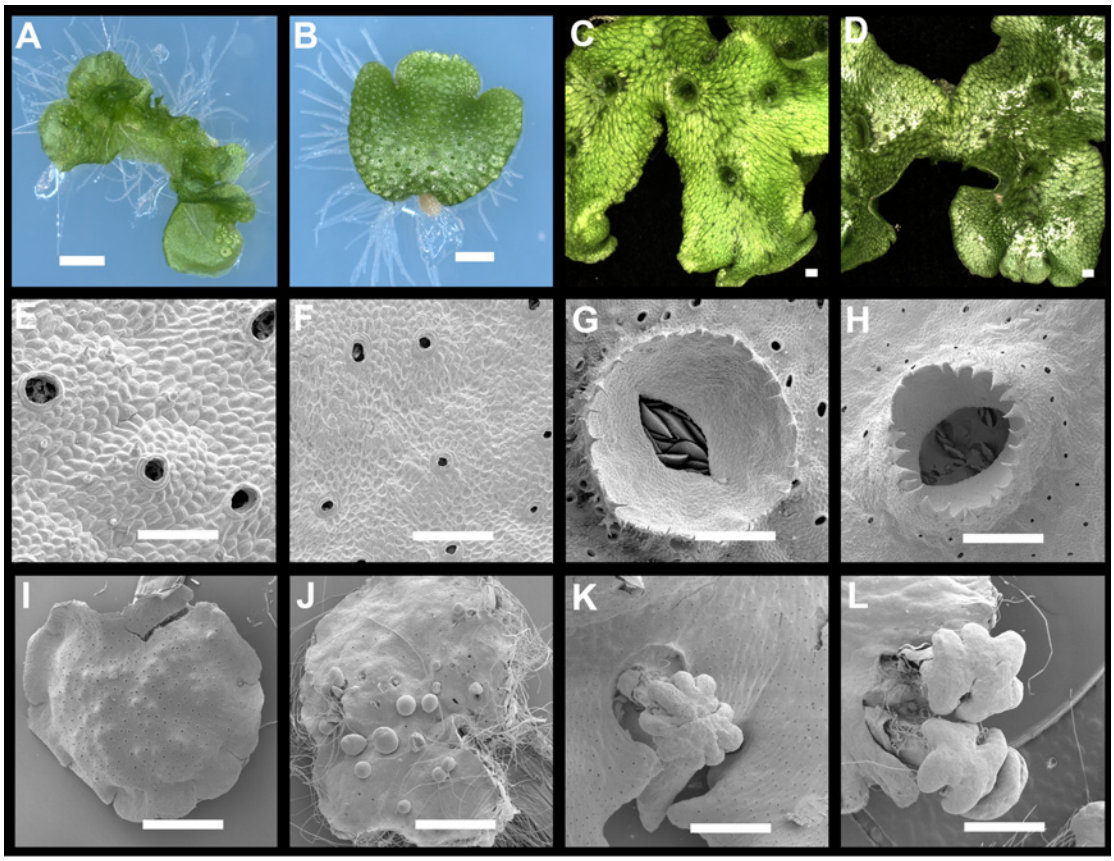

FIGURE 3. **Phenotypic characterization of loss-of-function *MpARF3* lines. (A)** Wild type sporeling at early development with multiple notches expanding in several directions, scale bar = 1mm. **(B)** Young *EF1:MpmiR160* sporeling with a characteristic shape in which growth only occurs from one side of the thallus. The intermediate lobe between notches is wide, scale bar = 1mm. **(C)** Mature wild type thallus, scale bar = 1 mm. **(D)** Mature *EF1:MpmiR160* thallus that preserves an overall simplicity without many gemmae cups and and an bulkier lobes between notches, scale bar = 1 mm. (**E**) Wild type close up of dorsal thallus cells in the wild type, scale bar = 0.2 mm. (**F**) *EF1:MpmiR160* plants have diminished cell size, scale bar = 0.2 mm. (**G**) Gemmae cup of the wild type with normal set of gemmae inside, scale bar = 0.5 mm. (**H**) *EF1:MpmiR160* plants often lack mature gemmae inside the cups, although it is possible to see small propagules that are delayed in their maturation. Gemmae propagation in *EF1:MpmiR160* plants is very rare, scale bar = 0.5 mm. **(I)** Wild type antheridia with a mix of air pores and pores connecting antheridia, scale bar = 1.2 mm. **(J)** *EF1:MpmiR160* antheridiophores are aberrant with external antheridia, excessive rhizoid growth in the edges and fewer airpores, scale

bar = 1 mm. **(K)** Wild type young archegoniophore, scale bar = 1.2 mm. **(L)** *EF1:MpmiR160* archegoniophores are sometimes fused and have a diminished number of airpores, scale bar = 1.2 mm.

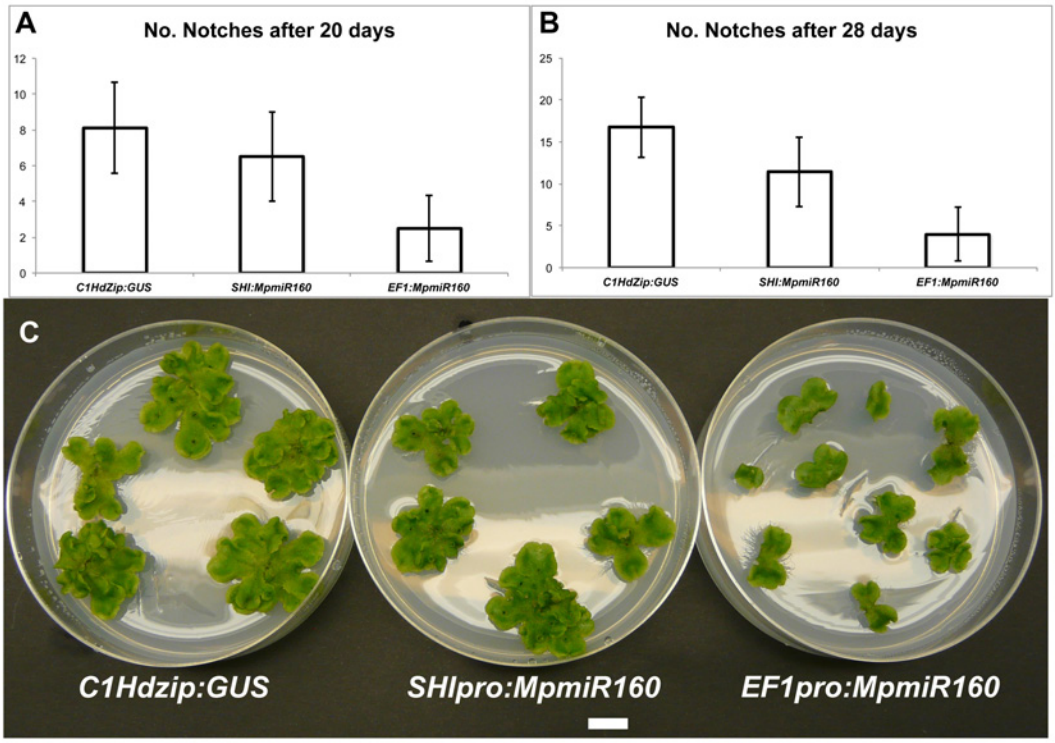

FIGURE 4. **Thallus bifurcation is delayed by *MpmiR160*. (A)** Simultaneously transformed lines after 20 days of growth show an average of 8 notches for wild type and only 2 for *EF1:MpmiR160* plants. i.e 2 extra apical meristem divisions in the wild type. *SHI:MpmiR160* plants are somehow intermediate in this process. **(B)** Apical meristem count after an additional week shows a similar difference between the populations. **(C)** Photographed lines showing a phenotypic grade for bifurcation frequency after 30 days of growth, scale bar = 1 cm.

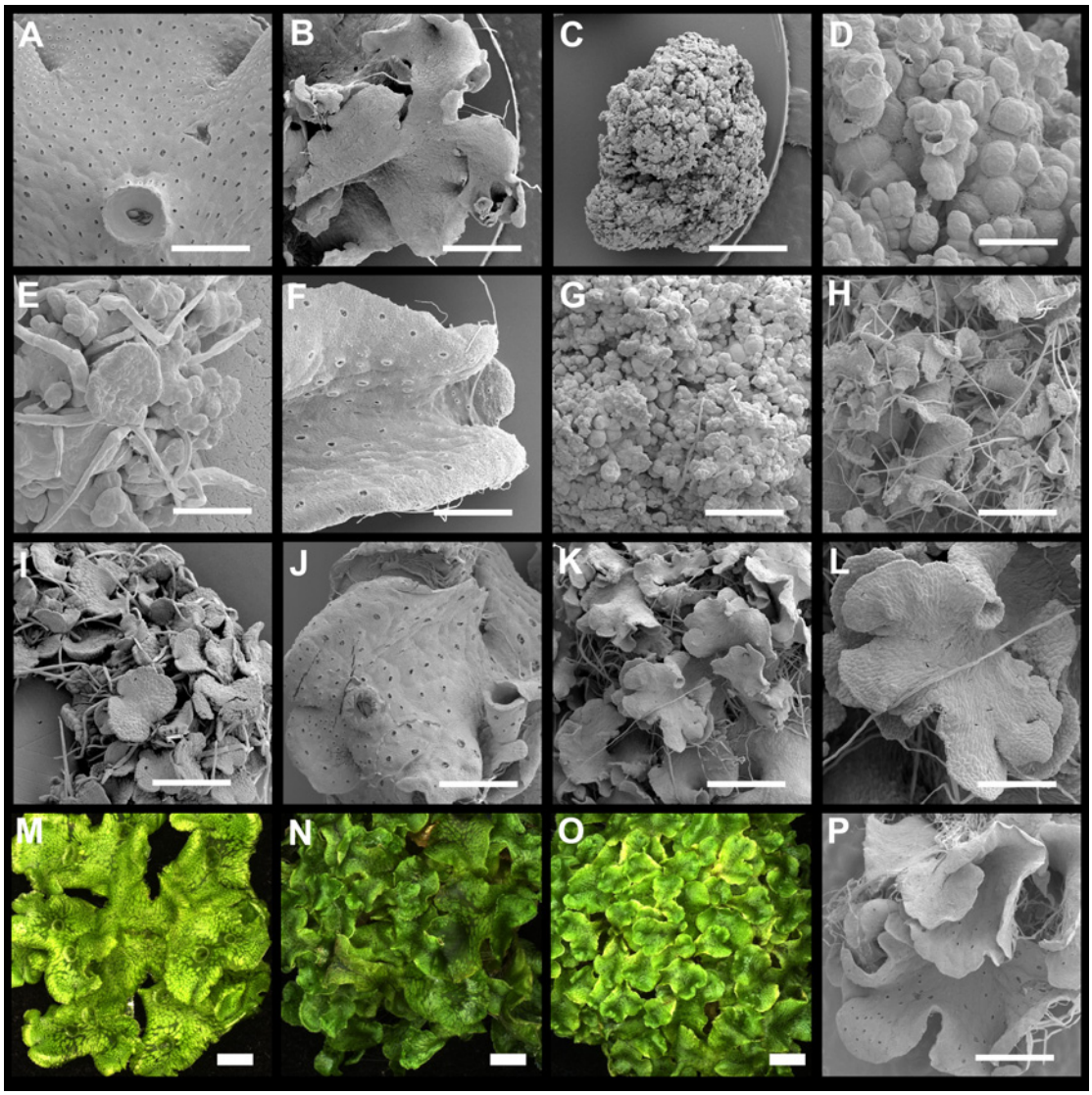

FIGURE 5. Gain of function phenotypes of *MpARF3* reproduce undifferentiated cell states. (A) Wild type mature thallus, scale bar = 1.5 mm. **(B)** *EF1:MpARF3* mature plants without airpores or gemmae cups but still able to form a bifurcated thallus with ventral rhizoids, scale bar = 1.36 mm. **(C)** *EF1:MpARF3*^{m} mature lines after more than 30 days of growth remains as an undifferentiated clump of cells, scale bar = 1.2 mm. (**D)** Close up to morphology of *EF1:MpARF3*^{m} cells, scale bar = 86 µm. **(E)** Wild type sporelings 10 days after plating, scale bar = 100 µm. **(F)** *MpARF3:MpARF3* line with a wild type phenotype, scale bar = 0.6 mm. **(G)** Strong *MpARF:MpARF3*^{m} lines also have a conversion to undifferentiated cell states, scale bar = 300 µm. **(H)** Weaker *MpARF:MpARF3*^{m} lines resemble an agglomeration of prothalli, scale bar = 0.6 mm. **(I)** Collection of wild type sporelings at prothallus stage

14 days after plating in normal media, scale bar = 0.43 mm. **(J)** *MpARF3:MpARF3Δ* line with a wild type phenotype, scale bar = 1.2 mm. **(K)** *MpARF:MpARF3^{m}Δ* lines show an excessive bifurcation and underdeveloped thalli, scale bar = 1mm. **(L)** *MpARF:MpARF3^{m}Δ* prothalli-like tissue has no airpores nor geamme cups but forms two potential apical notch initials, scale bar = 0.38 mm. **(M)**. Wild type mature thallus, scale bar = 1mm. (**N)** *SHI:MpARF3* plants show an increase in bifurcation, scale bar = 1mm. **(O)** *SHI:MpARF3^{m}* lines show a similar phenotype to *SHI:MpARF3* lines, scale bar = 1 mm. **(P)** SEM of *SHI:MpARF3^{m}* lines are able to form air pores but not gemmae cups, scale bar = 1.2mm.

Table 1. Comparison of number of notches after 20 days of growth between control and *MpmiR160* expressing lines.			
Line	Average No. Notches	Standard Deviation	N
C1HdZip:GUS	8.11	2.53	51
SHI:MpmiR160	6.51	2.5	41
EF1:MpmiR160	2.51	1.85	79

Ttest *EF1:MpmiR160* vs *C1HDZip:GUS* P=1.04×10^{-22}
Ttest *SHI:MpmiR160* vs *C1HDZip:GUS* P=0.005

Table 2.

Table 2. Comparison of number of notches after 28 days of growth between control and *MpmiR160* expressing lines.			
Line	Average No. Notches	Standard Deviation	N
C1HdZip:GUS	16.7	3.55	72
SHI:MpmiR160	11.43	4.15	37
EF1:MpmiR160	4	3.25	39

Ttest *EF1:MpmiR160* vs *C1HDZip:GUS* P=1.38×10^{-27}
Ttest *SHI:MpmiR160* vs *C1HDZip:GUS* P=8.61×10^{-08}

Table 3. Phenotype frequencies (No. Individuals) of primary transformants in MpARF3 Gain-of-function Experiments.			
ARF3pro:ARF3wt		*ARF3pro:ARF3^{m}*	
Wild type	Strong thallus reduction	Weak or WT	Strong thallus reduction
63	44	18	93

MATERIALS AND METHODS

Cloning of MpARF3. Wild type cDNA from day 8 Gemmalings was used to amplify MpARF3 with KOD polymerase and gene specific primers based on preliminary genomic assemblies provided by JGI. An initial outter PCR was done using primers MpARF3-F5 and MpARF3-R5, this PCR reaction gave no product and it was used as a template for a nested PCR with primers MpARF3-F3 and MpARF3-R3, which gave a 2.4kb fragment. This preliminary cDNA was cloned in pCRII, sequencing results showed an alternative transcript that lacked domains 3 and 4 of protein-protein interaction (*MpARF3Δ34*). Because it was difficult to amplify the full length MpARF3 transcript, domains 3 and 4 were synthesized in vitro (Genescript) from nucleotide 1891 of the MpARF3 CDS where there is a natural BstXI site, the synthesized $MpARF3^{D34}$ (total of 592 bp) was engineered with a HindIII site 3' of the stop codon.

The cloned *MpARF3ΔD34* cDNA was used as a template to amplify just the coding region of the transcript using primers MpARF10codingKpnI-F and MpARF10codingHindIII-R with KOD polymerase, this new shorter PCR product was also cloned in pcRII and sequenced and subcloned into EF1:BJ36 v2.0 using KpnI and HindIII and subsequently subcloned into HART with NotI sites to create *pEF1: MpARF3ΔD34* was subsequently cut with BstxI and HindIII to insert the full length D34 and create the *pEF1:MpARF3* construct.

PCR Mutagenesis of MpARF3. Using the pcRII cloned- *MpARF3ΔD34* cDNA as a template, assembly PCR was used to create miR-resistant *MpARF3ΔD3*. Primers M13-R and MpARF10m6-Fwd were used to create a 893 bp mutagenized fragment 1, and primers MpARF3-F3 and MpARF10m6-Rev to create a 1651 bp fragment 2. The assembly was performed using both fragments as templates and primers MpARF10codingKpnI-F and MpARF10codingHindIII-R to amplify a 2.3 kb fragment. PCR products were cloned in pCRII and sequenced. Subcloning into EF1:BJ36 and HART and addition of the full length *D34* was done as described for *pEF1:MpARF3*.

MpARF3 Promoter cloning. Gene specific primers NdeI-MpARF3proSeqF3 and MpARF10proKpnI-Rev were used to amplify a 3.6kb fragment from a PAC

containing MpARF3 and provided by Takayuki Kochi from Kyoto University. Such fragment was cloned in pcRII and sequenced. NdeI and KpnI were used to Subclone pMpARF3 into pRITA, a shuttle vector with a MCS 5' of the GUS reporter gene with a 3'nos terminator to create *pMpARF3:GUS*. NdeI and KpnI were used to subclone pMpARF3 into *pEF1: MpARF3ΔD34* and *pEF1:MpARF3 ^{m}ΔD34* to create *pMpARF3:MpARF3ΔD34 and pMpARF3: MpARF3^{m}ΔD34*. BstxI and HindIII were used to subclone *MpARF3^{D34}* into *pMpARF3:MpARF3ΔD34 and pMpARF3: MpARF3^{m}ΔD34*.

GUS reporter lines. GUS reporter gene was amplified from pRITA with primers KpnI-GUS-F and HindIII-GUS-miR160bsR that adds a miR160 binding site to the GUS CDS before the stop codon. KpnI and HindIII were used to subclone *GUS-miR160* into *pMpARF3:GUS*. The second version of the transcriptional fusion was created by amplifying the wild type MpARF3 3'UTR with primers 3'UTRMpARF3HindIII-F and 3'UTRMpARF3XbaI-R and primers 3'UTR-MpARF3miR160bs-F-HindIII and 3'UTRMpARF3XbaI-R to amplify a 3'UTR with a miR160 binding site. HindIII and XbaI were used to subclone the *wt* 3'UTR and 3'UTR-miR160bs into pMpARF3:MpARF3 and subsequently GUS was amplified with primers KpnI-GUS-F and HindIII-GUS-Rev to insert it into *pMpARF3:MpARF3:3'UTR* with KpnI and HindIII and create *pMpARF3:GUS:3'UTR* and *pMpARF3:GUS:3'UTR-miR160bs*. All fragments were previously cloned into pCRII and sequenced and subcloned into HART using NotI.

miR160. A minimal (220bp) *Arabidopsis MIR160a* precursor was provided by John Alvarez in pBSK. XhoI and EagI were used to clone into the Gateway entry vector pENTER2B cut with SalI and NotI. An LR reaction was performed to recombine into pKIGWB2 binary vector provided by Kimizune Ishizaki.

The *Marchantia MpMIR160* precursor was amplified using primers EcoRI-MpmiR160-F and KpnI-MpmiR160-R, cloned in pCRII and sequenced. EcoRI and KpnI were used to subclone *MpmiR160* into EF1:BJ36 V2.0 and later NotI was used to subclone into HART. SHI:MpmiR160 was obtained by amplifying MpmiR160 from *EF1:MpmiR160 BJ36* with primers KpnI-MpmiR160-F and HindIII-MpmiR160-R and subcloned into *pSHI:GUS* (in pRITA) created by Magnus Eklund using KpnI and HindIII.

Marchantia spores were simultaneously transformed with *pC1HDZIP:GUS* (an inocous reporter line) SHI:MpmiR160 HART, and EF1:MpmiR160, primary transformants were transferred to new selection plates after 10 days of initial selection and after 20 days after plating I counted apical notches for all surviving transformants using a dissecting scope. The same measurement was performed 8 days later.

Transformations. *Marchantia* transformations were described as in the previous chapter.

GUS Staining. Plants were induced in the GUS staining solution (0.5mM Potassium Ferrocyanid, 0.5mM Potassium Ferricyanide and 1mM X-Gluc) for 1hour at 37° C and later cleared with ethanol.

Primer Name	**Sequence (5′-3′)**
MpARF3-F5	TTCGTGCGAGCCGGACTTAGGTCGTGGCAG
MpARF3-R5	GTTGACTGTCAAGCATACTGTCAATGGTGC
MpARF3-F3	TGCTAAAATTGCGCCACCGCTCTCCGGCTC
MpARF3-R3	GTTTTGCCGTTGCTAGAGGGGTCGACACGG
MpARF10codingKpnI-F	**GGTACC**ATGCCCGGGCCAAGCCCTGGGTGTG
MpARF10-coding-R HindIII	**AAGCTT**TCACCAGGCGCCTTGCGGACTTTGC
MpARF10m6-F	GAAGTTACTGCCGGAATGCAAGGCGCTCGTCATGATCGAGT
MpARF10m6-R	ACTCGATCATGACGAGCGCCTTGCATTCCGGCAGTAACTTC
MpARF3-Pro-SeqF3-NdeI	AT**CATATG**CGAAAGTCAAATGTTTCGACAGG
MpARF10proKpnI-Rev	A**GGTACC**CCCAAACAGAAAGGAGCCGGAGAGCGGTG
KpnI-GUS-F	A**GGTACC**ATGGTCCGTCCTGTAGAAACCCCAACC
HIII-GUS-miR160bsR	A**AAGCTT**TCAATGCCTGGCTCCCTGCATGCCCGC
3′UTRMpARF3HindIII-F and	**AAGCTT**ACGCGATGTTCTATAGAGATGGAG
3′UTRMpARF3XbaI-R	**TCTAGA**GAACACGATTTCCGACTTTCTTGATTGGG
3′UTR-MpARF3miR160bs-F-HindIII	**AAGCTT**GGGCATGCAGGGAGCCAGGCAACGCGATGTTCTATAGAG ATGGAG
HindIII-GUS-R	**AAGCTT**TCATTGTTTGCCTCCCTGCTGCGG
EcoRI-MpmiR160-F	A**GAATTC**ATGGGTGAGATTGTCACACTCACTCACAACC
KpnI-MpmiR160-R	A**GGTACC**TCCACCAGAAACACTGACCCCGTGTATGACC
KpnI-MpmiR160-F	A**GGTACC**ATGGGTGAGATTGTCACACTCACTCACAACC
HindIII-MpmiR160-R	A**AAGCTT**TCCACCAGAAACACTGACCCCGTGTATGACC

GENERAL CONCLUSIONS

The present study is an initial attempt to understand the role of auxin in patterning the body plan of *Marchantia polymorpha*. The decision to study auxin biology was motivated not only by the importance of auxin in controlling basic ontogenetic processes in flowering plants and mosses, but also by of the observations of old physiologists and botanists linking auxin, gravity and light with the establishment of dorsiventrality in *Marchantia* (Fitting, 1935-1939; Halbsguth, 1936, 1953; Rousseau, 1950-1954; Taren, 1958; Kaul et al, 1972; Otto, 1976; Otto and Halbsguth, 1976). Furthermore, a theoretical framework linking the sophistication of the auxin genetic toolkit with the evolution of plant organismal complexity was put forward more than 10 years ago (Cooke et al 2002), but this has been barely tested with the tools of developmental genetics.

The design and objectives of this thesis changed over the years depending on the availability of isolated genes and the tools required to create experimental work that was possible to interpret, consistent and replicable. Thus, the results presented in this thesis are not connected with dorsiventrality but surprisingly, they fit in the context of auxin as a promoter of developmental transitions, as it has been observed in the moss *Physcomitrella patens*: By abolishing auxin responses or over-activating class C *ARF* genes, a gametophyte cannot produce complex developmental processes: from protonemal filaments to a leafy gametophore in mosses (Eklund et al., 2010b; Prigge et al., 2010), or from a prothallus to a branching thallus in liverworts. Although, *Marchantia* possesses many derived characters (such as air chambers, gemmae cups and gametophores), these findings could point at an ancestral role for auxin in developmental transitions. Similar inferences could be applied in other shared processes amongst land plants such as branching or the production of new meristematic tissue.

To summarize my findings: 1. The conservation of representatives of the auxin genetic toolkit, from *Arabidopsis* to *Marchantia*, suggests that the ancestral embryophyte had a sophisticated auxin genetic toolkit capable of auxin synthesis, transport, conjugation, and transcriptional responses. 2. The *Marchantia* genome may resemble the ancestral genomic state as single paralogues compose the main families involved in auxin biology. 3. There is a macro evolutionary trend for gene

duplications within these families but no novel gene family has evolved to control auxin homeostasis since the divergence of embryophytes. Therefore, a detailed study of the genetic toolkits of streptophytic algae could elucidate embryophyte specific gene families. 4. Mutations affecting general auxin transcriptional responses in *Marchantia* disrupt the organized growth and patterning of the thallus, suggesting a crucial role for auxin as a controller of developmental organization in liverworts. 5. Pharmacological experiments show that auxin patterns specific structures and processes in both early and late stages of development. 6. The class C *ARF* gene in *Marchantia* potentially controls gene regulation independently of auxin maxima and it promotes undifferentiated cell states. 7. Class C *ARF* regulation by *miR160* existed in the common ancestor of all embryophytes.

This thesis has also provided a series of testable questions for future work in the field of auxin transcriptional responses. For example, do class A and C *ARF* genes antagonistically control developmental processes? Is *miR160* regulation of class C *ARF* genes embryophyte specific? How do different AUX/IAA and ARF proteins interact and how do such interactions affect the overall auxin transcriptional responses? What is the role of the newly discovered genes with protein-protein interaction D34 in the auxin response pathway? What specific genes are de-repressed in *TPL* dominant negative lines and why is there a phenotypic similarity between loss-of-function of *TPL* and gain-of-function class C *ARF* genes? How do *ARF* genes pattern sporophyte development? And finally, how do different phytohormones interact to pattern the morphology of the thallus?

As a final remark, it is necessary to perform forward genetic screens to truly explore all aspects of auxin biology in an unbiased and systematic way. Some of the genetic backgrounds generated in this thesis could be used to produce mutagenized populations that could lead to the identification novel genes involved in auxin responses.

This is one of the first attempts to use the tools of developmental genetics to understand liverwort development, and despite its limitations, it expands the understanding of the morphogenetic roles of auxin in another branch of the green tree of life. Hopefully, this work will demonstrate that *Marchantia* is a promising model system for the study of developmental genetics. Expanding phylogenetic coverage of available model organisms contributes to the understanding of how novel phenotypes emerged from simpler beginnings.

REFERENCES

Abel, S., and Theologis, A. (1996). Early genes and auxin action. Plant Physiol **111,** 9-17.

Abel, S., Nguyen, M.D., and Theologis, A. (1995). THE PS-IAA4/5-LIKE FAMILY OF EARLY AUXIN-INDUCIBLE MESSENGER-RNAS IN ARABIDOPSIS-THALIANA. J. Mol. Biol. **251,** 533-549.

Aida, M., Beis, D., Heidstra, R., Willemsen, V., Blilou, I., Galinha, C., Nussaume, L., Noh, Y.S., Amasino, R., and Scheres, B. (2004). The PLETHORA genes mediate patterning of the Arabidopsis root stem cell niche. Cell **119,** 109-120.

Ainley, W.M., Walker, J.C., Nagao, R.T., and Key, J.L. (1988). SEQUENCE AND CHARACTERIZATION OF 2 AUXIN-REGULATED GENES FROM SOYBEAN. J. Biol. Chem. **263,** 10658-10666.

Allen, E., Xie, Z., Gustafson, A.M., and Carrington, J.C. (2005). microRNA-directed phasing during trans-acting siRNA biogenesis in plants. Cell **121,** 207-221.

Andersen, E.N. (1929). MORPHOLOGY OF SPOROPHYTE OF MARCHANTIA DOMINGENSIS. Bot Gaz **88,** 150-166.

Andersen, E.N. (1931). Discharge of sperms in Marchantia domingensis. Bot Gaz **92,** 0066-0084.

Apostolakos, P., Galatis, B., and Mitrakos, K. (1982). Studies on the Development of the Air Pores and Air Chambers of Marchantia-Paleacea .1. Light-Microscopy. Ann Bot-London **49,** 377-396.

Arazi, T., Talmor-Neiman, M., Stav, R., Riese, M., Huijser, P., and Baulcombe, D.C. (2005). Cloning and characterization of micro-RNAs from moss. Plant Journal **43,** 837-848.

Ashihara, Y., Komatsu, A., Nishihama, K., Ishizaki, K., Yamato, K.T., Oyama, T., Aoki, S., and Kohchi, T. (2012). The light-induced dorsiventral patterning of gemmalings in *Marchantia polymorpha*. In International Marchantia Workshop 2012 (Kumamoto, Japan).

Ashton, N.W., Grimsley, N.H., and Cove, D.J. (1979). Analysis of gametophytic development in the moss, Physcomitrella patens, using auxin and cytokinin resistant mutants. Planta **144,** 427-435.

Axtell, M.J., and Bartel, D.P. (2005). Antiquity of microRNAs and their targets in land plants. Plant Cell **17,** 1658-1673.

Axtell, M.J., Snyder, J.A., and Bartel, D.P. (2007). Common functions for diverse small RNAs of land plants. Plant Cell **19,** 1750-1769.

Axtell, M.J., Jan, C., Rajagopalan, R., and Bartel, D.P. (2006). A two-hit trigger for siRNA biogenesis in plants. Cell **127,** 565-577.

Ballas, N., Wong, L.M., and Theologis, A. (1993). IDENTIFICATION OF THE AUXIN-RESPONSIVE ELEMENT, AUXRE, IN THE PRIMARY INDOLEACETIC ACID-INDUCIBLE GENE, PS-IAA4/5, OF PEA (PISUM-SATIVUM). J. Mol. Biol. **233,** 580-596.

Ballas, N., Wong, L.M., Ke, M., and Theologis, A. (1995). Two auxin-responsive domains interact positively to induce expression of the early indoleacetic acid-inducible gene PS-IAA4/5. Proc Natl Acad Sci U S A **92,** 3483-3487.

Banks, J.A., Nishiyama, T., Hasebe, M., Bowman, J.L., Gribskov, M., dePamphilis, C., Albert, V.A., Aono, N., Aoyama, T., Ambrose, B.A.,

Ashton, N.W., Axtell, M.J., Barker, E., Barker, M.S., Bennetzen, J.L., Bonawitz, N.D., Chapple, C., Cheng, C.Y., Correa, L.G.G., Dacre, M., DeBarry, J., Dreyer, I., Elias, M., Engstrom, E.M., Estelle, M., Feng, L., Finet, C., Floyd, S.K., Frommer, W.B., Fujita, T., Gramzow, L., Gutensohn, M., Harholt, J., Hattori, M., Heyl, A., Hirai, T., Hiwatashi, Y., Ishikawa, M., Iwata, M., Karol, K.G., Koehler, B., Kolukisaoglu, U., Kubo, M., Kurata, T., Lalonde, S., Li, K.J., Li, Y., Litt, A., Lyons, E., Manning, G., Maruyama, T., Michael, T.P., Mikami, K., Miyazaki, S., Morinaga, S., Murata, T., Mueller-Roeber, B., Nelson, D.R., Obara, M., Oguri, Y., Olmstead, R.G., Onodera, N., Petersen, B.L., Pils, B., Prigge, M., Rensing, S.A., Riano-Pachon, D.M., Roberts, A.W., Sato, Y., Scheller, H.V., Schulz, B., Schulz, C., Shakirov, E.V., Shibagaki, N., Shinohara, N., Shippen, D.E., Sorensen, I., Sotooka, R., Sugimoto, N., Sugita, M., Sumikawa, N., Tanurdzic, M., Theissen, G., Ulvskov, P., Wakazuki, S., Weng, J.K., Willats, W., Wipf, D., Wolf, P.G., Yang, L.X., Zimmer, A.D., Zhu, Q.H., Mitros, T., Hellsten, U., Loque, D., Otillar, R., Salamov, A., Schmutz, J., Shapiro, H., Lindquist, E., Lucas, S., Rokhsar, D., and Grigoriev, I.V. (2011). The Selaginella Genome Identifies Genetic Changes Associated with the Evolution of Vascular Plants. Science **332,** 960-963.

Barbez, E., Kubes, M., Rolcik, J., Beziat, C., Pencik, A., Wang, B., Rosquete, M.R., Zhu, J., Dobrev, P.I., Lee, Y., Zazimalova, E., Petrasek, J., Geisler, M., Friml, J., and Kleine-Vehn, J. (2012). A novel putative auxin carrier family regulates intracellular auxin homeostasis in plants. Nature **485,** 119-122.

Barnes, C.R., and Land, W.J.G. (1907). Bryological papers I. The origin of air chambers - Contributions from the Hull Botanical Laboratory, 100. Bot Gaz **44,** 0197-0213.

Barnes, C.R., and Land, W.J.G. (1908). Bryological papers II. The origin of the cupule of marchantia - Contributions from the hull botanical laboratory 120. Bot Gaz **46,** 401-409.

Benkova, E., Ivanchenko, M.G., Friml, J., Shishkova, S., and Dubrovsky, J.G. (2009). A morphogenetic trigger: is there an emerging concept in plant developmental biology? Trends Plant Sci. **14,** 189-193.

Benkova, E., Michniewicz, M., Sauer, M., Teichmann, T., Seifertova, D., Jurgens, G., and Friml, J. (2003). Local, efflux-dependent auxin gradients as a common module for plant organ formation. Cell **115,** 591-602.

Bennett, M.J., Marchant, A., Green, H.G., May, S.T., Ward, S.P., Millner, P.A., Walker, A.R., Schulz, B., and Feldmann, K.A. (1996). Arabidopsis AUX1 gene: a permease-like regulator of root gravitropism. Science **273,** 948-950.

Berleth, T., and Jurgens, G. (1993). THE ROLE OF THE MONOPTEROS GENE IN ORGANIZING THE BASAL BODY REGION OF THE ARABIDOPSIS EMBRYO. Development **118,** 575-587.

Bierfreund, N.M., Reski, R., and Decker, E.L. (2003). Use of an inducible reporter gene system for the analysis of auxin distribution in the moss Physcomitrella patens. Plant Cell Reports **21,** 1143-1152.

Bierfreund, N.M., Tintelnot, S., Reski, R., and Decker, E.L. (2004). Loss of GH3 function does not affect phytochrome-mediated development in a moss, Physcomitrella patens. J Plant Physiol **161,** 823-835.

Binns, A.N., and Maravolo, N.C. (1972). APICAL DOMINANCE, POLARITY, AND ADVENTITIOUS GROWTH IN MARCHANTIA POLYMORPHA. American Journal of Botany **59,** 691-&.

Boot, K.J., Libbenga, K.R., Hille, S.C., Offringa, R., and van Duijn, B. (2012). Polar auxin transport: an early invention. J Exp Bot **63,** 4213-4218.

Bowman, J.L., Floyd, S.K., and Sakakibara, K. (2007). Green genes-comparative genomics of the green branch of life. Cell **129,** 229-234.

Braun, P., Carvunis, A.R., Charloteaux, B., Dreze, M., Ecker, J.R., Hill, D.E., Roth, F.P., Vidal, M., Galli, M., Balumuri, P., Bautista, V., Chesnut, J.D., Kim, R.C., de los Reyes, C., Gilles, P., Kim, C.J., Matrubutham, U., Mirchandani, J., Olivares, E., Patnaik, S., Quan, R., Ramaswamy, G., Shinn, P., Swamilingiah, G.M., Wu, S., Byrdsong, D., Dricot, A., Duarte, M., Gebreab, F., Gutierrez, B.J., MacWilliams, A., Monachello, D., Mukhtar, M.S., Poulin, M.M., Reichert, P., Romero, V., Tam, S., Waaijers, S., Weiner, E.M., Cusick, M.E., Tasan, M., Yazaki, J., Ahn, Y.Y., Barabasi, A.L., Chen, H.M., Dangl, J.L., Fan, C.Y., Gai, L.T., Ghoshal, G., Hao, T., Lurin, C., Milenkovic, T., Moore, J., Pevzner, S.J., Przulj, N., Rabello, S., Rietman, E.A., Rolland, T., Santhanam, B., Schmitz, R.J., Spooner, W., Stein, J., Vandenhaute, J., Ware, D., and Arabidopsis Interactome Mapping, C. (2011). Evidence for Network Evolution in an Arabidopsis Interactome Map. Science **333,** 601-607.

Brodie, H.J. (1951). The Splash-Cup Dispersal Mechanism in Plants. Can J Bot **29,** 224-234.

Brunoud, G., Wells, D.M., Oliva, M., Larrieu, A., Mirabet, V., Burrow, A.H., Beeckman, T., Kepinski, S., Traas, J., Bennett, M.J., and Vernoux, T. (2012). A novel sensor to map auxin response and distribution at high spatio-temporal resolution. Nature **482,** 103-U132.

Campbell, D.H. (1918). Mosses and Ferns. (New york: The Macmillan Company).

Carlsbecker, A., Lee, J.Y., Roberts, C.J., Dettmer, J., Lehesranta, S., Zhou, J., Lindgren, O., Moreno-Risueno, M.A., Vaten, A., Thitamadee, S., Campilho, A., Sebastian, J., Bowman, J.L., Helariutta, Y., and Benfey, P.N. (2010). Cell signalling by microRNA165/6 directs gene dose-dependent root cell fate. Nature **465,** 316-321.

Carter, J.L., and Nickell, G.L. (1967). The Effects of Various Wavelengths of Visible Light on Thallus Growth and Gemmae CupProduction in Marchantia polymorpha L. (Marchantiaceae). The Southwestern Naturalist **12,** 113-118.

Chen, R., Hilson, P., Sedbrook, J., Rosen, E., Caspar, T., and Masson, P.H. (1998). The arabidopsis thaliana AGRAVITROPIC 1 gene encodes a component of the polar-auxin-transport efflux carrier. Proc Natl Acad Sci U S A **95,** 15112-15117.

Cheng, Y., Dai, X., and Zhao, Y. (2007). Auxin synthesized by the YUCCA flavin monooxygenases is essential for embryogenesis and leaf formation in Arabidopsis. Plant Cell **19,** 2430-2439.

Cho, S.H., Coruh, C., and Axtell, M.J. (2012). miR156 and miR390 Regulate tasiRNA Accumulation and Developmental Timing in Physcomitrella patens. Plant Cell **24,** 4837-4849.

Chopra, R.N., and Sood, S. (1970). Effect of Light Intensity and Sucrose on the Production of Gemma Cups and Gemmae in Marchantia nepalensis. The Bryologist **73,** 592-596.
Chopra, R.N., and Kumra, P.K. (1988). Biology of bryophytes. (New Delhi: New Age Internationa Ltd.).
Cooke, T.J., Poli, D., Sztein, A.E., and Cohen, J.D. (2002). Evolutionary patterns in auxin action. Plant Mol Biol **49,** 319-338.
Cribbs, J.E. (1918). A Columella in Marchantia Polymorpha. Bot Gaz **65,** 91-96.
Darwin, C.R. (1880). The Power of Movement in Plants. (London: Murray).
Davidonis, G.H., and Munroe, M.H. (1972). Apical Dominance in Marchantia - Correlative Inhibition of Neighbor Lobe Growth. Bot Gaz **133,** 177-184.
De Smet, I., Voss, U., Lau, S., Wilson, M., Shao, N., Timme, R.E., Swarup, R., Kerr, I., Hodgman, C., Bock, R., Bennett, M., Jurgens, G., and Beeckman, T. (2011). Unraveling the Evolution of Auxin Signaling. Plant Physiol **155,** 209-221.
Dharmasiri, N., Dharmasiri, S., and Estelle, M. (2005a). The F-box protein TIR1 is an auxin receptor. Nature **435,** 441-445.
Dharmasiri, N., Dharmasiri, S., Weijers, D., Lechner, E., Yamada, M., Hobbie, L., Ehrismann, J.S., Jurgens, G., and Estelle, M. (2005b). Plant development is regulated by a family of auxin receptor F box proteins. Dev. Cell **9,** 109-119.
Dhonukshe, P., Aniento, F., Hwang, I., Robinson, D.G., Mravec, J., Stierhof, Y.D., and Friml, J. (2007). Clathrin-mediated constitutive endocytosis of PIN auxin efflux carriers in Arabidopsis. Curr Biol **17,** 520-527.
Dickson, H. (1932). Polarity and the production of adventitious growing points in Marchantia polymorpha. Ann Bot-London **46,** 683-U646.
Ding, Z., Wang, B., Moreno, I., Duplakova, N., Simon, S., Carraro, N., Reemmer, J., Pencik, A., Chen, X., Tejos, R., Skupa, P., Pollmann, S., Mravec, J., Petrasek, J., Zazimalova, E., Honys, D., Rolcik, J., Murphy, A., Orellana, A., Geisler, M., and Friml, J. (2012). ER-localized auxin transporter PIN8 regulates auxin homeostasis and male gametophyte development in Arabidopsis. Nat Commun **3,** 941.
Douin, M.R. (1920). Le capitule de Marchantia polymorpha expliqué par Leitgeb et ses disciples. Revue générale de botanique **32,** 57-71.
Douin, M.R. (1921). Reserches sur les Marchantiées. Revue générale de botanique **33,** 34-62; 99-145; 190-209.
Douin, M.R. (1923). Reserches sur le gamétophyte des Marchantiées. Revue générale de botanique **35,** 213-226.
Durand, E.J. (1908). The Development of the Sexual Organs and Sporogonium of Marchantia polymorpha. Bulletin of the Torrey Botanical Club **35,** 321-335.
Eklund, D.M., Staldal, V., Valsecchi, I., Cierlik, I., Eriksson, C., Hiratsu, K., Ohme-Takagi, M., Sundstrom, J.F., Thelander, M., Ezcurra, I., and Sundberg, E. (2010a). The Arabidopsis thaliana STYLISH1 Protein Acts as a Transcriptional Activator Regulating Auxin Biosynthesis. Plant Cell **22,** 349-363.
Eklund, D.M., Thelander, M., Landberg, K., Staldal, V., Nilsson, A., Johansson, M., Valsecchi, I., Pederson, E.R.A., Kowalczyk, M., Ljung, K., Ronne, H., and Sundberg, E. (2010b). Homologues of the Arabidopsis thaliana

SHI/STY/LRP1 genes control auxin biosynthesis and affect growth and development in the moss Physcomitrella patens. Development **137,** 1275-1284.

Eshed, Y., Baum, S.F., Perea, J.V., and Bowman, J.L. (2001). Establishment of polarity in lateral organs of plants. Curr Biol **11,** 1251-1260.

Esmon, C.A., Tinsley, A.G., Ljung, K., Sandberg, G., Hearne, L.B., and Liscum, E. (2006). A gradient of auxin and auxin-dependent transcription precedes tropic growth responses. Proc Natl Acad Sci U S A **103,** 236-241.

Fahlgren, N., Montgomery, T.A., Howell, M.D., Allen, E., Dvorak, S.K., Alexander, A.L., and Carrington, J.C. (2006). Regulation of AUXIN RESPONSE FACTOR3 by TAS3 ta-siRNA affects developmental timing and patterning in Arabidopsis. Curr Biol **16,** 939-944.

Finet, C., and Jaillais, Y. (2012). Auxology: when auxin meets plant evo-devo. Dev. Biol. **369,** 19-31.

Finet, C., Timme, R.E., Delwiche, C.F., and Marleta, F. (2010). Multigene Phylogeny of the Green Lineage Reveals the Origin and Diversification of Land Plants. Curr. Biol. **20,** 2217-2222.

Finet, C., Berne-Dedieu, A., Scutt, C.P., and Marletaz, F. (2012). Evolution of the ARF Gene Family in Land Plants: Old Domains, New Tricks. Mol Biol Evol.

Fitting, H. (1935). Untersuchungen über die Induktion der Dorsiventralität bei den keimenden Brutkörpern von Marchantia und Lunularia. I. Die Induktoren und ihre Wirkungen. (Studies on the induction of Dorsiventralität in germinating propagules of Marchantia and Lunularia. I. The inducers and their effects.). Jahrbücher für wissenschaftliche Botanik **82,** 333-376

Fitting, H. (1936). Untersuchungen über die Induktion der Dorsiventralität bei den Marehantieen brutkörpern. II. Die Schwerkraft als Induktor der Dorsiventralität. (Studies on the induction of Dorsiventralität in Marehantieen brood bodies. II Gravity as an inducer of Dorsiventralität.). Jahrbücher für wissenschaftliche Botanik **82,** 696-740

Fitting, H. (1937a). IV. Das Substrat als Induktor der Dorsiventralität. (IV The substrate as the inductor Dorsiventralität.). Jahrbücher für wissenschaftliche Botanik **85,** 243-266

Fitting, H. (1937b). Untersuchungen über die Induktion der Dorsiventralität bei den Brutkörperkeimlingen der Marchantieen. III. Das Licht als Induktor der Dorsiventralität. (Studies on the induction of Dorsiventralität in propagules seedlings Marchantieen. III. Light as the inductor Dorsiventralität.). Jahrbücher für wissenschaftliche Botanik **85,** 169-242

Fitting, H. (1938). V. Die Umkehrbarkeit der durch Aussenfaktoren induzierten Dorsiventralität. (V. The reversibility of the induced by external factors Dorsiventralität.). Jahrbücher für wissenschaftliche Botanik **86,** 107-227

Fitting, H. (1939). Untersuchungen über den Einfluss von Licht und Dunkelheit auf die Entwicklung von Moosen. I. Die Brutkörper der Marchantieen. (Investigations on the influence of light and darkness on the development of mosses. I. The propagules of Marchantieen.). Jahrbücher für wissenschaftliche Botanik **88,** 633-722

Fitting, H. (1942). Untersuchungen über den Einfluss von Licht und Dunkelheit auf die Entwicklung von Moosen. II. Die Thalli der Leber- und Laubmoose.

(Investigations on the influence of light and darkness on the development of mosses. II The thalli of the liver and mosses.). Jahrbücher für wissenschaftliche Botanik **90,** 595-704

Floyd, S.K., and Bowman, J.L. (2004). Gene regulation: Ancient microRNA target sequences in plants. Nature **428,** 485-486.

Floyd, S.K., and Bowman, J.L. (2007). The ancestral developmental tool kit of land plants. Int. J. Plant Sci. **168,** 1-35.

Floyd, S.K., Zalewski, C.S., and Bowman, J.L. (2006). Evolution of class III homeodomain-leucine zipper genes in streptophytes. Genetics **173,** 373-388.

Förster, K. (1926). DIE WIRKUNG ÄUSSERER FAKTOREN AUF ENTWICKLUNG UND GESTALTBILDUNG BEI MARCHANTIA POLYMORPHA (THE EFFECT OF EXTERNAL FACTORS IN DEVELOPMENT AND EDUCATION IN SHAPE Marchantia polymorpha). (Aus dem Botanischen Institut der Universität Leipzig).

Friml, J., Vieten, A., Sauer, M., Weijers, D., Schwarz, H., Hamann, T., Offringa, R., and Jurgens, G. (2003). Efflux-dependent auxin gradients establish the apical-basal axis of Arabidopsis. Nature **426,** 147-153.

Fujita, T., Sakaguchi, H., Hiwatashi, Y., Wagstaff, S.J., Ito, M., Deguchi, H., Sato, T., and Hasebe, M. (2008). Convergent evolution of shoots in land plants: lack of auxin polar transport in moss shoots. Evol Dev **10,** 176-186.

Gaal, D.J., Dufresne, S.J., and Maravolo, N.C. (1982). TRANSPORT OF C-14-LABELED INDOLEACETIC-ACID IN THE HEPATIC MARCHANTIA-POLYMORPHA. Bryologist **85,** 410-418.

Galweiler, L., Guan, C., Muller, A., Wisman, E., Mendgen, K., Yephremov, A., and Palme, K. (1998). Regulation of polar auxin transport by AtPIN1 in Arabidopsis vascular tissue. Science **282,** 2226-2230.

Garcia, D., Collier, S.A., Byrne, M.E., and Martienssen, R.A. (2006). Specification of leaf polarity in Arabidopsis via the trans-acting siRNA pathway. Curr Biol **16,** 933-938.

Goebel, K.v. (1905). Organography of Plants especially of the Archegoniatae and Spermatophyta. (Oxford).

Goedecke, F. (1935). ÜBER DAS ZUSAMMENWIRKEN DER RICHTUNGSFAKTOREN BEI MARCHANTIA POLYMORPHA (ON THE INTERACTION OF THE DIRECTION OF FACTORS Marchantia polymorpha). Aus dem Botanischen Institut der Universität Rostock**,** 132-153.

Graff, P.W. (1936). Invasion by Marchantia polymorpha Following Forest Fires. Bulletin of the Torrey Botanical Club **63,** 67-74.

Gray, W.M., Kepinski, S., Rouse, D., Leyser, O., and Estelle, M. (2001). Auxin regulates SCF(TIR1)-dependent degradation of AUX/IAA proteins. Nature **414,** 271-276.

Gray, W.M., del Pozo, J.C., Walker, L., Hobbie, L., Risseeuw, E., Banks, T., Crosby, W.L., Yang, M., Ma, H., and Estelle, M. (1999). Identification of an SCF ubiquitin-ligase complex required for auxin response in Arabidopsis thaliana. Genes Dev **13,** 1678-1691.

Guilfoyle, T.J., and Hagen, G. (2001). Auxin response factors. Journal of Plant Growth Regulation **20,** 281-291.

Guilfoyle, T.J., and Hagen, G. (2007). Auxin response factors. Curr Opin Plant Biol **10,** 453-460.

Gutierrez, L., Bussell, J.D., Pacurar, D.I., Schwambach, J., Pacurar, M., and Bellini, C. (2009). Phenotypic Plasticity of Adventitious Rooting in Arabidopsis Is Controlled by Complex Regulation of AUXIN RESPONSE FACTOR Transcripts and MicroRNA Abundance. Plant Cell **21,** 3119-3132.

Hagen, G., and Guilfoyle, T.J. (1985). Rapid induction of selective transcription by auxins. Mol. Cell. Biol. **5,** 1197-1203.

Hagen, G., Uhrhammer, N., and Guilfoyle, T.J. (1988). REGULATION OF EXPRESSION OF AN AUXIN-INDUCED SOYBEAN SEQUENCE BY CADMIUM. J. Biol. Chem. **263,** 6442-6446.

Hagen, G., Martin, G., Li, Y., and Guilfoyle, T.J. (1991). AUXIN-INDUCED EXPRESSION OF THE SOYBEAN GH3 PROMOTER IN TRANSGENIC TOBACCO PLANTS. Plant Mol Biol **17,** 567-579.

Halbsguth, W. (1936). Untersuchungen über die Morphologie der Marehantieen-Brutkörper. (Studies on the morphology of the Marehantieen-propagules). Jahrbücher für wissenschaftliche Botanik **84** 290-334.

Halbsguth, W., and KOHLENBACH, H.-W. (1953). EINIGE VERSUCHE ÜBER DIE WIRKUNG VON HETEROAUXIN AUF DIE SYMMETRIEENTWICKLUNG DER BRUTKÖRPERKEIMLINGE VON MARCHANTIA POLYMORPHA L. (SOME EXPERIMENTS ON THE EFFECT OF THE SYMMETRY heteroauxin DEVELOPMENT OF NUCLEAR BODY seedlings of Marchantia polymorpha L.). Planta **42,** 349-366.

Hamann, T., Mayer, U., and Jurgens, G. (1999). The auxin-insensitive bodenlos mutation affects primary root formation and apical-basal patterning in the Arabidopsis embryo. Development **126,** 1387-1395.

Hammond, S.M. (2005). Dicing and slicing: the core machinery of the RNA interference pathway. FEBS Lett **579,** 5822-5829.

Hardtke, C.S., and Berleth, T. (1998). The Arabidopsis gene MONOPTEROS encodes a transcription factor mediating embryo axis formation and vascular development. Embo J **17,** 1405-1411.

Hardtke, C.S., Ckurshumova, W., Vidaurre, D.P., Singh, S.A., Stamatiou, G., Tiwari, S.B., Hagen, G., Guilfoyle, T.J., and Berleth, T. (2004). Overlapping and non-redundant functions of the Arabidopsis auxin response factors MONOPTEROS and NONPHOTOTROPIC HYPOCOTYL 4. Development **131,** 1089-1100.

Harper, R.M., Stowe-Evans, E.L., Luesse, D.R., Muto, H., Tatematsu, K., Watahiki, M.K., Yamamoto, K., and Liscum, E. (2000). The NPH4 locus encodes the auxin response factor ARF7, a conditional regulator of differential growth in aerial Arabidopsis tissue. Plant Cell **12,** 757-770.

He, W.R., Brumos, J., Li, H.J., Ji, Y.S., Ke, M., Gong, X.Q., Zeng, Q.L., Li, W.Y., Zhang, X.Y., An, F.Y., Wen, X., Li, P.P., Chu, J.F., Sun, X.H., Yan, C.Y., Yan, N., Xie, D.Y., Raikhel, N., Yang, Z.B., Stepanova, A.N., Alonso, J.M., and Guo, H.W. (2011). A Small-Molecule Screen Identifies L-Kynurenine as a Competitive Inhibitor of TAA1/TAR Activity in Ethylene-Directed Auxin Biosynthesis and Root Growth in Arabidopsis. Plant Cell **23,** 3944-3960.

Heisler, M.G., Atkinson, A., Bylstra, Y.H., Walsh, R., and Smyth, D.R. (2001). SPATULA, a gene that controls development of carpel margin tissues in Arabidopsis, encodes a bHLH protein. Development **128,** 1089-1098.

Heisler, M.G., Ohno, C., Das, P., Sieber, P., Reddy, G.V., Long, J.A., and Meyerowitz, E.M. (2005). Patterns of auxin transport and gene expression during primordium development revealed by live imaging of the Arabidopsis inflorescence meristem. Curr. Biol. **15,** 1899-1911.

Hendelman, A., Buxdorf, K., Stav, R., Kravchik, M., and Arazi, T. (2012). Inhibition of lamina outgrowth following Solanum lycopersicum AUXIN RESPONSE FACTOR 10 (SlARF10) derepression. Plant Mol Biol **78,** 561-576.

Henfrey, A. (1853). XII. On the Development of the Spores and Elaters of Marchantia polymorpha. Transactions of the Linnean Society **21,** 103-110.

Hobbie, L., and Estelle, M. (1994). Genetic Approaches to Auxin Action. Plant Cell Environ **17,** 525-540.

Ikeno, S. (1903). Beiträge zur Kenntnis der pflanzlichen Spermatogenese: Die Spermatogenese von Marchantia polymorpha (Contributions to the knowledge of plant spermatogenesis: Spermatogenesis of Marchantia polymorpha). Beihefte zum Botanischen Centralblatt **15,** 5-88.

Ishizaki, K., Chiyoda, S., Yamato, K.T., and Kohchi, T. (2008). Agrobacterium-mediated transformation of the haploid liverwort Marchantia polymorpha L., an emerging model for plant biology. Plant Cell Physiol **49,** 1084-1091.

Ishizaki, K., Nonomura, M., Kato, H., Yamato, K.T., and Kohchi, T. (2012). Visualization of auxin-mediated transcriptional activation using a common auxin-responsive reporter system in the liverwort Marchantia polymorpha. Journal of Plant Research **125,** 643-651.

Jang, G., Yi, K., Pires, N.D., Menand, B., and Dolan, L. (2011). RSL genes are sufficient for rhizoid system development in early diverging land plants. Development **138,** 2273-2281.

Johri, M.M., and Desai, S. (1973). AUXIN REGULATION OF CAULONEMA FORMATION IN MOSS PROTONEMA. Nature-New Biology **245,** 223-224.

Jones, V.A., and Dolan, L. (2012). The evolution of root hairs and rhizoids. Annals of Botany **110,** 205-212.

Jurgens, G. (2001). Apical-basal pattern formation in Arabidopsis embryogenesis. Embo J **20,** 3609-3616.

Kagale, S., Links, M.G., and Rozwadowski, K. (2010). Genome-Wide Analysis of Ethylene-Responsive Element Binding Factor-Associated Amphiphilic Repression Motif-Containing Transcriptional Regulators in Arabidopsis. Plant Physiol **152,** 1109-1134.

Kaul, K.N., Tripathi, B.K., and Mitra, G.C. (1961a). MORPHOGENETIC RESPONSES OF THALLUS OF MARCHANTIA TO SEVERAL GROWTH SUBSTANCES. Current Science **30,** 131-&.

Kaul, K.N., Mitra, G.C., and Tripathi, B.K. (1961b). Morphognetic responses of the thallus of Marchantia to several growth substances. Current Science **30,** 131-133.

Kaul, K.N., Mitra, G.C., and Tripathi, B.K. (1962). Responses of Marchantia in Aseptic Culture to Well-known Auxins and Antiauxins. Ann Bot-London **26,** 447-466.

Kepinski, S., and Leyser, O. (2005). The Arabidopsis F-box protein TIR1 is an auxin receptor. Nature **435,** 446-451.

Kienitz-Gerloff, F. (1874). Vergleichende Untersuchungen über die Entwickelungsgeschichte des Lebermoos - Sporogoniums (Comparative studies available via the evolutionary history of liverworts - Sporogoniums). Botanische Zeitung **32,** 161-172; 193-204; 209-221; 225-238.

Kim, J., Harter, K., and Theologis, A. (1997). Protein-protein interactions among the Aux/IAA proteins. Proc Natl Acad Sci U S A **94,** 11786-11791.

Klambt, D., Knauth, B., and Dittmann, I. (1992). AUXIN DEPENDENT GROWTH OF RHIZOIDS OF CHARA-GLOBULARIS. Physiologia Plantarum **85,** 537-540.

Kny, L. (1865). Beiträge zur Entwickelungs geschichte der laubigen Lebermoose (Contributions to the history of development of the leafy liverworts). Jahrbücher für wissenschaftliche Botanik **4,** 64-100.

Kny, L. (1890). Botanische wandtafeln mit erläuterndem text (Botanical wall panels with explanatory text). (Berlin: Wiegandt. Hempel & Parey).

Krogan, N.T., Ckurshumova, W., Marcos, D., Caragea, A.E., and Berleth, T. (2012). Deletion of MP/ARF5 domains III and IV reveals a requirement for Aux/IAA regulation in Arabidopsis leaf vascular patterning. New Phytol **194,** 391-401.

Kuo, M.H., Brownell, J.E., Sobel, R.E., Ranalli, T.A., Cook, R.G., Edmondson, D.G., Roth, S.Y., and Allis, C.D. (1996). Transcription-linked acetylation by Gcn5p of histones H3 and H4 at specific lysines. Nature **383,** 269-272.

LaRue, C.D., and Narayanaswami, S. (1957). Auxin Inhibition in the Liverwort Lunularia. New Phytologist **56,** 61-70.

Laux, T., Mayer, U., Busch, M., Mayer, K., Ruiz, R.A.T., Berleth, T., and Jurgens, G. (1994). ESTABLISHING BODY PATTERN IN ARABIDOPSIS. Dev. Biol. **163,** 533-533.

Leitgeb, H. (1880a). Die Inflorescenzen der Marchantiaceen. Sitzungsberichte der Kaiserlichen Akademie der Wissenschaften, Wien **81,** 123-143.

Leitgeb, H. (1880b). Die Athemöffnungen der Marchantiaceen. Sitzungsberichte der Kaiserlichen Akademie der Wissenschaften, Wien **81,** 40-54.

Leitgeb, H. (1881). Untersuchungen über die Lebermoose. Vol. VI. Die Marchantieen. (Studies on the liverworts. Vol VI. The Marchantieen.). (Jena).

Leyser, H.M.O., Pickett, F.B., Dharmasiri, S., and Estelle, M. (1996). Mutations in the AXR3 gene of Arabidopsis result in altered auxin response including ectopic expression from the SAUR-AC1 promoter. Plant Journal **10,** 403-413.

Leyser, H.M.O., Lincoln, C.A., Timpte, C., Lammer, D., Turner, J., and Estelle, M. (1993). ARABIDOPSIS AUXIN-RESISTANCE GENE-AXR1 ENCODES A PROTEIN RELATED TO UBIQUITIN-ACTIVATING ENZYME-E1. Nature **364,** 161-164.

Li, H., Xu, L., Wang, H., Yuan, Z., Cao, X., Yang, Z., Zhang, D., Xu, Y., and Huang, H. (2005). The Putative RNA-dependent RNA polymerase RDR6 acts

synergistically with ASYMMETRIC LEAVES1 and 2 to repress BREVIPEDICELLUS and MicroRNA165/166 in Arabidopsis leaf development. Plant Cell **17,** 2157-2171.

Li, Y., Liu, Z.B., Shi, X.Y., Hagen, G., and Guilfoyle, T.J. (1994). An Auxin-Inducible Element in Soybean SAUR Promoters. Plant Physiol **106,** 37-43.

Liscum, E., and Briggs, W.R. (1996). Mutations of Arabidopsis in potential transduction and response components of the phototropic signaling pathway. Plant Physiol **112,** 291-296.

Liscum, E., and Reed, J.W. (2002). Genetics of Aux/IAA and ARF action in plant growth and development. Plant Mol Biol **49,** 387-400.

Liu, P.P., Montgomery, T.A., Fahlgren, N., Kasschau, K.D., Nonogaki, H., and Carrington, J.C. (2007). Repression of AUXIN RESPONSE FACTOR10 by microRNA160 is critical for seed germination and post-germination stages. Plant Journal **52,** 133-146.

Liu, X.D., Huang, J., Wang, Y., Khanna, K., Xie, Z.X., Owen, H.A., and Zhao, D.Z. (2010). The role of floral organs in carpels, an Arabidopsis loss-of-function mutation in MicroRNA160a, in organogenesis and the mechanism regulating its expression. Plant Journal **62,** 416-428.

Liu, Z.B., Ulmasov, T., Shi, X.Y., Hagen, G., and Guilfoyle, T.J. (1994). SOYBEAN GH3 PROMOTER CONTAINS MULTIPLE AUXIN-INDUCIBLE ELEMENTS. Plant Cell **6,** 645-657.

Long, J.A., Ohno, C., Smith, Z.R., and Meyerowitz, E.M. (2006). TOPLESS regulates apical embryonic fate in Arabidopsis. Science **312,** 1520-1523.

Long, J.A., Woody, S., Poethig, S., Meyerowitz, E.M., and Barton, K. (2002). Transformation of shoots into roots in Arabidopsis embryos mutant at the TOPLESS locus. Development **129,** 2797-2806.

Ludwig-Muller, J., Decker, E.L., and Reski, R. (2009a). Dead end for auxin conjugates in Physcomitrella? Plant Signal Behav **4,** 116-118.

Ludwig-Muller, J., Julke, S., Bierfreund, N.M., Decker, E.L., and Reski, R. (2009b). Moss (Physcomitrella patens) GH3 proteins act in auxin homeostasis. New Phytologist **181,** 323-338.

Luschnig, C., Gaxiola, R.A., Grisafi, P., and Fink, G.R. (1998). EIR1, a root-specific protein involved in auxin transport, is required for gravitropism in Arabidopsis thaliana. Genes Dev **12,** 2175-2187.

Mallory, A.C., Bartel, D.P., and Bartel, B. (2005). MicroRNA-directed regulation of Arabidopsis AUXIN RESPONSE FACTOR17 is essential for proper development and modulates expression of early auxin response genes. Plant Cell **17,** 1360-1375.

Maravolo, N.C. (1976). POLARITY AND LOCALIZATION OF AUXIN MOVEMENT IN HEPATIC, MARCHANTIA-POLYMORPHA. American Journal of Botany **63,** 526-531.

Maravolo, N.C., and Voth, P.D. (1966). MORPHOGENIC EFFECTS OF 3 GROWTH SUBSTANCES ON MARCHANTIA GEMMALINGS. Botanical Gazette **127,** 79-&.

Mashiguchi, K., Tanaka, K., Sakai, T., Sugawara, S., Kawaide, H., Natsume, M., Hanada, A., Yaeno, T., Shirasu, K., Yao, H., McSteen, P., Zhao, Y.D., Hayashi, K., Kamiya, Y., and Kasahara, H. (2011). The main auxin biosynthesis pathway in Arabidopsis. Proc Natl Acad Sci U S A **108,** 18512-18517.

Mattsson, J., Ckurshumova, W., and Berleth, T. (2003). Auxin signaling in Arabidopsis leaf vascular development. Plant Physiol **131,** 1327-1339.
Mayer, U., Ruiz, R.A.T., Berleth, T., Misera, S., and Jurgens, G. (1991). MUTATIONS AFFECTING BODY ORGANIZATION IN THE ARABIDOPSIS EMBRYO. Nature **353,** 402-407.
McCarty, D.R., Hattori, T., Carson, C.B., Vasil, V., Lazar, M., and Vasil, I.K. (1991). THE VIVIPAROUS-1 DEVELOPMENTAL GENE OF MAIZE ENCODES A NOVEL TRANSCRIPTIONAL ACTIVATOR. Cell **66,** 895-905.
McClure, B.A., Hagen, G., Brown, C.S., Gee, M.A., and Guilfoyle, T.J. (1989). TRANSCRIPTION, ORGANIZATION, AND SEQUENCE OF AN AUXIN-REGULATED GENE-CLUSTER IN SOYBEAN. Plant Cell **1,** 229-239.
McNaught, H.L. (1929). Development of sporophyte of Marchantia chenopoda. Bot Gaz **88,** 400-416.
Menand, B., Yi, K., Jouannic, S., Hoffmann, L., Ryan, E., Linstead, P., Schaefer, D.G., and Dolan, L. (2007). An ancient mechanism controls the development of cells with a rooting function in land plants. Science **316,** 1477-1480.
Meyers, B.C., Axtell, M.J., Bartel, B., Bartel, D.P., Baulcombe, D., Bowman, J.L., Cao, X., Carrington, J.C., Chen, X., Green, P.J., Griffiths-Jones, S., Jacobsen, S.E., Mallory, A.C., Martienssen, R.A., Poethig, R.S., Qi, Y., Vaucheret, H., Voinnet, O., Watanabe, Y., Weigel, D., and Zhu, J.K. (2008). Criteria for annotation of plant MicroRNAs. Plant Cell **20,** 3186-3190.
Miller, M.W., and Voth, P.D. (1962). Geotropic Responses of Marchantia. The Bryologist **65,** 146-154.
Mirbel, M. (1835a). Researches anatomiques et physiologiques sur le Marchantia polymorpha. (Anatomical and physiological researches on Marchantia polymorpha.). Mém. Acad. Roy. Sc. Inst. France **13,** 337-436.
Mirbel, M. (1835b). Researches anatomiques et physiologiques sur le Marchantia polymorpha. (Anatomical and physiological researches on Marchantia polymorpha.). Mém. Acad. Roy. Sc. Inst. France. **13,** 337-436
Moon, J., Parry, G., and Estelle, M. (2004). The ubiquitin-proteasome pathway and plant development. Plant Cell **16,** 3181-3195.
Mravec, J., Kubes, M., Bielach, A., Gaykova, V., Petrasek, J., Skupa, P., Chand, S., Benkova, E., Zazimalova, E., and Friml, J. (2008). Interaction of PIN and PGP transport mechanisms in auxin distribution-dependent development. Development **135,** 3345-3354.
Mravec, J., Skupa, P., Bailly, A., Hoyerova, K., Krecek, P., Bielach, A., Petrasek, J., Zhang, J., Gaykova, V., Stierhof, Y.D., Dobrev, P.I., Schwarzerova, K., Rolcik, J., Seifertova, D., Luschnig, C., Benkova, E., Zazimalova, E., Geisler, M., and Friml, J. (2009). Subcellular homeostasis of phytohormone auxin is mediated by the ER-localized PIN5 transporter. Nature **459,** 1136-1140.
Muller, A., Guan, C., Galweiler, L., Tanzler, P., Huijser, P., Marchant, A., Parry, G., Bennett, M., Wisman, E., and Palme, K. (1998). AtPIN2 defines a locus of Arabidopsis for root gravitropism control. Embo J **17,** 6903-6911.
Murphy, A.S., Hoogner, K.R., Peer, W.A., and Taiz, L. (2002). Identification, purification, and molecular cloning of N-1-naphthylphthalmic acid-

binding plasma membrane-associated aminopeptidases from Arabidopsis. Plant Physiol **128,** 935-950.

Nagai, I. (1919). Induced Adventitious Growth in the Gemnnae of Marchantia. The Botanical Magazine **33,** 99-109.

Nagpal, P., Walker, L.M., Young, J.C., Sonawala, A., Timpte, C., Estelle, M., and Reed, J.W. (2000). AXR2 encodes a member of the Aux/IAA protein family. Plant Physiol **123,** 563-573.

Nakazawa, M., Yabe, N., Ichikawa, T., Yamamoto, Y.Y., Yoshizumi, T., Hasunuma, K., and Matsui, M. (2001). DFL1, an auxin-responsive GH3 gene homologue, negatively regulates shoot cell elongation and lateral root formation, and positively regulates the light response of hypocotyl length. Plant J **25,** 213-221.

Napier, R.M., David, K.M., and Perrot-Rechenmann, C. (2002). A short history of auxin-binding proteins. Plant Mol Biol **49,** 339-348.

Ninnemann, H., and Halbsguth, W. (1965). Rolle des Phytochroms beim Etiolement von Marchantia polymorpha. Naturwissenschaften **52,** 110-111.

Noh, B., Murphy, A.S., and Spalding, E.P. (2001). Multidrug resistance-like genes of Arabidopsis required for auxin transport and auxin-mediated development. Plant Cell **13,** 2441-2454.

O'Hanlon, M.E. (1926). Germination of Spores and Early Stages in Development of Gametophyte of Marchantia polymorpha. Bot Gaz **82,** 215-222.

Oeller, P.W., Keller, J.A., Parks, J.E., Silbert, J.E., and Theologis, A. (1993). STRUCTURAL CHARACTERIZATION OF THE EARLY INDOLEACETIC ACID-INDUCIBLE GENES, PS-IAA4/5 AND PS-IAA6, OF PEA (PISUM-SATIVUM L). J. Mol. Biol. **233,** 789-798.

Okada, K., Ueda, J., Komaki, M.K., Bell, C.J., and Shimura, Y. (1991). Requirement of the Auxin Polar Transport System in Early Stages of Arabidopsis Floral Bud Formation. Plant Cell **3,** 677-684.

Okushima, Y., Overvoorde, P.J., Arima, K., Alonso, J.M., Chan, A., Chang, C., Ecker, J.R., Hughes, B., Lui, A., Nguyen, D., Onodera, C., Quach, H., Smith, A., Yu, G.X., and Theologis, A. (2005). Functional genomic analysis of the AUXIN RESPONSE FACTOR gene family members in Arabidopsis thaliana: Unique and overlapping functions of ARF7 and ARF19. Plant Cell **17,** 444-463.

Otto, K.-R. (1976). Der Einfluss von ausseren Faktoren auf die Bildung von Primärrhizoiden bei Brutkörpern von Marchantia polymorpha 1. (The influence of outer factors in the formation of primary rhizoids propagules of Marchantia polymorpha). Z. Pflanzenphysiol. **80,** 189-196.

Otto, K.-R., and Halbsguth, W. (1976). Die Forderung der Bildung von Primärrhizoiden an Brutkörpern von Marchantia polymorpha L. durch Licht und IES (The demand of the formation of primary rhizoids of propagules of Marchantia polymorpha L. by light and IAA). Z. Pflanzenphysiol. **80,** 197-205.

Ouellet, F., Overvoorde, P.J., and Theologis, A. (2001). IAA17/AXR3: Biochemical insight into an auxin mutant phenotype. Plant Cell **13,** 829-841.

Ouyang, J., Shao, X., and Li, J. (2000). Indole-3-glycerol phosphate, a branchpoint of indole-3-acetic acid biosynthesis from the tryptophan biosynthetic pathway in Arabidopsis thaliana. Plant J **24,** 327-333.

Pagnussat, G.C., Alandete-Saez, M., Bowman, J.L., and Sundaresan, V. (2009). Auxin-Dependent Patterning and Gamete Specification in the Arabidopsis Female Gametophyte. Science **324,** 1684-1689.

Pekker, I., Alvarez, J.P., and Eshed, Y. (2005). Auxin response factors mediate Arabidopsis organ asymmetry via modulation of KANADI activity. Plant Cell **17,** 2899-2910.

Petrasek, J., and Friml, J. (2009). Auxin transport routes in plant development. Development **136,** 2675-2688.

Prasad, K., Grigg, S.P., Barkoulas, M., Yadav, R.K., Sanchez-Perez, G.F., Pinon, V., Blilou, I., Hofhuis, H., Dhonukshe, P., Galinha, C., Mahonen, A.P., Muller, W.H., Raman, S., Verkleij, A.J., Snel, B., Reddy, G.V., Tsiantis, M., and Scheres, B. (2011). Arabidopsis PLETHORA transcription factors control phyllotaxis. Curr Biol **21,** 1123-1128.

Prigge, M.J., Lavy, M., Ashton, N.W., and Estelle, M. (2010). Physcomitrella patens Auxin-Resistant Mutants Affect Conserved Elements of an Auxin-Signaling Pathway. Curr. Biol. **20,** 1907-1912.

Prior, P.V., and Riggs, V.C. (1963). The Effects of Several Growth Regulators on Gametophytes of Riccia fluitans. The Bryologist **66,** 55-61.

Przemeck, G.K., Mattsson, J., Hardtke, C.S., Sung, Z.R., and Berleth, T. (1996). Studies on the role of the Arabidopsis gene MONOPTEROS in vascular development and plant cell axialization. Planta **200,** 229-237.

Qiao, M., Zhao, Z.J., Song, Y.G., Liu, Z.H., Cao, L.X., Yu, Y.C., Li, S., and Xiang, F.N. (2012). Proper regeneration from in vitro cultured Arabidopsis thaliana requires the microRNA-directed action of an auxin response factor. Plant Journal **71,** 14-22.

Reinhardt, D., Mandel, T., and Kuhlemeier, C. (2000). Auxin regulates the initiation and radial position of plant lateral organs. Plant Cell **12,** 507-518.

Remington, D.L., Vision, T.J., Guilfoyle, T.J., and Reed, J.W. (2004). Contrasting modes of diversification in the Aux/IAA and ARF gene families. Plant Physiol **135,** 1738-1752.

Rensing, S.A., Lang, D., Zimmer, A.D., Terry, A., Salamov, A., Shapiro, H., Nishiyama, T., Perroud, P.F., Lindquist, E.A., Kamisugi, Y., Tanahashi, T., Sakakibara, K., Fujita, T., Oishi, K., Shin-I, T., Kuroki, Y., Toyoda, A., Suzuki, Y., Hashimoto, S., Yamaguchi, K., Sugano, S., Kohara, Y., Fujiyama, A., Anterola, A., Aoki, S., Ashton, N., Barbazuk, W.B., Barker, E., Bennetzen, J.L., Blankenship, R., Cho, S.H., Dutcher, S.K., Estelle, M., Fawcett, J.A., Gundlach, H., Hanada, K., Heyl, A., Hicks, K.A., Hughes, J., Lohr, M., Mayer, K., Melkozernov, A., Murata, T., Nelson, D.R., Pils, B., Prigge, M., Reiss, B., Renner, T., Rombauts, S., Rushton, P.J., Sanderfoot, A., Schween, G., Shiu, S.H., Stueber, K., Theodoulou, F.L., Tu, H., Van de Peer, Y., Verrier, P.J., Waters, E., Wood, A., Yang, L.X., Cove, D., Cuming, A.C., Hasebe, M., Lucas, S., Mishler, B.D., Reski, R., Grigoriev, I.V., Quatrano, R.S., and Boore, J.L. (2008). The Physcomitrella genome reveals evolutionary insights into the conquest of land by plants. Science **319,** 64-69.

Rose, S., and Bopp, M. (1983). UPTAKE AND POLAR TRANSPORT OF INDOLEACETIC-ACID IN MOSS RHIZOIDS. Physiologia Plantarum **58,** 57-61.

Rose, S., Rubery, P.H., and Bopp, M. (1983). THE MECHANISM OF AUXIN UPTAKE AND ACCUMULATION IN MOSS PROTONEMATA. Physiologia Plantarum **58,** 52-56.

Rouse, D., Mackay, P., Stirnberg, P., Estelle, M., and Leyser, O. (1998). Changes in auxin response from mutations in an AUX/IAA gene. Science **279,** 1371-1373.

Rousseau, J. (1950). Action de l'acide indol beta-acétique sur les propagules de marchantia polymorpha et Lunularia cruciata (Action beta-indol acetic propagules on Marchantia polymorpha and Lunularia cruciata). Comptes rendus hebdomadaires des séances de l'Académie des sciences **230,** 675-676.

Rousseau, J. (1951a). Action des acides 2.4-dichloro-phénoxy-acétique et 2.5-dichloro-thio-acétique sur les propagules de Marchantia polymorpha L. (Action of acids 2.4-dichloro-phenoxy-acetic acid and 2.5-dichloro-thio-acetic propagules on Marchantia polymorpha L.). Comptes rendus hebdomadaires des séances de l'Académie des sciences **232,** 749-751.

Rousseau, J. (1951b). Action de l'acide x napthaléne acétique sur les corbeilles á propagules de Marchantia polymorpha L. et de Lunularia cruciata Adans. (Action naphthalene acetic acid on baskets á propagules Marchantia polymorpha L. and Lunularia cruciata Adans.). Comptes rendus hebdomadaires des séances de l'Académie des sciences **232,** 107-108.

Rousseau, J. (1952a). Influence des hétéroauxines sur la croissance des corbeilles a propagules de Marchantia polymorpha L. et de Lunularia cruciata Adans. (Influence of auxins on the growth of propagules of baskets has Marchantia polymorpha L. and Lunularia cruciata Adans.) Revue Bryologique et Lichénologique **75,** 239-241.

Rousseau, J. (1952b). Action de l'acide 2.4-dichlorophénoxyacétique sur les spores de Marchantia polymorpha L. (Action of the acid 2,4-dichlorophenoxyacetic on spores Marchantia polymorpha L.). Comptes rendus hebdomadaires des séances de l'Académie des sciences **234,** 988-990.

Rousseau, J. (1953). Action de hétéroauxines sur les thalles de Lunularia cruciata Adans. et de Marchantia polymorpha L. (Action of auxins on thalli Lunularia cruciata Adans. and Marchantia polymorpha L.). Revue Bryologique et Lichénologique **76,** 22-25.

Rousseau, J. (1954). Action des hétéroauxines á l'obscurité sur les propagules de Marchantia polymorpha L. (Action hétéroauxines favorite darkness of propagules of Marchantia polymorpha L.). Comptes rendus hebdomadaires des séances de l'Académie des sciences **238,** 2111-2112.

Ruegger, M., Dewey, E., Gray, W.M., Hobbie, L., Turner, J., and Estelle, M. (1998). The TIR1 protein of Arabidopsis functions in auxin response and is related to human SKP2 and yeast Grr1p. Genes Dev **12,** 198-207.

Ruegger, M., Dewey, E., Hobbie, L., Brown, D., Bernasconi, P., Turner, J., Muday, G., and Estelle, M. (1997). Reduced naphthylphthalamic acid binding in the tir3 mutant of Arabidopsis is associated with a reduction in

polar auxin transport and diverse morphological defects. Plant Cell **9,** 745-757.

Sabatini, S., Beis, D., Wolkenfelt, H., Murfett, J., Guilfoyle, T., Malamy, J., Benfey, P., Leyser, O., Bechtold, N., Weisbeek, P., and Scheres, B. (1999). An auxin-dependent distal organizer of pattern and polarity in the Arabidopsis root. Cell **99,** 463-472.

Schneider, M.J., Troxler, R.F., and Voth, P.D. (1967). Occurrence of Indoleacetic Acid in the Bryophytes. Bot Gaz **128,** 174-179.

Scott, G.A.M. (1963). Suppression of Gemma-Cups in Marchantia by High Humidity. Nature **200,** 1123-&.

Seo, P.J., Hong, S.Y., Kim, S.G., and Park, C.M. (2011). Competitive inhibition of transcription factors by small interfering peptides. Trends Plant Sci. **16,** 541-549.

Seo, P.J., Hong, S.-Y., Ryu, J.Y., Jeong, E.-Y., Kim, S.-G., Baldwin, I.T., and Park, C.-M. (2012). Targeted inactivation of transcription factors by overexpression of their truncated forms in plants. The Plant Journal **72,** 162-172.

Sessions, A., Nemhauser, J.L., McColl, A., Roe, J.L., Feldmann, K.A., and Zambryski, P.C. (1997). ETTIN patterns the Arabidopsis floral meristem and reproductive organs. Development **124,** 4481-4491.

Smith, G.M. (1955). Crytogamic Botany Volume II Bryophytes and Pteridophytes. (New York: McGraw-Hill Book Company, Inc.).

Smith, Z.R., and Long, J.A. (2010). Control of Arabidopsis apical-basal embryo polarity by antagonistic transcription factors. Nature **464,** 423-U121.

Staswick, P.E., Serban, B., Rowe, M., Tiryaki, I., Maldonado, M.T., Maldonado, M.C., and Suza, W. (2005). Characterization of an Arabidopsis enzyme family that conjugates amino acids to indole-3-acetic acid. Plant Cell **17,** 616-627.

Stepanova, A.N., Yun, J., Robles, L.M., Novak, O., He, W., Guo, H., Ljung, K., and Alonso, J.M. (2011). The Arabidopsis YUCCA1 flavin monooxygenase functions in the indole-3-pyruvic acid branch of auxin biosynthesis. Plant Cell **23,** 3961-3973.

Stepanova, A.N., Robertson-Hoyt, J., Yun, J., Benavente, L.M., Xie, D.Y., DoleZal, K., Schlereth, A., Jurgens, G., and Alonso, J.M. (2008). TAA1-mediated auxin biosynthesis is essential for hormone crosstalk and plant development. Cell **133,** 177-191.

Stowe-Evans, E.L., Harper, R.M., Motchoulski, A.V., and Liscum, E. (1998). NPH4, a conditional modulator of auxin-dependent differential growth responses in Arabidopsis. Plant Physiol **118,** 1265-1275.

Strasburger, E. (1869). Die Geschlechtsorgane und die Befruchtung bei Marchantia polymorpha L. (The sex organs and fertilization in Marchantia polymorpha). Jahrbücher für wissenschaftliche Botanik **7,** 409-422. .

Szemenyei, H., Hannon, M., and Long, J.A. (2008). TOPLESS mediates auxin-dependent transcriptional repression during Arabidopsis embryogenesis. Science **319,** 1384-1386.

Sztein, A.E., Cohen, J.D., and Cooke, T.J. (2000). Evolutionary patterns in the auxin metabolism of green plants. Int. J. Plant Sci. **161,** 849-859.

Sztein, A.E., Cohen, J.D., de la Fuente, I.G., and Cooke, T.J. (1999). Auxin metabolism in mosses and liverworts. American Journal of Botany **86,** 1544-1555.

Takase, T., Nakazawa, M., Ishikawa, A., Manabe, K., and Matsui, M. (2003). DFL2, a new member of the Arabidopsis GH3 gene family, is involved in red light-specific hypocotyl elongation. Plant Cell Physiol **44,** 1071-1080.

Takase, T., Nakazawa, M., Ishikawa, A., Kawashima, M., Ichikawa, T., Takahashi, N., Shimada, H., Manabe, K., and Matsui, M. (2004). ydk1-D, an auxin-responsive GH3 mutant that is involved in hypocotyl and root elongation. Plant J **37,** 471-483.

Talmor-Neiman, M., Stav, R., Klipcan, L., Buxdorf, K., Baulcombe, D.C., and Arazi, T. (2006). Identification of trans-acting siRNAs in moss and an RNA-dependent RNA polymerase required for their biogenesis. Plant J **48,** 511-521.

Tan, X., Calderon-Villalobos, L.I.A., Sharon, M., Zheng, C.X., Robinson, C.V., Estelle, M., and Zheng, N. (2007). Mechanism of auxin perception by the TIR1 ubiquitin ligase. Nature **446,** 640-645.

Tao, Y., Ferrer, J.L., Ljung, K., Pojer, F., Hong, F.X., Long, J.A., Li, L., Moreno, J.E., Bowman, M.E., Ivans, L.J., Cheng, Y.F., Lim, J., Zhao, Y.D., Ballare, C.L., Sandberg, G., Noel, J.P., and Chory, J. (2008). Rapid synthesis of auxin via a new tryptophan-dependent pathway is required for shade avoidance in plants. Cell **133,** 164-176.

Tarén, N. (1958). Regulating the Initial Development of Gemmae in Marchantia polymorpha. The Bryologist **61,** 191-204.

Taylor, T. (1837). De Marchantieis. Transactions of the Linnean Society **17,** 375-395.

Terol, J., Domingo, C., and Talon, M. (2006). The GH3 family in plants: Genome wide analysis in rice and evolutionary history based on EST analysis. Gene **371,** 279-290.

Theologis, A., Huynh, T.V., and Davis, R.W. (1985). RAPID INDUCTION OF SPECIFIC MESSENGER-RNAS BY AUXIN IN PEA EPICOTYL TISSUE. J. Mol. Biol. **183,** 53-68.

Tian, Q., and Reed, J.W. (1999). Control of auxin-regulated root development by the Arabidopsis thaliana SHY2/IAA3 gene. Development **126,** 711-721.

Timme, R.E., and Delwiche, C.F. (2010). Uncovering the evolutionary origin of plant molecular processes: comparison of Coleochaete (Coleochaetales) and Spirogyra (Zygnematales) transcriptomes. BMC Plant Biol **10,** 96.

Timme, R.E., Bachvaroff, T.R., and Delwiche, C.F. (2012). Broad phylogenomic sampling and the sister lineage of land plants. PLoS One **7,** e29696.

Tiwari, S.B., Hagen, G., and Guilfoyle, T. (2003). The roles of auxin response factor domains in auxin-responsive transcription. Plant Cell **15,** 533-543.

Tiwari, S.B., Wang, X.J., Hagen, G., and Guilfoyle, T.J. (2001). AUX/IAA proteins are active repressors, and their stability and activity are modulated by auxin. Plant Cell **13,** 2809-2822.

Ulmasov, T., Hagen, G., and Guilfoyle, T.J. (1997a). ARF1, a transcription factor that binds to auxin response elements. Science **276,** 1865-1868.

Ulmasov, T., Hagen, G., and Guilfoyle, T.J. (1999a). Dimerization and DNA binding of auxin response factors. Plant J **19,** 309-319.

Ulmasov, T., Hagen, G., and Guilfoyle, T.J. (1999b). Activation and repression of transcription by auxin-response factors. Proc Natl Acad Sci U S A **96,** 5844-5849.

Ulmasov, T., Liu, Z.B., Hagen, G., and Guilfoyle, T.J. (1995). Composite Structure of Auxin Response Elements. Plant Cell **7,** 1611-1623.

Ulmasov, T., Murfett, J., Hagen, G., and Guilfoyle, T.J. (1997b). Aux/IAA proteins repress expression of reporter genes containing natural and highly active synthetic auxin response elements. Plant Cell **9,** 1963-1971.

Utsuno, K., Shikanai, T., Yamada, Y., and Hashimoto, T. (1998). Agr, an Agravitropic locus of Arabidopsis thaliana, encodes a novel membrane-protein family member. Plant Cell Physiol **39,** 1111-1118.

Valio, I.F.M., and Schwabe, W.W. (1969). Growth and Dormancy in Lunularia Cruciata (L) Dum .4. Light and Temperature Control of Rhizoid Formation in Gemmae. J Exp Bot **20,** 615-&.

Vanneste, S., and Friml, J. (2009). Auxin: A Trigger for Change in Plant Development. Cell **136,** 1005-1016.

Vernoux, T., Brunoud, G., Farcot, E., Morin, V., Van den Daele, H., Legrand, J., Oliva, M., Das, P., Larrieu, A., Wells, D., Guedon, Y., Armitage, L., Picard, F., Guyomarc'h, S., Cellier, C., Parry, G., Koumproglou, R., Doonan, J.H., Estelle, M., Godin, C., Kepinski, S., Bennett, M., De Veylder, L., and Traas, J. (2011). The auxin signalling network translates dynamic input into robust patterning at the shoot apex. Mol Syst Biol **7**.

Vieten, A., Sauer, M., Brewer, P.B., and Friml, J. (2007). Molecular and cellular aspects of auxin-transport-mediated development. Trends Plant Sci. **12,** 160-168.

Villalobos, L., Lee, S., De Oliveira, C., Ivetac, A., Brandt, W., Armitage, L., Sheard, L.B., Tan, X., Parry, G., Mao, H.B., Zheng, N., Napier, R., Kepinski, S., and Estelle, M. (2012). A combinatorial TIR1/AFB-Aux/IAA co-receptor system for differential sensing of auxin. Nat. Chem. Biol. **8,** 477-485.

Vöchting, H. (1885). Über die regeneration der Marchantieen. (On the regeneration of Marchantieen). Jahrbücher für wissenschaftliche Botanik **16,** 367-.

Voigt, W.E.A. (1879a). Beitrag zur vergleichenden Anatomie der Marchantiaceen (Contribution to the comparative anatomy of Marchantiaceen). Botanische Zeitung **37,** 729-743.

Voigt, W.E.A. (1879b). Beitrag zur vergleichenden Anatomie der Marchantiaceen (Contribution to the comparative anatomy of Marchantiaceen). Botanische Zeitung **37,** 745-759.

Voth, P.D. (1940). Responses of Marchantia polymorpha to Nutrient Supply and Photoperiod. Bot Gaz **102,** 169-205.

Walker, L., and Estelle, M. (1998). Molecular mechanisms of auxin action. Curr Opin Plant Biol **1,** 434-439.

Wang, J.W., Wang, L.J., Mao, Y.B., Cai, W.J., Xue, H.W., and Chen, X.Y. (2005). Control of root cap formation by microRNA-targeted auxin response factors in Arabidopsis. Plant Cell **17,** 2204-2216.

Wann, F.B. (1925). Some of the factors involved in the sexual reproduction of Marchantia polymorpha. Am J Bot **12,** 307-U309.

Wenkel, S., Emery, J., Hou, B.H., Evans, M.M., and Barton, M.K. (2007). A feedback regulatory module formed by LITTLE ZIPPER and HD-ZIPIII genes. Plant Cell **19,** 3379-3390.

Went, F.W. (1926). On growth-accelerating substances in the coleoptile of Avena sativa. Proceedings Koninklijke Nederlandse Akademie van Wetenschappen **30,** 10-19.

Went, F.W. (1928). Wuchsstoff und Wachstum. Recueil des Travaux Botaniques Néerlandais **24,** 1-116.

Williams, L., Carles, C.C., Osmont, K.S., and Fletcher, J.C. (2005). A database analysis method identifies an endogenous trans-acting short-interfering RNA that targets the Arabidopsis ARF2, ARF3, and ARF4 genes. Proc Natl Acad Sci U S A **102,** 9703-9708.

Woodward, A.W., and Bartel, B. (2005). Auxin: Regulation, action, and interaction. Annals of Botany **95,** 707-735.

Worley, C.K., Zenser, N., Ramos, J., Rouse, D., Leyser, O., Theologis, A., and Callis, J. (2000). Degradation of Aux/IAA proteins is essential for normal auxin signalling. Plant Journal **21,** 553-562.

Wu, M.F., Tian, Q., and Reed, J.W. (2006). Arabidopsis microRNA167 controls patterns of ARF6 and ARF8 expression, and regulates both female and male reproduction. Development **133,** 4211-4218.

Yang, Z., and Rannala, B. (2012). Molecular phylogenetics: principles and practice. Nat Rev Genet **13,** 303-314.

Zhao, Y., Christensen, S.K., Fankhauser, C., Cashman, J.R., Cohen, J.D., Weigel, D., and Chory, J. (2001). A role for flavin monooxygenase-like enzymes in auxin biosynthesis. Science **291,** 306-309.

Zhao, Y., Hull, A.K., Gupta, N.R., Goss, K.A., Alonso, J., Ecker, J.R., Normanly, J., Chory, J., and Celenza, J.L. (2002). Trp-dependent auxin biosynthesis in Arabidopsis: involvement of cytochrome P450s CYP79B2 and CYP79B3. Genes Dev **16,** 3100-3112.